Computer Simulation Studies of the Association of Caffeine Molecules in Aqueous Solution and its Role as an Inhibitor on Amyloid Aggregation

A Thesis Submitted

in Partial Fulfillment of the Requirements

for the Degree of

DOCTOR OF PHILOSOPHY

by

Bhanita Sharma

to the

Department of Chemistry

Indian Institute of Technology Guwahati, India

2016

भारतीय प्रौद्योगिकी संस्थान गुवाहाटी
Indian Institute of Technology Guwahati

Dedicated to
my beloved family

भारतीय प्रौद्योगिकी संस्थान गुवाहाटी
Indian Institute of Technology Guwahati

Declaration

I hereby declare that the matter manifested in this thesis "*Computer Simulation Studies of the Association of Caffeine Molecules in Aqueous Solution and its Role as an Inhibitor on Amyloid Aggregation*" is the result of research carried out by me in the Department of Chemistry, Indian Institute of Technology Guwahati, India under the supervision of Dr. Sandip Paul.

In keeping with the general practice of reporting scientific observations, due acknowledgement has been made wherever the work described is based on the findings of other investigators.

Bhanita Sharma
IIT Guwahati

भारतीय प्रौद्योगिकी संस्थान गुवाहाटी
Indian Institute of Technology Guwahati

Certificate

It is certified that the work contained in this thesis entitled, "*Computer Simulation Studies of the Association of Caffeine Molecules in Aqueous Solution and its Role as an Inhibitor on Amyloid Aggregation*" has been carried out by Bhanita Sharma for the Degree of Doctor of Philosophy under my supervision and the same has not been submitted elsewhere for a degree.

Dr. Sandip Paul
Thesis Supervisor
Department of Chemistry
Indian Institute of Technology Guwahati
Guwahati-781039, India

भारतीय प्रौद्योगिकी संस्थान गुवाहाटी
Indian Institute of Technology Guwahati

Preface

Over the past few years, several studies have proposed the link between caffeine intake and reduced risk of developing Alzheimer's disease, a neurodegenerative disease. Recent studies on Alzheimer's disease transgenic mice have shown that caffeine significantly slows down or prevents the development of β amyloid plaques, which is associated with the development of Alzheimer's disease. However, the molecular mechanism of the therapeutic potential of caffeine is largely unknown. The entitled thesis seeks to address this issue by means of classical molecular dynamics simulation.

It is my great pleasure to express here few words of appreciation to the people who actually made this thesis a reality and an unforgettable experience for me.

Foremost, I would like to express my sincere gratitude and respect to my thesis supervisor Dr. Sandip Paul for his excellent guidance, constant encouragement, unstinting inspiration, and amicable cooperation during the course of this work. In my countless discussion sessions with him which I am going to treasure forever, he not only showed how science and its challenges could be made interesting to ease out a solution, but also taught me the way this fun conveyed to the others. I could not have imagined having a better advisor and mentor for my Ph.D study.

Besides my supervisor, I am indebted to Dr. Bhubaneswar Mandal, Dr. Debasis Manna and Dr. Sumana Dutta for periodically assessing my work and providing valuable suggestions for its improvement. My sincere thanks go to all other faculty members in the department for their kind help at various stages of my doctoral work.

I am grateful to Ashim Paul (Dr. Ashim Paul) and Sourav Kalita for their cooperation, help and cheerful association, which were very much available in times of need. No words will be sufficient to express my feelings to labmates Dr. Rahul Sarma, Dr. Subrata Paul, Gargi, Shubhadip, Krishna, Srijita, Saikat, Rabindra and Shubhajit whom I consider a part of my life. I am truly grateful to them for taking the time to listen to many questions arising in my mind and sharing their knowledge about computer simulations. I owe a lot to my friends Sabera, Nirmali, Aswini, Apurba, Naba, Jayanta, Ranjith da, Harikrishna and Debashis and all other research scholars in the department for their lively company during

my stay in IITG.

I take this opportunity to express my sincere thanks to all my teachers in school, college, and university days for helping and encouraging me in various aspects of life and academics. All of my learning from them will be an asset in every walk of my life. I am grateful to the institute and also Center for Development of Advanced Computing (CDAC) for the computational support.

Many thanks go to my family members for their understanding, encouragement, and patience in my every endeavor. Last but not the least, I would like to thank my parents Dinesh Sharma and Golapi Sharma for giving birth to me at the first place and supporting me spiritually throughout my life. This thesis would not have seen the light of this day without their great wishes, immense patience, and great sacrifice. A famous quote reads- "Every journey begins with a single step"- and today, only because of my family, I move a step uphill towards my zenith.

Bhanita Sharma

2016

"A scientific truth does not triumph by convincing its opponents and making them see the light, but rather because its opponents eventually die and a new generation grows up that is familiar with it."

– Max Planck

भारतीय प्रौद्योगिकी संस्थान गुवाहाटी
Indian Institute of Technology Guwahati

Outline of the Thesis

भारतीय प्रौद्योगिकी संस्थान गुवाहाटी
Indian Institute of Technology Guwahati

Chapter 1

Introduction

"Folding and unfolding are crucial ways of regulating biological activity and targeting proteins to different cellular locations. Aggregation of misfolded proteins that escape the cellular quality-control mechanisms is a common feature of a wide range of highly debilitating and increasingly prevalent diseases."

– C. M. Dobson *Nature* **426**, 884 (2003)

■ PROTEIN AGGREGATION AND AMYLOIDOSIS

Neurodegenerative disorders typically result in a range of debilitating cognitive impairments including confusion, disorientation, loss of motor skills, and memory loss. The molecular origin of several neurodegenerative diseases including Alzheimer's disease, Parkinson's disease, Huntington's disease and prion protein diseases has been associated with the aggregation of proteins into amyloid fibrils [1-5]. In order to perform their biological function, most proteins adopt a defined three dimensional conformation, that is the most thermodynamically favorable: their native state, which is determined by the primary amino acid sequence and the local environment [6, 7]. However, although the native protein structure is thermodynamically stable, it does not necessarily imply that there is no other conformation, which exhibits a lower free energy state than the native state [8, 9]. Due to some variations in external parameters such as temperature, pH or solvent the natural folding equilibrium is disturbed and as a consequence protein misfolding and finally aggregation can be observed.

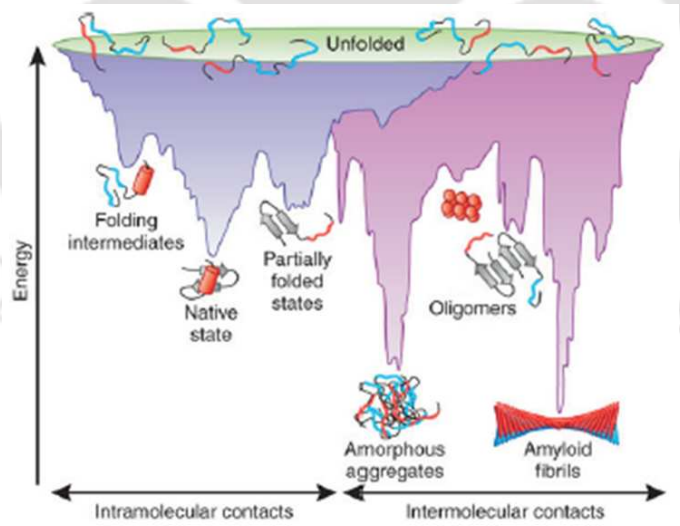

Figure 1-1. *Energy landscape scheme of protein folding and aggregation. The purple regime shows the multitude of conformations funneling to the native state via intramolecular contacts; and the pink area shows the conformations moving toward amorphous aggregates or amyloid fibrils via intermolecular contacts. Aggregate formation can occur from intermediates populated during de novo folding or by destabilization of the native state into partially folded states. Figure adapted from reference [10]*

The deposition of proteins in the form of amyloid fibrils and plaques within the extracellular space in the tissues of the body is the characteristic feature of more than 20 degenerative conditions affecting either the central nervous system or a variety of peripheral tissues. In particular, the Alzheimer's disease (AD) is the most common form of dementia that is affecting more than 44 million people worldwide. This leads to the loss of connections between the nerve cells, and eventually to the death of nerve cells and loss of brain tissues. Alzheimer's is a progressive disease. This means that gradually, over time, more parts of the brain are damaged leading to severe memory loss. AD is caused by the formation of extracellular senile plaques, mainly composed of amyloid peptide (Aβ), and intracellular neurofibrillary tangles formed by hyperphosphorylated tau protein [11, 12]. The extracellular senile plaques are made of Aβ, which comprises of mainly 39-42 residue long peptide fragments. These are formed by the cleavage of amyloid precursor protein (APP) in the presence of γ-secretase [13]. Therapeutic strategies that are currently being pursued for AD, mainly focus on these two AD-related proteins, Aβ and Tau. Of these, Aβ has attracted more attention by far.

At present, there is no drug treatment available that can cure AD or any other common type of dementia. Medicines that are used for AD can only temporarily help to mask the symptoms. Inhibiting the aggregation of protein is now being considered as an effective therapeutic strategy for the treatment of AD, and therefore, researchers are looking for drugs that can inhibit the amyloid formation to treat the underlying disease or delay its progression [14-21]. However, despite intensive research on this front, only a few novel aggregation inhibitors that showed potential to cope with the disease based on this strategy, have been rejected in clinical trials due to their undesirable side effects. Typical Aβ aggregation inhibitors such as some inorganic nanoparticles, sulfonated dyes etc. are often toxic and some of them are also carcinogenic [22]. Whereas a variety of biopolymers and macromolecules that can act as inhibitors, have the difficulty of transportation through the blood-brain barrier (BBB). The BBB is the homeostatic defence mechanism against pathogens and toxins. It determines whether or not a given drug (unless lipid soluble, small (<600 Da), electrically neutral and weakly basic), can reach the central nervous system (CNS), limiting the brain penetration by polymers. Therefore, much effort has been made recently mainly focusing on the development of a drug which is safe, readily available, passes through BBB and at the same time can prevent or delay the progress of the AD disease. Recent longitudinal studies spanning 4-10 years suggested that regular moderate amount of caffeine intake prevents memory decline in older people, and reduces the risk of

developing Alzheimer's disease. Several other researches on AD transgenic mice have shown that caffeine significantly decreases the level of Aβ amyloid plaques both in brain and in the blood of mice that were exhibiting symptoms of the disease [23-26]. Another study investigated the effect of caffeine in mice bred to mimic the other hallmark of Alzheimer's - the tau deposits. It reported that caffeine intake is beneficial in mice that develop tau deposit similar to those seen in humans [27]. The proposed link between caffeine intake and the reduction of AD disease probability suggests a possible role of caffeine in therapeutic utility against AD. Caffeine (see Fig.1.2) is inherently safe, naturally produced by several plants, inexpensive and normally found in the diet [28, 29]. It is an example of a planar, hetero-atomic bicyclic, aromatic ring compound that, although somewhat polar, exhibits limited aqueous solubility. The simultaneous presence of hydrophobic methyl (-CH3) groups and extended flat hydrophobic faces, as well as three hydrophilic proton acceptors groups makes it a good selection for our study. The oral intake of caffeine rapidly passes through the BBB due to its amphiphilic nature, and reach the brain tissues.

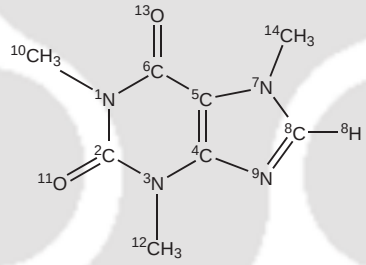

Figure 1-2. *The structure and atomic numbering of caffeine molecule*

Caffeine can be classified as an alkaloid [30, 31] and is regularly consumed in sources such as tea, coffee, chocolate and beverages and included in many medicines [28, 29]. It is naturally produced by several plants, including coffee beans, guarana, cacao beans, and tea etc. It acts as a natural pesticide that paralyzes and kills certain insects feeding on the plants [32]. It possesses purine ring system in its backbone and is a biologically important compound.

Caffeine undergoes self-association in water above its solubility limit. Moreover, no theoretical studies have been conducted so far to the best of our knowledge, to understand the effect of caffeine as an inhibitor to amyloid formation. On molecular level, it would be interesting to understand how a small molecule like caffeine might inhibit amyloid formation, interacts with proteins and ultimately destabilizes amyloid assemblies. Literature

survey on caffeine self and hetero association has shown that only recently some theoretical and experimental studies have been carried out of the effects of several dissolutes on the association properties of caffeine [33-39]. For example, the studies of interaction of chemical denaturants like 8 M urea and 6 M guanidium chloride on caffeine have shown the disruption of caffeine aggregates [33, 37]. Again, the study of the influence of solvent and solution ionic strength on the formation of caffeine and actinocin heterodimers are reported to be energy-preferable. Hence, caffeine can decrease the concentration of aromatic ligand in biological systems, and thus decreases its biological activity [35]. It has also been shown that caffeine has an ability to act on DNA intercalates and thus reducing the toxicity of them [40]. In addition to this, caffeine has a negative effect on the pharmacological activity of a number of aromatic anticancer drugs due to the competition of caffeine over drugs for DNA binding sites [41-44]. Caffeine is a base analogous to adenosine nucleotide and it is known as a central nervous system stimulant [45, 46]. It also increases the dopamine levels in the body by slowing down the rate of dopamine reabsorption [47]. Caffeine is one of the many xanthine derivatives that acts as a nonselective antagonist on the A_1 and A_{2A} receptors. So, caffeine is used extensively as a drug for different pharmacological diseases.

Moreover, recent experimental evidences suggested that although the amyloid plaques are one of the hallmarks of these diseases, the neurotoxicity may be caused by oligomers formed in the early stage of fibril formation [48-50]. Thus, drugs that can prevent the formation of early oligomeric intermediates or make them unstable, are major concerns in the field of drug discovery against AD. The initial stages of oligomers formation are difficult to characterize in experimental studies, since Aβ peptide is highly amyloidogenic. In this context, we note that computer simulation can provide the information required to capture the early steps of amyloid formation and demonstrate insights of the behavior of the drugs that can inhibit Aβ aggregation. Different theoretical and experimental studies showed that caffeine molecules form complexes with different biomolecules, DNA, and drug molecules with π-stacking interaction [51, 52]. Caffeine molecule also self-aggregates in aqueous solution and its aromatic ring plays a central role to form high-order caffeine clusters [53-58]. In this regard, it is to be noted that several previous studies argued that it is the aggregated forms of the small molecule inhibitors that show inhibiting action against the biomolecular aggregations. Therefore, caffeine molecule seems to be a potential candidate as an inhibitor of amyloid formation and can act as a potent drug controlling amyloid disease.

Therefore, in the current study, an effort has been made to understand the molec-

ular mechanism of inhibition of protein aggregation by caffeine. For this, first, we will try to understand the self-association of caffeine in molecular details in different chemical and physical environments and the thermodynamics of caffeine association. Then we extend our study on molecular interaction between caffeine and protein oligomers, which will shed lights on the mechanism of amyloid inhibition by caffeine. The simulation works and concluding remarks are presented in the subsequent six chapters. The next section of the present chapter deals with the basic techniques of MD simulation that is employed in our work. The details analyses of the applications of these techniques for specific systems are given in later chapters. This is followed by a brief description of the work presented in the current thesis.

■ METHODOLOGY

In this thesis, classical molecular dynamics (MD) simulation technique has been employed. It has been widely used to investigate the structure and dynamics of biomolecular systems, such as proteins, nucleic acids, and small molecules like amino acids and sugars. In MD simulation, the potential energy function (U) is described by all interactions between the atoms that are covalently bonded as well as non-bonded interactions between atoms and molecules in the condensed phase. The interactions between particles are governed by the so-called force field parameterization [59]. Note that, through out this thesis, specific AMBER10/12 force field parameter sets are used [60, 61].

The potential energy function is written as a sum of bonded and non-bonded interaction terms

$$U = U_{bond} + U_{angle} + U_{dihedral} + U_{vdw} + U_{Coulomb} \tag{1.1}$$

The first three terms (U_{bond}, U_{angle}, $U_{dihedral}$) are the bonded terms, which describe the bond stretching, angle bending, and torsion rotation, and the last two terms are for the non-bonded potential. In bonded terms, the bond and angle contributions are described by harmonic potentials and all of the interactions between directly bonded atoms (1-2 interactions), angles (1-3 interactions, where two atoms bonded to a common atom), and torsion (interactions between pairs of 1-4 atoms) are defined as:

$$U_{bond} = \sum_{bonds} K_b(b_{ac} - b_{eq})^2 \tag{1.2}$$

$$U_{angle} = \sum_{angles} K_\theta(\theta_{ac} - \theta_{eq})^2 \tag{1.3}$$

$$U_{dihedral} = \sum_{dihedrals} \frac{V_n}{2}(1 + cos(n\phi - \delta)) \tag{1.4}$$

The letters b, θ, ϕ, and δ represent the bond length, bond angle, dihedral angle, and phase angle, respectively. The subscripts ac stands for actual and eq stands for equilibrium. The parameters K_b, K_θ, and V_n are the force constants for bond, bond angle, and dihedral angle, respectively.

The non-bonded potentials are calculated using two terms, the first one is the Lennard-Jones term (U_{vdw}) [62] describing the van der Waals interaction [63], and the second one is the Coulomb term ($U_{coulomb}$) [64] that deals with the electrostatic interactions between particles having partial charges on them. The non-bonding interaction terms are defined as:

$$U_{vdw} = \sum_i \sum_{i<j} 4\epsilon_{ij}\left[\left(\frac{\sigma_{ij}}{r_{ij}}\right)^{12} - \left(\frac{\sigma_{ij}}{r_{ij}}\right)^{6}\right] \tag{1.5}$$

$$U_{coulomb} = \sum_i \sum_{i<j} [\frac{q_i q_j}{4\pi\epsilon_o r_{ij}}] \tag{1.6}$$

where the overall sum is over all the atom pairs i and j. σ and ϵ are the Lennard-Jones separation at minimum (i.e. equilibrium distance) and well depth energy, respectively. r_{ij} is the inter-atomic distance. q_i and q_j are the partial charges on interaction sites i and j and ϵ_o is the electrical permittivity.

The aim of the MD simulation is to observe the evolution of atomic coordinates in time. We consider an N-particle system characterized by the following Hamiltonian

$$H = \sum_{i=1}^{N} \frac{p_i^2}{2m} + U(\mathbf{r}^N) \tag{1.7}$$

where m is the mass of each particle, p_i is the momentum of the i-th particle and $U(\mathbf{r}^N)$ is the total potential energy of the system which includes the all particle-particle interactions. The coordinates of the particles are denoted by $\mathbf{r}^N = \{\mathbf{r}_1, \cdots, \mathbf{r}_N\}$. The position and velocity of i-th particle is represented by $\mathbf{r}_i$ and $\mathbf{v}_i$, respectively. The method of molecular dynamics consists of solving the equation

$$a_i = \frac{\mathbf{F_i}}{m_i} \tag{1.8}$$

where $i = 1, 2, ...N$, m_i is the mass of i-th particle and $\mathbf{F}_i$ is the force acting on particle i. This equation is obtained easily from the Lagrangian

$$L = \frac{1}{2}\sum_{i=1}^{N} m_i \mathbf{v_i}.\mathbf{v_i} - \frac{1}{2}\sum_{i=1}^{N}\sum_{j\neq i}^{N} u(r_{ij}) \tag{1.9}$$

where the potential U has been assumed to be the sum of pair potentials u_{ij}. The Lagrangian equation of motion is

$$\frac{d}{dt}(\frac{\partial L}{\partial \dot{q}_i}) - \frac{\partial L}{\partial \dot{q}_i} = 0 \tag{1.10}$$

It is clear from Eq. 1.10 that the dynamics of particles is described by 3N number of second order differential equations.

It is also possible to write down the Hamiltonian (H) for the system and solve the the Hamiltonian equations of motion

$$\dot{\mathbf{q}}_k = \frac{\partial H}{\partial p_k} \tag{1.11}$$

$$\dot{\mathbf{p}}_k = -\frac{\partial H}{\partial q_k} \tag{1.12}$$

where $\mathbf{q}_k$ and $\mathbf{p}_k$ represent generalized coordinates and momenta. For a system with pairwise interaction potential, the Hamiltonian is

$$H = \frac{1}{2}\sum_{i=1}^{N} m_i \mathbf{v_i}.\mathbf{v_i} + \frac{1}{2}\sum_{i=1}^{N}\sum_{j\neq i}^{N} u(r_{ij}) \tag{1.13}$$

and Eqs. 1.11 and 1.12 yield

$$\frac{dr_i}{dt} = \frac{\mathbf{p_i}}{m_i} \tag{1.14}$$

$$-\dot{\mathbf{p}}_i = -\nabla \mathbf{u} = \mathbf{F_i} \tag{1.15}$$

where i=1,2,....N. There are now $6N$ first order differential equations to be solved.

The equation of motion is solved numerically to yield particle velocities and positions as a function of time. It is usually integrated by using finite difference approach. The Verlet algorithm is one of the most commonly used algorithm for this purpose [65]. The advantage of the use of Verlet algorithm is that its implementation is straightforward and storage requirements are modest. Although, it has the disadvantage of moderate precision during the calculation and velocity does not appear explicitly in the Verlet integration. As an improvement to the Verlet algorithm, the leap-frog algorithm [66] has been developed. But, it has a disadvantage that the positions and velocities are not synchronized. As an alternative of Verlet or the leapfrog algorithm, Velocity Verlet algorithm has been developed and the following relations are used to calculate new position and velocity at the same time:

$$r(t+dt) = r(t) + v(t)dt + \frac{1}{2}a(t)dt^2 \tag{1.16}$$

$$v(t+dt) = v(t) + \frac{1}{2}[a(t) + a(t+dt)]dt \tag{1.17}$$

To calculate the velocities at time t+dt, this method requires acceleration at time t and t+dt. In the present work, we have employed Velocity Verlet algorithm.

■ PRESENT WORK

Alzheimer's disease is a devastating neurodegenerative disease triggered by the aggregation of amyloid-β peptide (Aβ) into amyloid fibrils. At present, there is no drug treatment available that can cure AD or any other common type of dementia. Recent longitudinal studies spanning 4-10 years suggested that regular moderate amount of caffeine intake prevents memory decline in older people, and reduces the risk of developing Alzheimer's disease. Several research studies on AD transgenic mice have shown that caffeine significantly decreases the level of Aβ amyloid and slows down or prevents the development of β amyloid plaques both in brain and in the blood of mice that were exhibiting symptoms of the disease. It has also been revealed that caffeine intake is beneficial in mice that already developed tau deposit similar to those seen in humans. On the other hand, caffeine is a widely consumed psychoactive substance and acts as a central nervous system stimulant. It is also extensively used as a drug for different pharmacological diseases. Caffeine is inherently safe, naturally produced by several plants, inexpensive and normally found in the diet. Due to caffeine's unhindered traversal of the blood-brain-barrier (BBB), oral intake of caffeine rapidly acts on the central nervous system and brain tissues. All these findings suggest a possible role of caffeine in therapeutic utility against AD. However, the molecular mechanism of the therapeutic potential of caffeine is largely unknown. Therefore, exploring effect of caffeine on the amyloid aggregation by means of classical molecular dynamics (MD) simulations is the goal of the present thesis.

For unveiling the role of caffeine, we first aim to study the self-association of caffeine in molecular details in different chemical and physical environments.

The present chapter (**Chapter 1**) of the thesis includes a review of related experimental and theoretical works that exist in the literature together with the basic techniques of MD simulations.

From the studies of different small molecule inhibitors it is known that inhibitors inhibit amyloid formation by forming chemical aggregates with the like molecules. It has been reported that caffeine molecules self-aggregate in water above its threshold concentration of 0.1M. Moreover, it is also a well known fact that hydrophobic interaction is

markedly influenced by the presence of salt ions in water. Salt ions are naturally present in all biological systems and an essential component of living systems. In fact, the ionic environment in water is indispensable for making the ideal structure or conformation of biological macromolecules. Again, since the thermodynamics of self-association is strongly temperature dependent, therefore, the caffeine-caffeine interaction is expected to be affected largely by temperature change. Thus, a complete understanding of caffeine self-association requires a knowledge of temperature dependence propensity of caffeine association. Therefore, motivated by the above considerations, in **Chapters 2 and 3** we have investigated the self-association properties of caffeine in pure water, in different concentration of NaCl salt in water, and at different temperatures. In **Chapters 2**, the effect of salt concentration on association propensities of caffeine molecules is investigated by employing classical MD simulations in isothermal-isobaric ensemble of eight caffeine molecules in pure water and three different NaCl salt concentrations. The concentration of caffeine was taken almost at the solubility limit. We have calculated radial distribution functions (rdfs) of caffeine-caffeine and caffeine-water considering center of masses of caffeine and water. Further, to study the local structure of salt solution, we have also calculated the ion-ion, ion-water and water-water rdfs and the rdfs involving selected atomic sites of caffeine and different solution species. The molecular orientation of liquid water around hydrophobic solutes is governed by the optimization of hydrogen bonding interactions. We have shown the contours of water density within 3.4 Å around a caffeine monomer in a frame fixed with respect to the center of mass of its monomer. The solvent accessible surface area (SASA) describes the area over which the contact between solute and solvent can occur. We have calculated the SASA of caffeine molecules in different solutions. Then, we have shown the preferential interaction parameter of caffeine for a caffeine molecule over water at different concentrations of salt solution. In aqueous solution, caffeine molecules can form hydrogen bonds with water. Caffeine molecule has three hydrogen bonding sites, and these are two carbonyl oxygen and the ring nitrogen atom. These atoms can only act as hydrogen acceptors. Therefore, we have carried out an analysis of the number of hydrogen bonds formed between water and hydrogen acceptor sites of caffeine molecules.

In **Chapter 3**, we have investigated the temperature induced self association of caffeine molecules in aqueous solution both in presence and absence of salt NaCl at a regime of temperatures ranging from 275 K to 350 K with a temperature difference of 25 K. Water, the common environment for most biological processes, plays a significant role in binding thermodynamics. Water structure in the vicinity of a hydrophobic solute influences the

thermodynamics of hydrophobic hydration as well as water-mediated interactions between them. For small hydrophobic solutes, an adjacent water molecule can straddle the solute to make hydrogen bonds to other water molecules, with neither of its protons or lone pairs directly pointing at the solute, and therefore, there is no loss of any hydrogen bonds. Thus, due to the restriction of rotational freedom of water molecules adjacent to the solutes, the aggregation of such small hydrophobic solutes is entropy driven. As a consequence, with increasing temperature the aggregation of small hydrophobic solutes are found to be enhanced. In contrast, there is a significant difference in the hydration of large hydrophobic solutes. Hydration of large hydrophobic solutes leads to breaking of some hydrogen bonds between water molecules, as it becomes impossible for water molecules to straddle the surface and still maintaining the hydrogen bonds to other water molecules. Therefore, when such large hydrophobic solutes aggregate in aqueous solution, the structured water molecules around the hydrophobic solutes are liberated, which results in regaining of lost hydrogen bonds, and, therefore, aggregation is enthalpy driven. As predicted by Chandler, for hydrophobic solutes in the bulk water at standard conditions, the cross-over from one regime to the other occurs at solute size of 1 nm. In the context of caffeine association in aqueous solution it is to be noted that the simultaneous presence of hydrophobic methyl (-CH3) groups and extended flat hydrophobic faces, as well as three hydrophilic proton acceptor groups makes it a good selection for our study. Although, the size of caffeine molecule is considerably shorter than the 1 nm limit (the size of caffeine is 6.5 Å), some experimental and theoretical studies showed that the self-association of caffeine is enthalpy driven. Contrary to these studies entropy driven association of caffeine molecules is also reported. However, since both entropy and enthalpy are strongly temperature- dependent, therefore, the thermodynamic stability of caffeine-caffeine interaction is expected to be affected largely by change in temperature. Thus, a complete understanding of caffeine self-association requires a knowledge of temperature dependent propensity of caffeine association. However, a very few experimental or theoretical studies have been carried out to investigate the effect of temperature change on caffeine aggregation. Although Origlia-Luster et al. and Sanjeewa et al. have carried out temperature induced caffeine aggregation in binary caffeine-water system [67, 68], their studies were limited to just some thermodynamic calculations. However, no experimental or theoretical study has been carried out on simultaneous effects of temperature and salt on caffeine aggregation. Further, salt ions are important components in the aqueous environment in biological systems, and the hydrophobic interaction is greatly influenced by the presence of salts. A great deal of research

works have been devoted to explore the interaction between hydrophobic solutes and their hydration in different aqueous media. It was observed that, as the solute-water attractions are turned on, the solvation thermodynamics also change. Therefore, the solvation behavior of the solute critically depends on the strength of the solute-solvent attraction. Therefore, a detailed knowledge of the effects of salt and temperature on hydrophobic interactions is of fundamental interest for the understanding of aggregation phenomena in biological systems. We have considered caffeine-caffeine center of mass rdf and cluster structure analyses to understand the association propensity of caffeine. To get a clear picture on thermodynamics of association, we have also calculated potentials of mean force (PMF) as a function of caffeine-caffeine distance, and then calculated enthalpic and entropic contribution to caffeine association.

The 'hydrophobic effect' is one of the most significant forces in biological systems. It plays a major role in many different biomolecular processes including conformational changes in proteins, protein-protein interaction, enzyme-substrate binding etc. However, intermolecular protein-protein association may lead to aggregation of proteins into amyloid fibers, which is associated with a growing list of diseases, such as Alzheimers disease, Parkinsons disease and Huntingtons disease, type 2 diabetes mellitus and the prion diseases. The hydrophobic effect is recognized to be the major driving force in protein-protein interactions. Therefore, an extensive study of hydrophobic interaction is important to get a clear understanding of how such protein aggregation can be inhibited. It is also useful to use a smaller molecular system which can mimic hydrophobic aggregation in biomolecules to carry out an atomic and molecular level description of hydrophobic effect. In fact, due to complexity in structure and size and the presence of variety of polar and nonpolar side chains in protein, the range of possible interactions is too vast. This makes it difficult to investigate them in atomistic detail in theoretical study too. Therefore, simple hydrophobic model systems are often chosen as an alternative to understand the solute-solute, solute-solvent interactions. Therefore, in **Chapter 4**, we have explored the inhibition of self-aggregation of a hydrophobic model solute di-t-butyl-methane (DTBM) by caffeine in water. To shed lights into the aggregation propensity of DTBM molecules in water and in different caffeine solutions, we have calculated the number of free monomer DTBM molecules in different systems. Then, in order to gain insights into the intermolecular interaction between DTBM molecules we have considered the site-site distribution functions of DTBM molecules, hydration of DTBM, and the average number of caffeine molecules around DTBM. To get a pictorial description of DTBM aggregation and the

effect of caffeine molecules on it we have shown spatial density plots of DTBM around DTBM, water around DTBM, and caffeine around DTBM. Again, as the ability of self-assembly formation is a general property of small organic molecule inhibitors, therefore, we have carried out cluster structure analyses of caffeine for different systems to analyze the self-association of caffeine in different systems. To explain the mechanism of inhibition of hydrophobic aggregation of DTBM by caffeine aggregates, we have calculated the binding affinities, preferential interaction parameters, and the effect of caffeine cluster's size on DTBM aggregation. We then studied the aggregation behavior of DTBM in previously aggregated caffeine systems to further verify our mechanism.

Although the hydrophobic effect is one of the major factors stabilizing the tertiary structures of proteins, hydrogen bonding and electrostatic interactions play crucial roles in protein aggregation. Therefore, in **Chapter 5** we report the inhibiting effect of caffeine on amyloid aggregation with more realistic 18-residue amyloid-β derived switch-peptide. Our study focuses on the effect of caffeine on the aggregation of amyloid-β derived switch-peptide with varied stoichiometric ratio of caffeine to peptide. For this we have carried out secondary structure analyses of peptide in pure water and in different stoichiometric ratios of caffeine solutions to examine the formation of ordered β-sheets structure. Calculations of rdfs, residue-residue contact map, interaction energy and SASA as well as hydrogen bond analyses are carried out to understand the disaggregation tendency of peptide in presence of different ratios of caffeine to peptide.

In **Chapter 6** we have considered seven residue peptide Aβ_{16-22}, one of the shortest length peptide that can form amyloid in vitro. This peptide with sequence KLVFFAE (16-22) is amphiphilic, and found to be critical for fibrillization. The LVFF sequence (17-20) in the Aβ_{16-22} peptide is the central hydrophobic core (CHC) in Aβ peptide. The aromatic residues (FF) in the Aβ_{16-22} peptide play an important role in the molecular recognition and self-assembly process that lead to amyloid fibril formation (due to stacking interaction). Again, the N-terminal residue of Aβ_{16-22} peptide has positively charged lysine and C-terminal has negatively charged glutamic acid. The electrostatic interaction between peptides (due to presences of opposite charges on terminal residues) leads to stabilization of anti-parallel strands. Therefore, Aβ_{16-22} is an attractive model system to probe the mechanism of inhibition of the formation of peptide oligomers by caffeine. We have carried out classical molecular dynamics simulation of five amyloid forming Aβ_{16-22} peptide in pure water and in a regime of caffeine solutions, with different caffeine : peptide stoichiometric ratios. We have carried out secondary structure analyses to analyse the formation of β-

sheets in pure water and the effect of caffeine solution in the prevention of ordered β structure. Residue-residue contact map analyses are explored to examine the interaction between different peptides. The interactions of aromatic phenylalanine residues of peptide with caffeine are calculated to understand the mechanism of caffeine action on amyloid inhibition.

At the end, in **Chapter 7**, we present the summary of the results together with our view on caffeine's action on inhibition of protein aggregation.

Chapter 2

Association of Caffeine Molecules in Aqueous Solution

"The hydrophobic effect–the tendency for oil and water to segregate- is important in diverse phenomena, from the cleaning of laundry, to the creation of micro-emulsions to make new materials, to the assembly of proteins into functional complexes. This effect is multifaceted depending on whether hydrophobic molecules are individually hydrated or driven to assemble into larger structures. Despite the basic principles underlying the hydrophobic effect being qualitatively well understood, only recently have theoretical developments begun to explain and quantify many features of this ubiquitous phenomenon."

– D. Chandler *Nature* **437**, 640 (2005)

Overview:

The effect of salt concentration on association properties of caffeine molecule was investigated by employing molecular dynamics (MD) simulations in isothermal-isobaric ensemble of eight caffeine molecules in pure water and three different salt(NaCl) concentration, at 300K temperature and 1 atm pressure. The concentration of caffeine was taken almost at the solubility limit. On addition of NaCl salt, we observe enhancement of first peak height and appearance of a second peak in the caffeine-caffeine distribution function suggesting association of caffeine molecules. This observation is supported by our calculated SASA values and structure visualization of our systems taken at 5 ns interval for different systems. Our calculated hydrogen bond properties reveal that NaCl has essentially no influence on the average water-caffeine hydrogen bonds. Also observed are: (i) decrease in probability of salt contact ion pair as well decrease in the solvent separated ion pair formation with increasing salt concentration, (ii) a modest second shell collapse in the water structure and (iii) dehydration of hydrophobic atomic sites of caffeine on addition of NaCl.

■ INTRODUCTION

Solute molecules when dissolved in water can significantly affect the structuring of water molecules in aqueous solutions [69]. When a solute molecule is present in aqueous environment, its functional groups must interact with the surrounding water, and its presence can impose a structuring pattern on the adjacent solvent molecules, which differs from that of pure bulk water [70, 71]. These solutes may self-aggregate in aqueous medium depending on the interaction of these solutes with water. Recent studies on interaction of caffeine molecule with solvent water showed highly complex hydration pattern compared to that of a smaller hydrophobic molecule such as methane. For small hydrophobic solutes, an adjacent water molecule can straddle the solute to make hydrogen bonds to other water molecules, with neither of its protons or lone pairs directly pointing at the solute, which would involve the loss of a hydrogen bond [72]. Therefore, the aggregation of such small hydrophobic solutes is entropy driven due to the restriction of rotational freedom of these water molecules adjacent to the solutes. However, in case of extended hydrophobic surface, water structural reorganization at the solute surface is required, as it becomes impossible for water molecules to straddle the surface and still form hydrogen bonds to other water molecules off to its side [69, 73]. Therefore, to maximize the total interaction, a water molecule prefers to sacrifice one possible bonding interaction by pointing one hydrogen atom or lone pair directly at the non-hydrogen bonding surface, as the resulting loss of one hydrogen bond is energetically favorable than the loss of three hydrogen bonds that would result if it adopted an orientation of waters as that of adjacent to a methane molecule [74-76]. Thus, when such larger hydrophobic solutes aggregate in aqueous solution, these hydrophobically structured water molecules are liberated, as the surface area accessible to water molecules decreases which results in regain of lost hydrogen bonds, and, therefore, aggregation is enthalpically driven. The aggregation of caffeine molecules in water is very interesting to study because of the simultaneous presence of hydrophobic methyl (-CH_3) groups and extended flat hydrophobic faces, as well as three proton acceptor groups (O11, O13, N9). There is no proton donor group in the caffeine molecule. Due to the close proximity of these different groups in the solute, structuring of solvent around one atom contributes to the structuring around adjacent atoms as well, and this results in highly anisotropic and very complex distribution of water molecules around caffeine molecule [69]. The presence of hydrophobic groups in the molecule limits its solubility in water and leads to association with itself or complexation with other drug molecules. In fact, several experimental and

theoretical studies were carried out on self and hetero-association of caffeine molecule in aqueous medium [33-36, 77] It is found in literature that caffeine molecules self-aggregates in water above the concentration of 0.1M [78]. To know how solute molecules influence in changing the structure of solvent water, is important to understand the properties of that solute in solution and its interaction with itself and other cosolutes.

Again it is well known that hydrophobic interaction is markedly influenced by the presence of salt ions in water [79]. Salt ions are naturally present in all biological systems and an essential component of living systems. In fact, the ionic environment in water is indispensable for making the ideal structure or conformation of biological macromolecules [80]. The effect of salt ions on the self-assembly of biological molecules is very significant. Depending on the nature and concentration of the salt solution, either association or dissolution of hydrophobic molecules in water may take place. There are some experimental data available on the solubility of caffeine in presence of urea, [33, 37] guanidium chloride [37], KCl [37], sucrose [38] and alcohol [81]. Recently some experimental studies on the effects of several cosolutes on the association properties of caffeine have shown the change of self-association constant in presence of some salts of Hofmeister series, increasing from $NaClO_4$ to NaSCN to NaCl to Na_2SO_4 [39]. Also, molecular level study on the influence of solvent and solution ionic strength on the self and hetero-association properties of caffeine and actinocin derivatives have been studied [35]. However, there are no information regarding the effect of different concentration of salt on self-association properties of caffeine, change in the possibility of formation of hydrogen bond with solvent, and change in solubility limit of caffeine upon addition of salt. Motivated by the above considerations, we explore the effect of different concentrations of NaCl salt on caffeine self-association.

In this chapter, we have carried out a series of molecular dynamics (MD) simulation to understand the self-association behavior of caffeine in pure water and in different concentration of NaCl salt in water. The goal of this chapter are: (i) to investigate the aggregate formation of caffeine at different concentration of salt solution, (ii) to provide a molecular level description of the interactions between caffeine, water and ions in solution, (iii) to study the structural arrangement of caffeine molecule in aggregates, and (iv) to examine any change in the possibility of formation of hydrogen bonds between hydration sites of caffeine and water at different salt concentrations. In the next section, we have presented a description of the models and simulation method. Results are discussed thereafter, and this part is ended with a section whereof we have included our concluding remarks with a brief summary.

■ MODELS AND SIMULATION METHOD

We have carried out molecular dynamics (MD) simulation of 8 caffeine molecules in pure water and as well as in aqueous NaCl solution of varying concentration. Since the solubility limit of caffeine in pure water was reported to be 0.1 M [78], we have considered all our systems near to its solubility limit. The systems considered in this study are summarized in Table 2-1. It is worth noting that we have kept the total number of water molecules fixed to 4500 in all cases and Na^+ and Cl^- ions were added without replacing the water molecules. Further note that since our goal is to understand the aggregation of caffeine molecules on slight change of NaCl concentration, we have considered the concentrations of NaCl in the dilute solution range.

Table 2-1. Overview of Systems[a]

System	N_{caff}	N_{wat}	N_{salt}	C_{salt}(M)	C_{caff}(M)	ρ (g cm^{-3})	Box Length(Å)
S0	8	4500	0	0	0.097	1.01	51.54
S1	8	4500	20	0.24	0.097	1.02	51.63
S2	8	4500	50	0.60	0.096	1.03	51.75
S3	8	4500	70	0.83	0.095	1.04	51.85

N_{caff}, N_{wat} and N_{salt} represent the number of caffeine, the number of water and the number of NaCl molecules respectively. C_{salt}, C_{caff} and ρ represent the salt concentration, caffeine concentration, box length and the density respectively.

In order to develop the partial charges of different atomic sites, the caffeine molecule was first optimized with HF/6-31G* using Gaussian03 [82], and then fitting the atomic charges using RESP module of AMBER10 [60]. The rest of the parameters for caffeine were generated using the general AMBER Force Field (GAFF) with the ANTECHAMBER module of AMBER10. The atomic partial charges developed for the present MD simulation are given in Table 2-2. Furthermore, in Table 2-1, we have compared the density of our caffeine-water system (S0) with the available experimental and other simulation density values reported elsewhere [77, 83]. We remark that although the agreement is little far from perfect, the experimental and simulation densities are in reasonable accord. For NaCl, we employ force field parameters developed by Joung and Cheatham [84]. We have used the popular extended simple point-charge (SPC/E) model for water [85].

Table 2-2. Partial charges for different atomic sites of caffeine. e is the elementary charge

Atom	Charge (e)	Atom	Charge (e)
N1	0.028	C2	0.333
N3	0.036	C4	0.222
C5	-0.019	C6	0.341
N7	0.043	C8	0.163
N9	-0.617	C10M	0.213
O11	-0.630	C12M	0.188
O13	-0.631	C14M	0.147

The MD simulations were carried out using the AMBER 10 suite of programs in isothermal isobaric (NPT) ensemble at 300 K temperature and 1 atm pressure with a time step of 2 fs. At the beginning of the simulation, caffeine molecules were randomly distributed in the cubic simulation box. To obtain a reasonable initial structure, for each system, the initial configurations (generated using the Packmol program [86]) were first energy minimized for 5000 steps with 2500 steps of steepest descent minimization followed by 2500 steps of conjugate gradient method. Each system was then heated slowly from 0 to 300K over 20 ps in the canonical (NVT) ensemble. To remove the edge effects, periodic boundary condition was applied for all the simulations and Langevin dynamics method with a collision frequency of 1 ps^{-1} was used to control the temperature. The Berendsen barostat [87] was used to maintain the pressure with a pressure relaxation time of 2 ps. Bonds involving hydrogen were constrained by applying the SHAKE algorithm and a cut off of 12.0 Å was applied for all nonbonding interactions. The long-range electrostatic interactions were treated using the particle mesh Ewald method. After 5 ns equilibration, the simulations were carried out for another 15 ns production run in NPT ensemble. The results reported in this Article are from these last 15 ns of simulation periods.

■ RESULTS AND DISCUSSION

Radial distribution function and Co-ordination number analysis

To understand the solvation and possible association of caffeine molecules in different salt concentrations, we have studied the molecular interaction between caffeine, water and ions (Na^+ and Cl^-). Radial distribution function (rdf) is an effective way of describing the average structure of molecules around a central reference molecule. We have calculated rdfs of caffeine-caffeine and caffeine-water considering center of masses of caffeine and water. Further, to study the local structure of salt solution, we have also calculated the ion-ion, ion-water and water-water rdfs and rdfs involving selected atomic sites of caffeine and different solution species. For further analysis, first shell water coordination number around caffeine is calculated using the relation:

$$n_{\alpha\beta} = 4\pi\rho_\beta \int_0^{r_c} r^2 g_{\alpha\beta}(r) dr \tag{2.1}$$

where $n_{\alpha\beta}$ represents the number of atoms of type β surrounding atom α in a shell extending from 0 to r_c (the distance of the first minimum in the rdf plot) and ρ_β is the number density of β in the system. So for the calculations of first shell coordination number, the typical values of r_1 and r_2 are zero and the distance of first minimum in the corresponding radial distribution function, respectively. Note that, the standard errors reported are calculated by using block averages over 3 ns. In Fig. 2-1, we have shown the rdf of caffeine-caffeine center of mass. The first peak and the first minimum of this distribution function appear at 3.7 Å and 6.4 Å respectively. It is interesting to note that though the concentrations of caffeine in all the four systems are very similar and are slightly below the solubility limit, the first peak height of g(r) increases with increasing salt concentration indicating increasing interaction between caffeine molecules. Further, on addition of NaCl a second peak also starts developing at 7.2 Å .

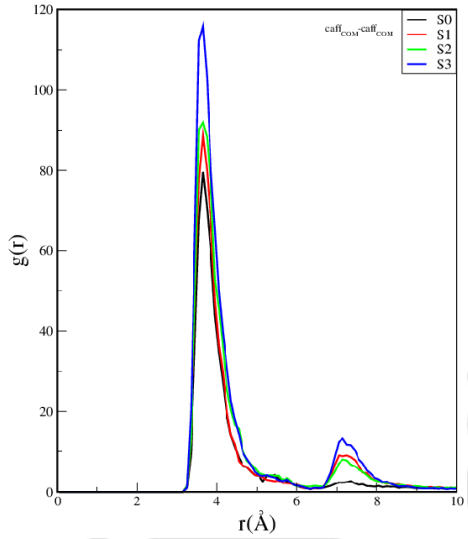

Figure 2-1. *Radial distribution functions of caffeine around caffeine as calculated from the center of mass of caffeine. Black, red, green and blue colors are for systems S0, S1, S2 and S3 respectively.*

In Fig. 2-2, we have shown the change in co-ordination number of caffeine around caffeine for first and second co-ordination shells of caffeine. In the same figure, we have also included the expected caffeine coordination numbers if the only change with added salt came through the number density of caffeine in different systems.

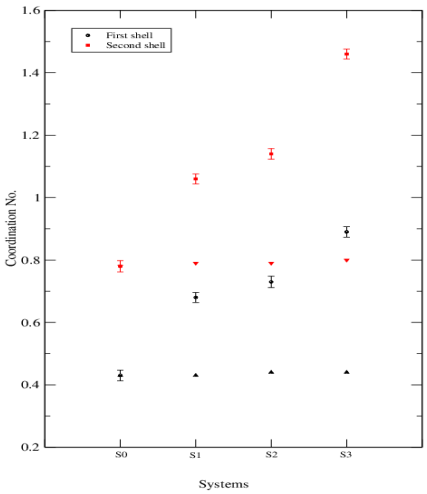

Figure 2-2. *change in co-ordination number of caffeine around caffeine for first and second coordination shell. Black and red colors are for upto first and second shell coordination number, respectively.*

It can be seen immediately that the number of caffeine molecules in the first and second coordination shells increases with increasing salt concentrations. These findings suggest a possible association of caffeine molecules with increasing salt concentration.

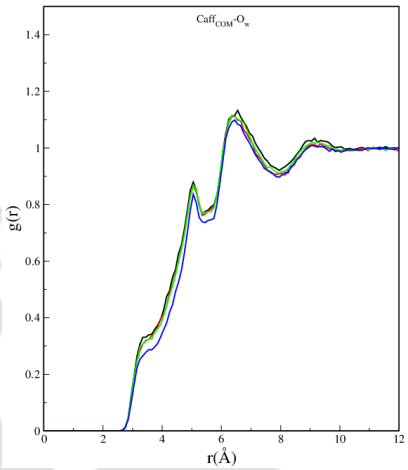

Figure 2-3. *Radial distribution functions of water around the center of mass of caffeine. Black, red, green and blue colors are for systems S0, S1, S2 and S3 respectively.*

Further, if the association of caffeine takes place it would be reflected in its hydration pattern. So, to understand the effect of NaCl concentration on caffeine hydration we have computed the average structure of water around caffeine through rdf of water oxygen atom around center of mass of caffeine (Fig. 2-3) in each system. The first peak height of this distribution function in all the four systems are below the bulk limit which can be attributed to the exclusion of water from the vicinity of caffeine. Further, the peak height decreases with increasing NaCl concentration indicating more exclusion of water molecules from caffeine with increasing salt concentration.

Caffeine molecule contains different types of functional groups and they have different hydration patterns. Although somewhat polar, caffeine molecule shows limited aqueous solubility and is relatively hydrophobic due to its weakly hydrating faces. It has been reported that both in pure water and in presence of Na^+ and Cl^- ions, a caffeine molecule makes hydrogen bonds with three water molecules [35]. The hydrophilic sites of caffeine are the two carbonyl oxygen atoms O11 and O13, as well as the ring atom N9 and they serve as hydrogen bond acceptors to water. Moreover, H8 proton may also interact with water molecules due to its higher than normal positive partial charges (see Table 2-2).

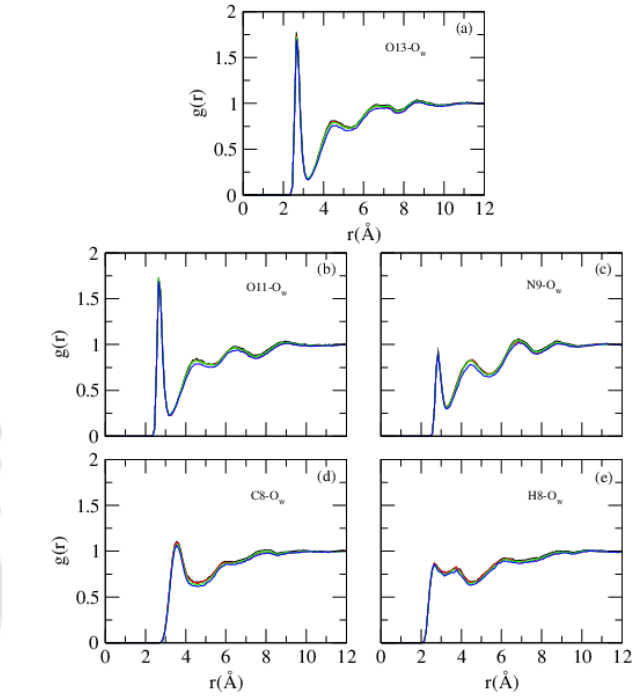

Figure 2-4. *Radial distribution functions of water oxygen atom around selective atomic sites of caffeine. (a) O13-O_w, (b) O11-O_w, (c) N9-O_w, (d) C8-O_w and (d) H8-O_w. Black, red, green and blue colors are for systems S0, S1, S2 and S3 respectively.*

In Fig. 2-4, we show the rdfs of water oxygen atom around each of these hydration sites in pure water as well as in different salt concentration. In the same figure the rdf involving water oxygen atom and nonpolar C8 carbon (to which H8 is attached to) is also shown.

Table 2-3. Hydration number around selected atomic sites of caffeine atoms

Atoms	S0	S1	S2	S3
O11	2.0635 ± 0.0165	2.0477 ± 0.0123	2.0226 ± 0.0162	1.9503 ± 0.0144
O13	1.9801 ± 0.0192	1.9314 ± 0.0136	1.9303 ± 0.0174	1.8436 ± 0.0143
N9	1.3522 ± 0.0245	1.3509 ± 0.0181	1.3312 ± 0.0211	1.2820 ± 0.0192
H8	2.5146 ± 0.0148	2.5031 ± 0.0137	2.4357 ± 0.0152	2.0518 ± 0.0131
C8	7.6482 ± 0.1473	7.5302 ± 0.1241	7.2384 ± 0.1384	7.0147 ± 0.1469
Na^+	-	5.3813 ± 0.1310	5.0132 ± 0.1194	4.8737 ± 0.1619
Cl^-	-	7.5204 ± 0.1628	7.4421 ± 0.1096	7.3820 ± 0.1450

The appearances of the first peak positions of these rdfs (for O11, O13 and N9 in particular) suggest the existence of hydrogen bonding interactions between caffeine and water. Further, the number of first shell water molecules (i.e., hydration number) around different atomic sites of caffeine calculated using Eq. (1) is shown in Table 2-3. The hydration number values indicate presence of two water molecules in the first hydration shell of each sites of O11 and O13 atoms. Though our calculated hydration number for these two atomic sites match well with the values reported earlier for caffeine in pure water, for N9 atom the hydration number reported here is slightly lower than that reported earlier [77]. The small deviation in this value might be due to the fact of different caffeine and water models considered in our study. As can be seen from the Table 2-3, the hydration number decreases for all atomic sites of caffeine including the hydrophilic carbonyl oxygens, but the effect is much more pronounced for C8 and H8 atoms. In this regard it is worth noting that we have observed that on addition of salt, a peak at around 4 Å in the C8-C8 distribution function (not shown) started developing, which was originally absent in system S0. Further, the FT-IR (Fourier transform-infrared spectroscopy) study of caffeine-water binary solution reported that, compared to monomeric caffeine unit where complete hydration of C=O groups of caffeine is possible, stacking of caffeine molecule causes the partial hydration of its C=O groups [88].

To understand the solvation of different hydrophobic groups of caffeine we have computed rdfs involving hydrophobic methyl carbons (C10, C12 and C14) and oxygen of water and the same are presented in Fig. 2-5. In Fig. 2-5, we have shown the variation in the hydration numbers for these methyl carbon atoms for different salt concentrations. As can be seen from methyl-water rdfs (Fig. 2-5) that they start from zero at 2.7 Å and reach the value of bulk density at 3.4 Å. Therefore, below 3.4 Å water molecules are actually excluded from the solvation shell of methyl groups. Further, the height of the peak decreases slightly with increasing salt concentration. The change in peak height in the distribution function is prominent in case of system S3. It depicts exclusion of some water molecules around methyl groups of caffeine at higher NaCl concentration. In consistent with the above observation, with increasing NaCl concentration, the number of first shell water molecules around different hydrophobic groups of caffeine decreases and this effect is more pronounced as one moves from system S2 to S3 (see Fig. 2-5).

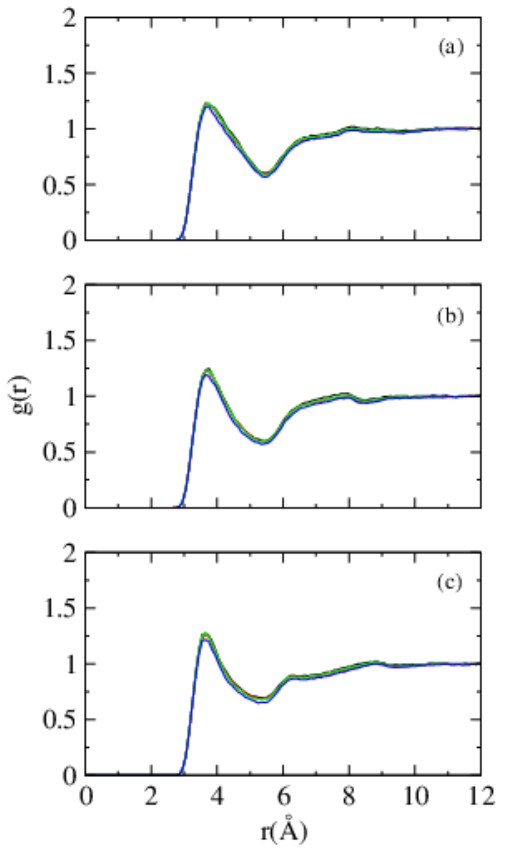

Figure 2-5. *Site-site radial distribution functions of C10, C12, and C14 methyl carbons with water oxygen. (a) C10-O_w, (b) C12-O_w, and (c) C14-O_w. Black, red, green and blue colors are for systems S0, S1, S2 and S3 respectively.*

The effect NaCl molecules on the local structure of water in caffeine solution can be studied by means of water-water distribution function and the same is shown in Fig. 2-6. The first and second peaks in this rdf characterize the hydrogen bonded first neighbor and the tetrahedrally located second neighbor, and they appear at about 2.75 Å and 4.5 Å respectively. We found that the peak height of $O_w - O_w$ correlation function is insensitive to ion concentrations considered here. However, a modest modification of the second shell is observed with increasing NaCl concentration. With increasing salt concentration the first valley becomes shallower and the second peak becomes less pronounced. These results are in accordance with the observed second shell breaking of water structure in aqueous salt solutions reported earlier [89].

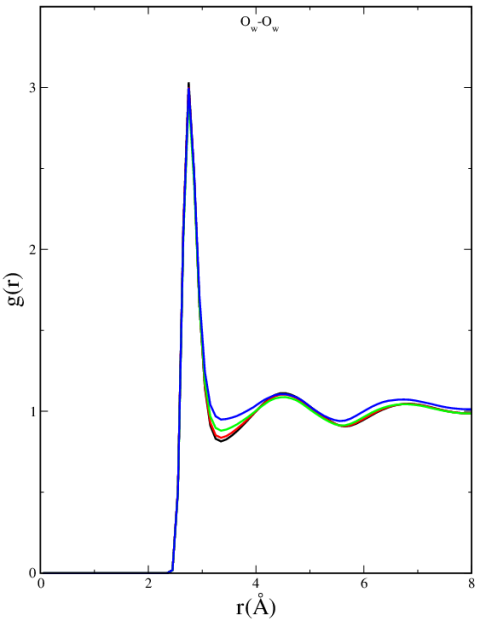

Figure 2-6. *Water oxygen-oxygen site-site radial distribution functions in all systems. Black, red, green and blue colors are for systems S0, S1, S2 and S3 respectively.*

The rdfs involving Na^+ and Cl^- ions for different salt concentrations are shown in Fig. 2-7. The appearance of a sharp peak at 2.8 Å suggests presence of contact ion pairs in all solutions. This correlation function also shows a pronounced second peak at 5.3 Å which corresponds to the presence of solvent separated ion pairs. With increasing salt concentration, we have observed decrease in the probability of contact ion pair formation as well as the probability of formation of solvent separated ion pair. However, the effect is much more prominent for the former. In this context we note that our observations are in contradiction with some previous simulation results of NaCl salt in water without caffeine [89], where it was found that the probability of contact ion pair formation increases. The differences in Na^+-Cl^- rdfs in our observations between pure salt water and the presence of caffeine in salt water directly point to some interactions of caffeine with ions in water (discussed below). In this regard we note that the results reported in Refs. 34 and 35 are in agreement qualitatively with each other despite of the fact of different models for water and salt used in those studies.

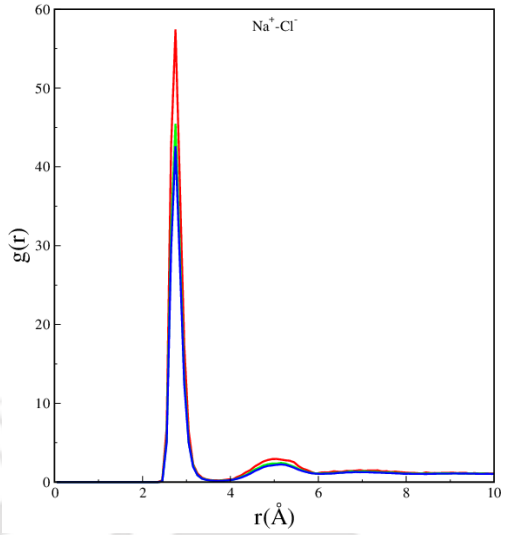

Figure 2-7. *Radial distribution functions between Na^+ and Cl^-. Red, green and blue colors are for systems S1, S2 and S3 respectively.*

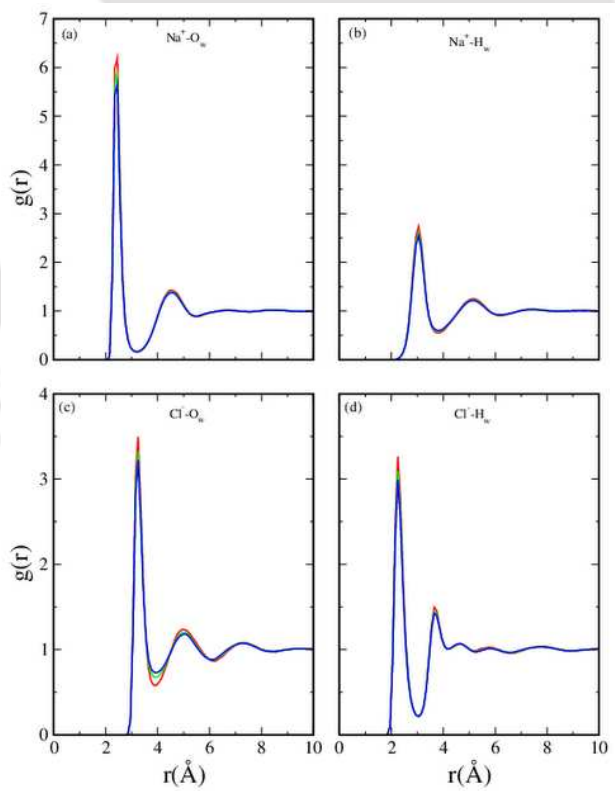

Figure 2-8. *Site-site radial distribution functions involving (a) Na^+-O_w, (b) Na^+-H_w, (c) Cl^--O_w and (d) Cl^--H_w respectively. Red, green and blue colors are for systems S1, S2 and S3 respectively.*

The ion-water pair correlation functions are presented in Fig. 2-8. These include Na^+-O_w, Na^+-H_w, Cl^--O_w and Cl^--H_w rdfs for three different concentrations of NaCl. The corresponding hydration number values are included in Table 2-3. With increasing ion concentration, since the probability of contact ion pair formation decreases (as observed in $Na^+ - Cl^-$ distribution function) one would expect increase of solvent separated ion pair formation and thereby a rise in the ion-water hydration number value.

However, contrary to this, we observe a decrease in peak height in ion-water rdfs and hydration number value with increasing ion concentration. The effect is more pronounced for Na^+-O_w rdf. This is due to the fact of strong interaction between Na^+ and O11 atomic sites of caffeine (discussed below). Further, the first peak of Na^+-H_w distribution function appears farther away than the first maximum in the Na^+-O_w distribution function. This suggests that the oxygen atoms of water molecules are pointing toward the Na^+ ion and the water hydrogen atoms are facing bulk water. The examination of the positions of first peak appearance of Cl^--O_w and Cl^--H_w indicates that the water hydrogen atoms point toward the chloride ion, whereas the oxygen atom of water molecule faces bulk water. Moreover, the calculated number of water molecules around a chloride ion decreases with increasing ion concentration. However, this decrease in the Cl^--O_w is less pronounced when compared with that of Na^+-O_w.

To investigate the interaction of caffeine molecules with ions, we have shown the rdfs between Na^+ ions around two electronegative carbonyl oxygens O11 and O13 and Cl^- ions around more electropositive hydrogen H8 of caffeine molecule (Fig. 2-9). The principal observation derived from the rdfs between Na^+ and carbonyl oxygens is that Na^+ ions exhibit an appreciable affinity for carbonyl oxygen O11 and as the concentration of salt increases, the interaction between Na^+ and O11 increases, as demonstrated by stronger peak height at higher concentration. This leads to decreasing contact ion pair formation in presence of caffeine with increasing salt concentration. The first peak height of rdf of Na^+ around O13 does not change much on increasing salt concentration, and it barely crosses unity suggesting weak interaction of Na^+ ions with O13. The rdfs involving Cl^- ions and H8 do not exhibit an appreciable amount of affinity of the former for the later in caffeine as can be seen from the first peak height which limits up to unity.

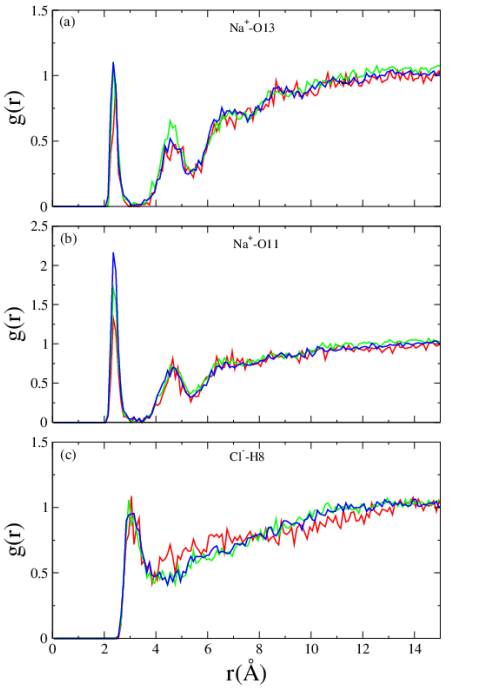

Figure 2-9. *Site-site radial distribution functions of Na^+ ion around O13 and O11, and Cl^- ion around H8 of caffeine. (a) Na^+-O13, (b) Na^+-O11 and (c) Cl^--H8 radial distribution functions. Red, green and blue colors are for systems S1, S2 and S3 respectively.*

Atomic density analysis:

The molecular orientation of liquid water around hydrophobic solutes is governed by the optimization of hydrogen bonding interactions. As already mentioned, the distribution of water molecules around caffeine is quite complex because of the complicated arrangement of hydrogen bonding functional groups in caffeine. We have carried out atomic density analysis using the Visual Molecular Dynamics (VMD) program. In Fig. 2-10 (a), we have shown the mass density map of water oxygen atom with a cell side of 0.5 Å within 3.4 Å around a caffeine monomer in the system S3. (Contour density is calculated for 5ns trajectory, when a caffeine molecule is remained as a monomer, and rest of the caffeines are taking part in aggregation. The monomer is kept fixed at the center of the simulation box with respect to the center of mass of the molecule.) In Fig. 2-10 (b), contour density is plotted in a single frame, when six caffeine molecules are stacking together. From the figure, we can clearly see that water density around caffeine is highly anisotropic and solvent

molecules prefer some positions of solutes more than the other, such as the two carbonyl oxygen atoms, the ring nitrogen atoms and the extended non-hydrogen bonding planar surfaces. There is a band of high solvent density wrapping around the two carbonyl oxygen atoms, as two water molecules are hydrogen bonded to these atoms. Another band of solvent density wraps around the ring nitrogen atoms and localizes over the hydrophobic faces.

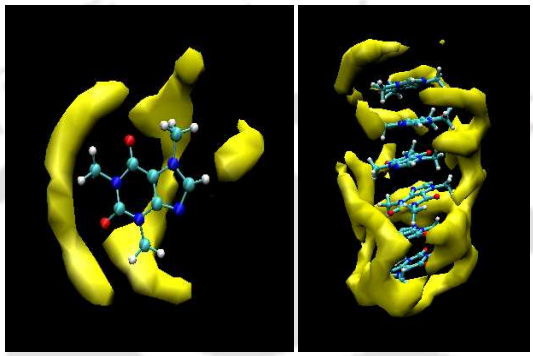

Figure 2-10. *Contours of solvent water density within 3.4 Å around caffeine monomer (a,left) and around caffeine molecules stacking together (b,right) during simulation.*

As discussed earlier, water molecules prefer to sacrifice one possible bonding interaction by pointing one hydrogen atom or lone pair directly at the non-hydrogen bonding surface, as the resulting loss of one hydrogen bond is energetically favorable than the loss of three hydrogen bonds that would result if it adopted an alternate orientation, such as, of waters adjacent to a methane molecule [69]. Therefore this kind of orientation is required to maximize the total interaction. In addition to this, the hydrophobic faces of caffeine are not a uniformly hydrophobic surface, but instead, has hydrogen bonding functional groups all around its periphery, and structuring of water molecules around these groups also contributes to the structuring requirements above and below the plane of the rings. A small clouds of water density is also observed around H8 hydrogen. Fig. 2-10 (b) represents the contours of solvent water density within 3.4 Å around six caffeine molecules stacking together. When the hydrophobic faces of caffeine molecules pair up by stacking one above another, the water molecules which were initially structured above and below the caffeine monomer surface, are now liberated and recover their lost hydrogen bonds. Experimental studies showed such pairing is enthalpically driven [90, 91]. From the figure it can be seen that water density is not symmetric around the stack, and water molecules prefer to occupy the the available hydrogen bonding sites around the periphery of caffeine molecules.

Clouds of water density hydrating the hydrophobic faces above and below the stack can also be seen, as water molecules present at these faces are free to interact with bulk water. The aggregation of caffeine molecules by such stacking results in decrease in surface area accessible to water molecules.

Cluster Structure Analysis:

To discuss caffeine self association in more details, we have carried out cluster structure analysis. We have defined clusters as an assembly of caffeine molecules where one caffeine molecule is within 6.4 Å of neighboring caffeine molecules in the cluster. Probability distribution of clusters of various sizes n, with respect to monomer, as calculated for all the systems are shown in Fig. 2-11.

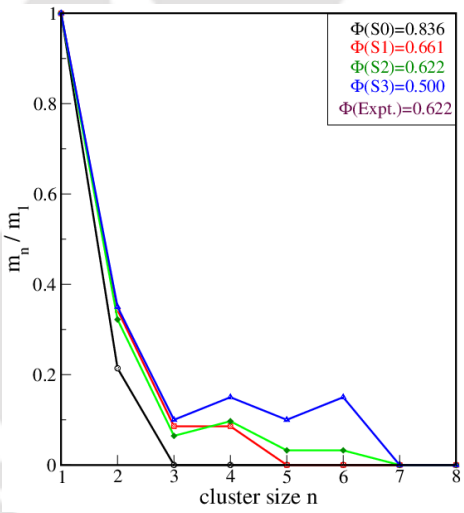

Figure 2-11. *Probability distribution of clusters of different sizes with respect to monomer, for all the systems. Black, red, green and blue colors are for systems S0, S1, S2 and S3 respectively.*

It is evident that, as the concentration of NaCl increases, more and more higher order clusters of caffeine are formed, and their probability with respect to monomer increases. Further, contrary to previously reported simulation results of caffeine-TIP4Pwater system [77], our cluster structure distribution for system S0 exhibits that, relative to monomer and dimer formation, the formation of higher order caffeine cluster is negligibly small. This discrepancy may be due to use of lower caffeine concentrations in our study (slightly below its solubility limit) as well as different caffeine and water models used in our study. From this distribution, we further estimated the osmotic coefficient (ϕ) values for different

systems and the same are also shown in Fig. 2-11. For system S0, the calculated value of ϕ is 0.84 as compared to the experimental value of 0.62 (measured at 302.8 K and 0.1116 M caffeine concentration) [90]. Addition of salt causes formation of more and more higher order clusters and as a result, the ϕ value decreases.

Solvent accessible surface area:

The solvent accessible area (SASA) describes the area over which contact between solute and solvent can occur. The SASA of caffeine molecules in the simulations have been computed using the VMD program, which is based on the algorithm of Shrake-Rupley [92] which creates many points on the surface of each (heavy) atom and determines whether each point is occluded or exposed to solvent. The probe radius of 1.4 Å have been used, which corresponds to the size of a water molecule.

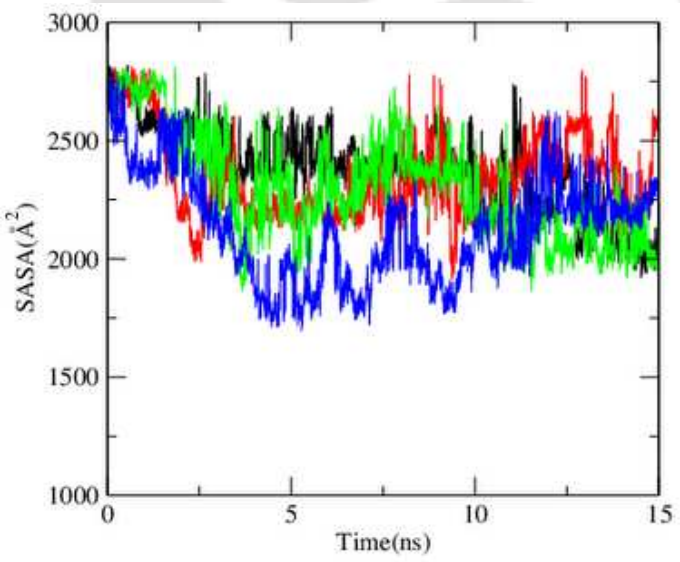

Figure 2-12. *Distribution of solvent accessible surface area(SASA) of caffeine in water as a function of simulation time. Black, red, green and blue colors are for systems S0, S1, S2 and S3 respectively.*

The distribution of SASA of caffeine molecules as a function of simulation time in all the systems is shown in Fig. 2-12. We observe that there is certain association among caffeine molecules as the simulation proceeds and association of caffeine occurs in higher extent for system S3. The average value of surface area accessible to solvent is summarized in Table 2-4, and we can see that the average SASA value decreases as NaCl concentration increases providing clear evidence of aggregation of caffeine on increasing salt concentration.

Table 2-4. Solvent accessible surface area per caffeine for different systems

System	SASA(Å^2)
S0	297.480 ± 3.021
S1	292.735 ± 5.853
S2	286.587 ± 5.942
S3	264.930 ± 6.056

The formation of caffeine aggregation in NaCl solution is further supported by the snapshots of different systems taken at 5 ns interval (discussed below).

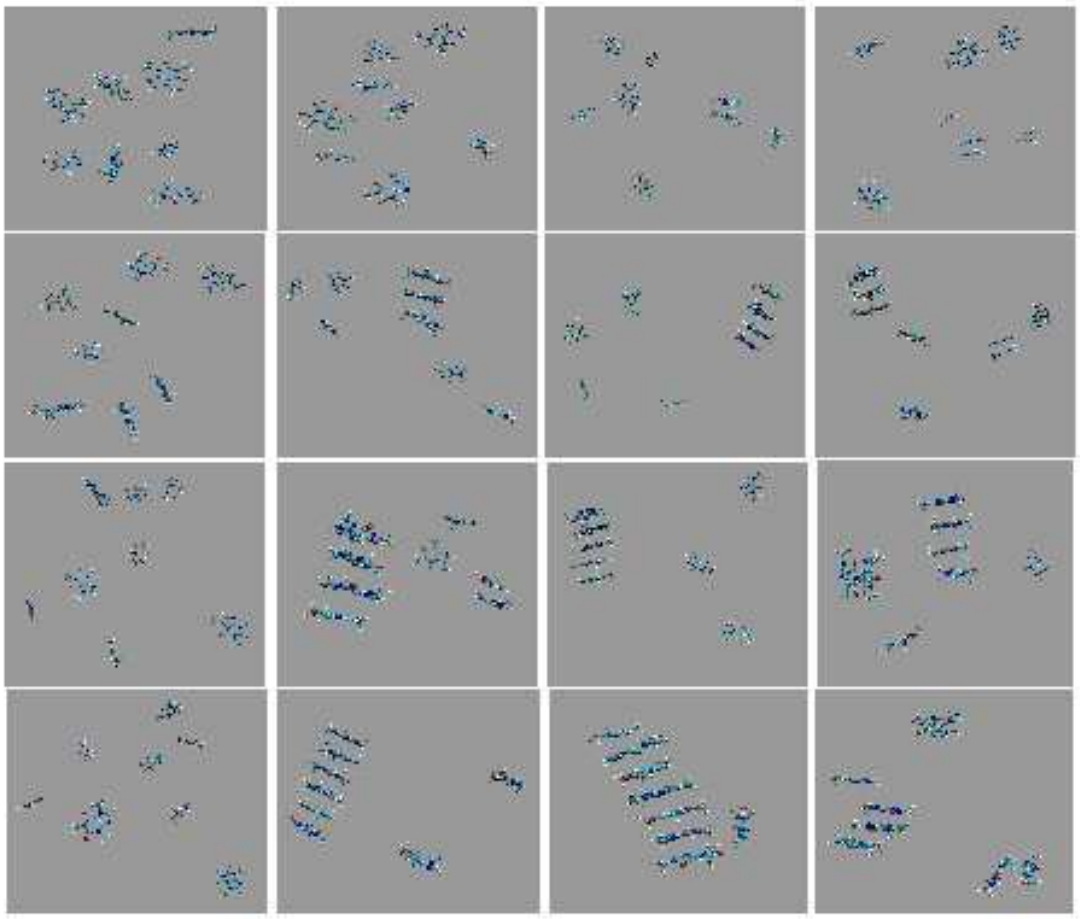

Figure 2-13.*Snapshots of MD simulations of systems S0, S1, S2, S3 (from top to bottom). From left to right for 0 ns, 5 ns, 10 ns and 15 ns respectively.*

From the visual observation of snapshots (see Fig. 2-13), it can be seen that the formation of larger aggregates occurs within a shorter time period in system S3, where

concentration of NaCl is the highest among all the systems.

Preferential interaction of caffeine:

From the visualization of different systems from initial to the final step in VMD, it is noticed that in system S0, where no salt was added, caffeine molecules were seen to be preferred to remain as monomer for most of the time of simulation. It took considerable amount of time for a dimer to form, which was not stable and broke into two monomeric units immediately after its formation. As the simulation proceeds, the formation and breaking of dimers continued in some interval, and at the end of simulation the system contains one dimer and six monomers. On addition of salt, a significant difference has been observed compared to system S0. We have observed a considerable aggregation (stacking) of caffeine molecules in those systems. Initially, dimer is formed, which after stabilization, gives rise to trimer and then tetramer is formed by capturing another monomeric unit. The progression of stacking continued in this fashion with many breaking events of larger aggregates to smaller one and again reformation of larger aggregates as the simulation proceeds. Finally, the stacks were stabilized and lasted uninterruptedly for nearly 1 ns. The snapshots of of different systems in 5 ns intervals are shown (Fig. 2-13).

The Kirkwood-Buff theory [93-98] provides a statistical thermodynamic framework for evaluating the preferential interaction parameter, τ, from molecular distribution function for a solute (c for caffeine), in a solvent mixture of water (w) and cosolutes (s) via

$$\tau_{sw}^{c} = \rho_s(G_{cs} - G_{cw}) \tag{2.2}$$

where G_{cs} and G_{cw} are Kirkwood-Buff G-factors, and ρ_s is the number density of cosolvent.

Preferential interaction parameter of caffeine with itself over water, τ_{cw}^{c}, can be calculated by considering a caffeine molecule as the solute, and it can be expressed as:

$$\tau_{cw}^{c} = \rho_c(G_{cc} - G_{cw}) \tag{2.3}$$

where the Kirkwood-Buff integrals G_{cc} and G_{cw}, can be obtained from the distribution function of caffeine around caffeine (g_{cc}(r)) and that of water around caffeine (g_{cw}(r)) respectively and ρ_c is the number density (N/V) of caffeine in the system [68].

For a grand canonical ensemble, G_{ij} (for species i and j) is defined as

$$G_{ij} = 4\pi \int_0^\infty [g_{ij}(r) - 1] r^2 dr \tag{2.4}$$

For a closed system, the above equation can be written as

$$G_{ij} \approx 4\pi \int_0^R [g_{ij}(r) - 1] r^2 dr \tag{2.5}$$

where R is the distance at which the integral approaches zero. A positive value of the preferential interaction parameter, τ_{cw}^c, indicates more preference of caffeine to itself over water.

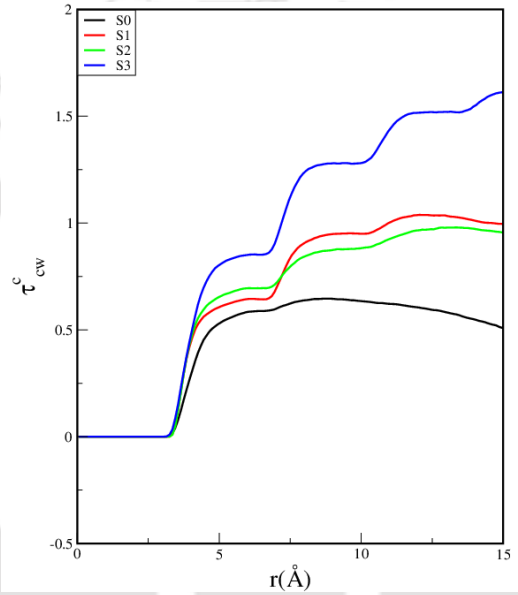

Figure 2-14. *Preferential interaction parameter of caffeine for a caffeine molecule over a water molecule (τ_{cw}^c). Black, red, green and blue colors are for systems S0, S1, S2 and S3 respectively.*

In Fig. 2-14, we have shown the change in the τ_{cw}^c value as function of distance for different concentration of salt solution. For system S0, the value of τ_{cw}^c is close to zero, which indicates that caffeine does not show much greater preference to another caffeine molecule over water molecule. This is obviously expected as the concentration of caffeine is almost at the solubility limit. Note that another computer simulation study of caffeine-water system without salt has also reported positive value of τ_{cw}^c. However, when salt is added in water, a relatively larger positive τ_{cw}^c values are obtained compared to S0, and S3 shows the largest value for the preferential parameter, indicating a greater preference of caffeine to other caffeine molecules over water molecules. Note that experimental findings also reveal high positive value of G_{cc} and negative value of G_{cw} for binary caffeine-water system [83]. These findings suggest strong caffeine-caffeine interactions and less hydration of caffeine molecules. Furthermore, our calculated potential of mean force (PMF) profiles of

caffeine (not shown), estimated from caffeine-caffeine center of mass distribution functions, for different salt concentrations show a positive gradient that does not approach to zero at large-r distances and acts as a corroborative evidence of caffeine association.

Hydrogen bond interaction:

In aqueous solution, caffeine molecules can form hydrogen bonds with water. It was already mentioned that caffeine molecule has three hydrogen bonding sites, and these are two carbonyl oxygen O11 and O13 and ring nitrogen atom N9. These atoms can only act as hydrogen acceptors. However, the H8 proton may also interact with water resembling to hydrogen bonding due to its high partial charge, but the first peak of $H8-O_w$ distribution function shows much broader peak than that of a true hydrogen bond donor proton [77].

Table 2-5. Average number of water-water (per water) and water-caffeine (per caffeine) hydrogen bonds in different systems

System	HB_{w-w}	HB_{O11-w}	H_{O13-w}	H_{N9-w}
S0	3.2875 ± 0.0022	1.6183 ± 0.0017	1.6423 ± 0.0011	1.0024 ± 0.0013
S1	3.2367 ± 0.0016	1.5746 ± 0.0013	1.5502 ± 0.0009	0.9932 ± 0.0017
S2	3.1733 ± 0.0023	1.5081 ± 0.0015	1.4936 ± 0.0010	0.9328 ± 0.0016
S3	3.1349 ± 0.0019	1.5732 ± 0.0012	1.5439 ± 0.0011	0.9643 ± 0.0009

w represents water and *O11, O13* and *N9* correspond to the different atomic sites of caffeine.

Therefore, we have carried out an analysis of the number of hydrogen bonds between water and above mentioned three hydrogen acceptor sites of caffeine molecules, and also the number of water-water hydrogen bonds per water molecule, and the results are listed in Table 2-5. Hydrogen bonds are calculated based on the location of the first minimum in the corresponding rdf as the cutoff distance between donor(D) and acceptor(A), and the angle of H-D-A are considered as 45^o. We found that all the systems are dominated by water-water hydrogen bonds and they change only slightly with increasing salt concentrations. We, further, observed that the average number of water-caffeine (per caffeine) hydrogen bond decreases only modestly on addition of salt. For example, the total number of hydrogen bonds formed by a caffeine molecule with water is 4.25 for system S0 and the same for system S3 is 4.07. Further insight into caffeine-water hydrogen bonds reveals that the decrease in its value is dominated by the change in hydrogen bonds involving

caffeine O13-water hydrogen atom. The lowering of C=O stretching frequency of caffeine in caffeine-water system (without salt) due to formation of stacking has also been reported experimentally [88]. In this context, we note that the formation of hydrogen bonds between caffeine and water depends on the availability of hydrophilic groups of caffeine for water molecules. The stacking between caffeine molecules may decrease the accessibility of hydrophilic groups for water molecules. Not only that, the structural arrangement of stacks may also affect the number of hydrogen bonding between caffeine and water. If polar and non-polar atomic groups of caffeine overlap in the stack, the possibility of formation of hydrogen bonds with water decreases. On the other hand if polar groups are available for hydrogen bonding with water, the number of caffeine-water hydrogen bonds should not change much.

■ SUMMARY AND CONCLUSIONS

In this chapter, we have investigated caffeine aggregation in presence of NaCl salt. We considered four different salt concentrations. From caffeine-caffeine center of mass distribution function we find that on addition of salt, the first peak height increases and a second peak at 8.5 Å started to develop. Since, in aqueous solution molecular association or dissolution of solute molecules is reflected in its hydration pattern, we, further, probed the solvation of caffeine molecules by means of caffeine center of mass-water distribution function. We observe that on addition of NaCl more and more water molecules are excluded from caffeine surface. The distribution functions followed by first shell coordination number values involving different atomic sites of caffeine and water center of mass further show that with increasing salt concentration, for the hydrophobic atomic sites of caffeine more and more dehydration takes place and the effect is more pronounced for higher NaCl concentration. Whereas, the hydrophilic atomic sites show only a slight change in the hydration number value.

We have also investigated the structural properties involving different solution species with variation of ion concentration as these are intimately related to the solvation pattern of caffeine. On contrary to aqueous NaCl solution without caffeine [89], we found that probability of contact ion pairs as well as solvent separated ion pairs decreases with increasing ion concentration. We trace this discrepancy is due to strong interactions between caffeine and salt. Furthermore, with increasing salt concentration a modest modification in the second solvation shell is also found in the oxygenoxygen radial distribution function

of water molecules.

To examine the solvation of caffeine more closely we have also calculated preferential interaction parameter. It is observed that with increasing salt concentration, a caffeine molecule prefers to interact with another caffeine over water molecules. This fact act as a corroborative evidence of what we observed in the caffeine-caffeine distribution function. Our SASA calculations also show association of caffeine molecules at higher NaCl concentration. The stacking arrangements among caffeine molecules can be observed from the structure visualization taken at 5 ns intervals. In this context we note that, NMR studies suggest that the self-association of caffeine in solution occurs through stacking with many possible orientations of stacks [99]. Finally, in consistent with observed distribution functions involving hydrophilic atomic sites of caffeine and water molecules, our hydrogen bond properties calculations also revealed a slight decrease in the caffeine-water average number of hydrogen bonds on addition of salt.

In the context, the present study shows the self-associtionn tendency of caffeine and the effects of NaCl salt on caffeine aggregation. The thermodynamics of self-association will be treated in **Chapter 3**.

भारतीय प्रौद्योगिकी संस्थान गुवाहाटी
Indian Institute of Technology Guwahati

Chapter 3

Caffeine Association : Enthalpy Entropy Crossover

"Hydrophobic interactions between small apolar groups at low concentrations in water are very different from those between large assemblies or relatively high concentrations of hydrophobic groups in water. The former is pertinent when considering, say, the aqueous solvation of a butane or butanol molecule. The latter is relevant to the solvation of macromolecules such as proteins."

– K. Lum, D. Chandler, J. D. Weeks *J. Phys. Chem. B* **103**, 4570 (1999)

Overview:

The previous chapter of this thesis dealt with the self-association of caffeine in pure water and salt solution (**Chapter 2**). In this chapter we have explored the thermodynamics of self association. To examine the molecular level understanding of temperature induced self association of caffeine molecules in aqueous solution both in presence and absence of salt NaCl, we have performed long MD simulations at regime of temperatures ranging from 275 K to 350 K with a temperature difference of 25 K. The calculations of different site-site radial distribution functions followed by coordination number analyses, the calculations of preferential interaction parameters, solvent accessible surface area and cluster structure analyses show a depletion in the caffeine association propensity with increasing temperature. We have also observed the salting out effect of caffeine molecules in salt solution. Simultaneous presence of polar and nonpolar groups in caffeine molecule leads to anisotropic hydration. In specific, the hydration tendency of caffeine hydrophobic sites increases with increasing temperature, while hydrophilic sites tend to be less hydrated. This leads to decrease in caffeine association. In accordance with some experimental studies on thermodynamics of caffeine association, we have also observed enthalpy driven association in pure water. But presence of salt leads to entropy driven association specifically at higher temperature. This is due to the fact of relatively stronger interactions of salt ions with caffeine at higher temperature.

■ INTRODUCTION

Water, the common environment for most biological processes, plays a significant role in binding thermodynamics. Water structure in the vicinity of a hydrophobic solute influences the thermodynamics of hydrophobic hydration as well as water-mediated interactions between them [69]. When a solute molecule is present in aqueous environment, its functional groups interact with the surrounding water. These solutes may self aggregate in aqueous medium depending upon the interaction of them with water. Water packs well near small hydrophobic solutes, and dewets gradually as the solute size is increased due to loss of attractive water-water interactions between water molecules near hydrophobic solutes. For small hydrophobic solutes, an adjacent water molecule can straddle the solute to make hydrogen bonds to other water molecules, with neither of its protons or lone pairs directly pointing at the solute, and therefore, there is no loss of any hydrogen bonds [72]. But due to the restriction of rotational freedom of water molecules adjacent to the solutes, the aggregation of such small hydrophobic solutes is entropy driven. As a consequence, with increasing temperature the aggregation of small hydrophobic solutes are found to be enhanced [100]. In contrast, there is a significant difference in the hydration of large hydrophobic solutes. Hydration of large hydrophobic solutes leads to breaking of some hydrogen bonds between water molecules, as it becomes impossible for water molecules to straddle the surface and still maintaining the hydrogen bonds to other water molecules [69, 73]. Therefore, when such larger hydrophobic solutes aggregate in aqueous solution, the structured water molecules around the hydrophobic solutes are liberated, which results in regaining of lost hydrogen bonds, and, therefore, aggregation is enthalpy driven. As predicted by Chandler, for hydrophobic solutes in the bulk water at standard conditions, the cross-over from one regime to the other occurs at solute size of 1 nm [74].

In the context of caffeine association in aqueous solution it is to be noted that the simultaneous presence of hydrophobic methyl (-CH3) groups and extended flat hydrophobic faces, as well as three hydrophilic proton acceptor groups makes it significant for our study. In the previous chapter (**Chapter 2**) we have observed that the water distribution around caffeine molecule is highly anisotropic and solvent molecules prefer some positions of solutes more than the other. We observed an enhancement in association of caffeine molecules in presence of NaCl salt, and tendency of association was more at higher salt concentration. Although, the size of caffeine molecule is considerably shorter than the

1 nm limit, some experimental and theoretical studies show that the self-association of caffeine is enthalpy driven [36, 67]. On the other hand, another study suggests entropy driven association of caffeine molecules [68]. However, since both entropy and enthalpy are strongly temperature-dependent therefore, the thermodynamic stability of caffeine-caffeine interaction is expected to be affected largely by temperature. Thus, a complete understanding of caffeine self-association requires a knowledge of temperature dependence propensity of caffeine association. However, a very few experimental or theoretical studies have been carried out to investigate the effect of temperature change on caffeine aggregation. Although Origlia-Luster et al. [67] and Sanjeewa et al. [68] have temperature induced caffeine aggregation in binary caffeine-water system, their studies were limited to just for some thermodynamic calculations. However, no experimental or theoretical study has been carried out on simultaneous effect of temperature and salt on caffeine aggregation. Further, salt ions are important components in the aqueous environment in biological systems, and the hydrophobic interaction is greatly influenced by the presence of salts. A great deal of research have been devoted to explore the interaction between hydrophobic solutes and their hydration in different aqueous media [101, 102]. It was observed that, as the solute-water attractions are turned on, the solvation thermodynamics also change. Therefore, the solvation behavior of the solute critically depends on the strength of the solute-solvent attraction. Therefore, a detailed knowledge of the effects of salt and temperature on hydrophobic interactions is of fundamental interest for the understanding of aggregation phenomena in biological systems.

In this chapter, we have investigated the self-association behavior of caffeine at different temperature, in pure water and in NaCl salt solution. Our goals are: (i) To quantify the simultaneous effects of NaCl salt ions and temperature on the thermodynamics of caffeine association. (ii) To study the effect of temperature on the hydration of hydrophobic and hydrophilic sites of caffeine. (iii) To examine any change in the formation of hydrogen bonds between hydrophilic sites of caffeine and water at different temperature. This is important because it affects the self association affinity of caffeine molecules. (iv) The molecular level understanding of interactions between caffeine, water and ions in solution and their effects on water structure, and (v) to explore the structural arrangements of caffeine molecule in its aggregated form.

What follows in this part are brief description of the models and simulation method, discussion of the results obtained, and finally, our concluding remarks and brief summary.

■ MODELS AND SIMULATION METHOD

We have carried out classical molecular dynamics (MD) simulations of caffeine molecules both in pure water and in aqueous NaCl solutions at four different temperatures (275 K, 300 K, 325 K and 350 K). The basic work is done with the AMBER generated force field for caffeine molecule as discussed in **Chapter 2** [53]. For NaCl, we employ force field parameters developed by Joung and Cheatham [84]. We have used the popular extended simple point-charge (SPC/E) [85] model for water. The initial configurations of our systems were prepared using packmol program [86]. MD simulations were performed with 15 caffeine molecules (and 100 $NaCl$ molecules in case of salt solutions) immersed in 4200 water molecules. The concentration of caffeine is taken above its solubility limit in pure water (0.1M) [78]. For systems containing $NaCl$, the salt concentrations are approximately 1.2 M. It is worth noting that for different systems, the total number of water molecules was kept fixed at 4200 in all cases and Na^+ and Cl^- ions were added without replacing the water molecules.

MD simulations were carried out using AMBER12 molecular dynamics package [61] in isothermal isobaric (NPT) ensemble at four different temperatures, 275, 300, 325 and 350 K and 1 atm pressure with a time step of 2 fs. The simulation protocols were identical to those described in **Chapter 2**. In order to obtain a reasonable initial structure, for each system, the initial configurations were first energy minimized for 5000 steps with 2500 steps of steepest descent minimization, followed by 2500 steps of conjugate gradient minimization. Each system was then heated slowly from 0 to the desired temperature over 40 ps in the canonical (NVT) ensemble. After 30 ns equilibration, the simulations were carried out for another 75 ns production run in NPT ensemble. We have used the final 50 ns of simulation for the analysis of our results.

Since, the results obtained from MD simulations may vary with the change in force field parameters used for different molecules thus it is important to examine if the results obtained in our study contain a general accepted view of caffeine aggregation. To this we have carried out another set of separate MD simulations in similar environments where we use the force field parameters of alkali halide ions Na^+ and Cl^- developed by Smith and coworkers [103]. Nevertheless, it is found that the change in force field parameters of Na^+ and Cl^- ions have very nominal impact on the results of our simulations (see below). Since the two different force field parameters of salt $NaCl$ yield very similar results for our caffeine model [53], it would be interesting to investigate the role of caffeine force field

parameters on its aggregation propensity in aqueous salt solutions. For this, by employing the caffeine force filed parameters of R. Sanjeewa and S. Weerasinghe [33], we have carried out another set of simulations using GROMACS (version 4.6.5) software package [104, 105]. As discussed above, since the force filed parameters of both the models of alkali halides $NaCl$ produce very similar results, we use the Smith model of $NaCl$ [103]. We follow the simulation procedure as described in Reference 11. The different systems we considered for this are briefly summarized in Table 3-1 .

Table 3-1. Overview of Simulations[a]

Sample No.	N_{caff}	N_{wat}	N_{salt}	T(K)	C_{caff} (M)	Box Length (Å)	ρ (g cm^{-3})
S0	15	4200	0	275 K	0.195	50.37	1.03
S1	15	4200	0	300 K	0.193	50.57	1.01
S2	15	4200	0	325 K	0.189	50.81	0.99
S3	15	4200	0	350 K	0.186	51.12	0.98
M0	15	4200	100	275 K	0.188	50.86	1.07
M1	15	4200	100	300 K	0.184	51.01	1.06
M2	15	4200	100	325 K	0.181	51.27	1.05
M3	15	4200	100	350 K	0.169	51.59	1.03
P0	15	4208	0	275 K	0.194	50.45	1.02
P1	15	4208	0	300 K	0.192	50.63	1.01
P2	15	4208	0	325 K	0.188	50.91	0.99
P3	15	4208	0	350 K	0.186	51.20	0.98
Q0	15	4208	100	275 K	0.189	50.83	1.07
Q1	15	4208	100	300 K	0.187	51.04	1.06
Q2	15	4208	100	325 K	0.184	51.33	1.04
Q3	15	4208	100	350 K	0.181	51.67	1.03

N_{caff}, N_{wat} and N_{salt}, respectively, represent the number of caffeine, the number of water and the number of NaCl in different systems. C_{caff} is the caffeine concentration in different systems. For system S0-S3 and M0-M3, we use the basic caffeine model [53] and Joung and Cheatham NaCl model [84]. For system P0-P3 and Q0-Q3, we use the Weerasinghe model for caffeine [33], and Smith model for $NaCl$ [103]

■ RESULTS AND DISCUSSION

Self-association of caffeine:

For molecular level understanding of the effect of temperature and NaCl salt on caffeine self-association, we have calculated the radial distribution function (rdf), g(r), involving center of mass of caffeine. Fig. 3-1 (a) and (b) represent the caffeine-caffeine rdf in pure water and in salt solution, respectively, at different temperatures. The first peak of g(r) appears at around 3.7 Å and a second peak also develops at 7.2 Å. It is interesting to note that, the first peak of g(r) becomes lower and sharper with increasing temperature from 275 K to 350 K, suggesting that the tendency for aggregation of caffeine molecules decreases as temperature is increased. This is in contrast to the effect of temperature on small hydrophobic molecules like methane, where increase in temperature results in increase in self-association of the solute [100].

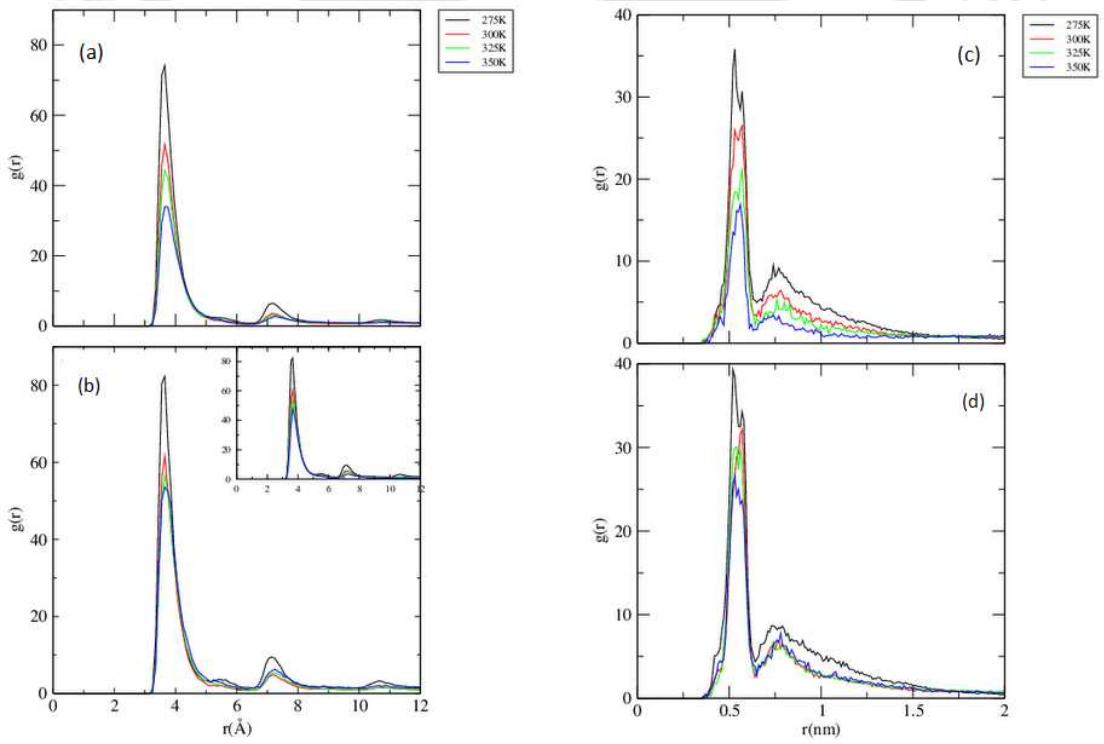

Figure 3-1. *Radial distribution functions of caffeine around caffeine as calculated from the center of mass of caffeine in (a,c) pure water, and (b,d) salt solution for Joung and Cheatham model of NaCl [84]. (a,b) shows rdf for basic caffeine model [53], and (c,d) for Weerasinghe model [33] of caffeine. Inset of (b) shows rdf for Smith model of NaCl [103]*

In order to investigate the effect of change of force field parameters of $NaCl$ on this rdf, in the inset of Fig. 3-1 (b) we show how this rdf evolves as temperature is changed for Smith model of $NaCl$. As can be seen that as temperature changes the rdfs behave in very similar fashion suggesting the aggregation propensity of our model caffeine is unaware of change in salt model considered in this study. Further, the analysis of the results for another set of simulations of caffeine with different force-field run in GROMACS software (i.e. Weerasinghe model [33]), we observed that at a particular temperature though the peak height of caffeine-caffeine rdf is much lower compared to the model used in our study (see Fig. 3-1 (c,d)), but the results show similar trends in rdf at different temperatures.

Further, from this pair correlation function, we have estimated the number of first shell caffeine molecules around a reference caffeine molecule. This coordination number can be calculated from the location of the first minimum in the corresponding rdf by the equation:

$$n_{\alpha\beta} = 4\pi\rho_\beta \int_0^{r_c} r^2 g_{\alpha\beta}(r) dr \tag{3.1}$$

where $n_{\alpha\beta}$ represents the number of atoms of type β surrounding atom α in a shell extending from 0 to r_c (the distance of the first minimum in the distribution function $g_{\alpha\beta}(r)$), and ρ_β is the number density of β in the system. The estimation of number of first shell caffeine molecules around a caffeine also supports the decrease in tendency of aggregation of caffeine at higher temperature (see Fig 3-2).

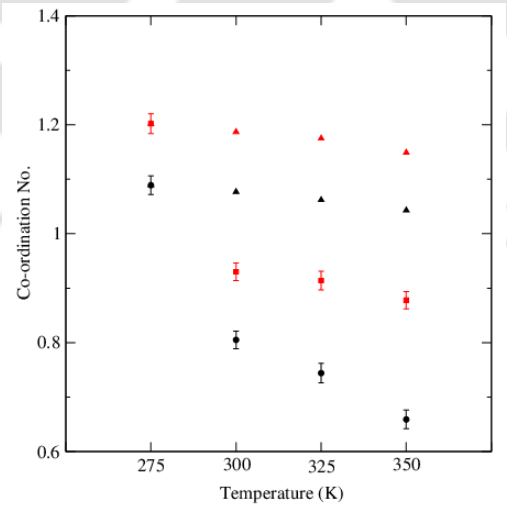

Figure 3-2. *Change in first shell co-ordination number of caffeine around caffeine with expected value. Black and red colors are for pure water and salt water, respectively. Triangles represent the caffeine coordination numbers if the only change with added salt came through the number density of caffeine.*

In salt solution, the peak height of g(r) is significantly higher and broader at all temperatures compared to pure water, indicating higher tendency of aggregation of caffeine molecules in presence of salt (Fig. 3-1 (b)). It was expected on the basis of our study discussed in **Chapter 1** [53], which reveals salting out effect of caffeine molecules on addition of NaCl salt and higher the concentration of salt, higher is the association of caffeine molecules. We have also noticed a higher first peak height in salt solution compared to that of pure water system as temperature increases from 275 K to 350 K. These findings are further supported by the spatial distribution plot of caffeine around caffeine, with an isovalue of 2.0 as shown in Fig. 3-3. The effects of temperature and salt can be clearly visible from the contour density plot, which shows the highest aggregation of caffeine molecules at 275 K temperature. Here we note that salt-induced enhancement in the caffeine-caffeine g(r) values fall within 15 for all temperatures considered here. As a result the potentials of mean force (PMFs) of caffeine-caffeine association may vary between 0.1-0.25k_BT suggesting that caffeine salting-out effect is of second-order.

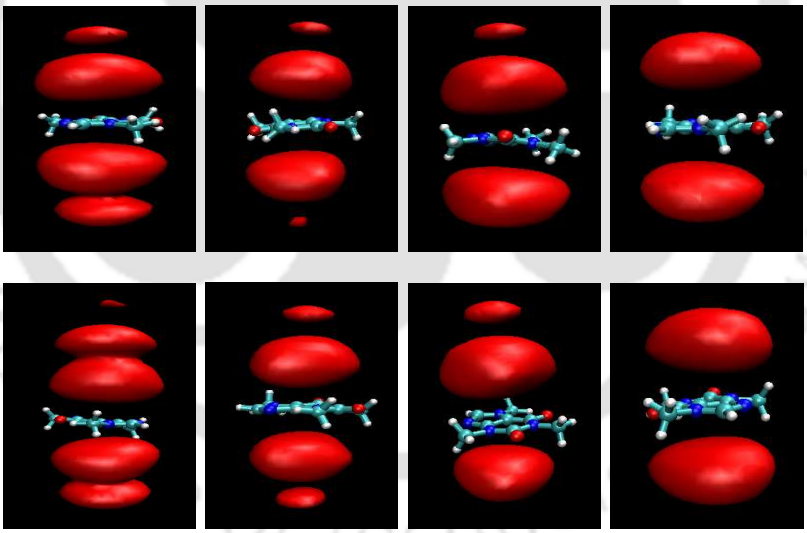

Figure 3-3.*Spatial distribution plot for caffeine around caffeine, with an isovalue of 2.0 for systems S0 to M3 from top left to bottom right.*

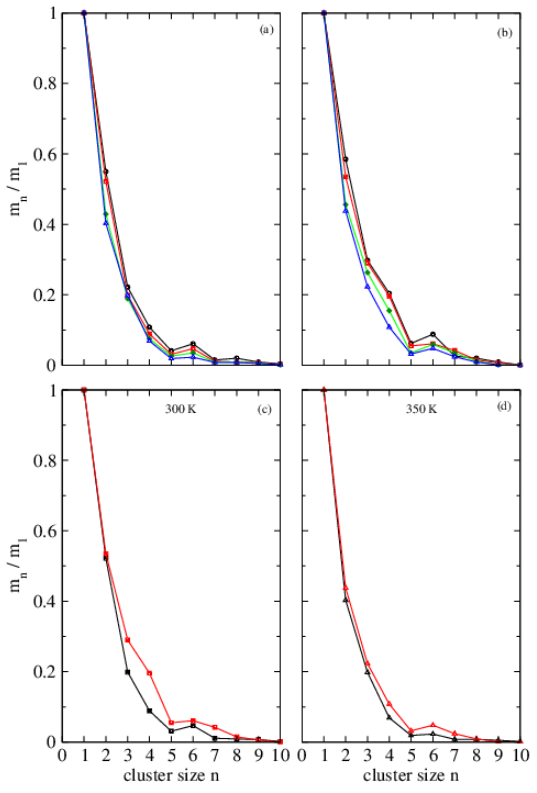

Figure 3-4. *Probability distribution of clusters of different sizes (m_n) with respect to monomer (m_1) in (a) pure water and (b) in salt solution. (c) and (d) are at a single temperature.*

Caffeine molecules are known to aggregate in aqueous solution by forming 'vertical-stacking' clusters. These stackings of caffeine molecules have also been demonstrated by various experimental techniques, like, vapor pressure osmometry, sedimentation equilibria, NMR, and other spectroscopic methods [43, 57, 58]. We have estimated the caffeine cluster sizes in different systems by considering clusters as an assembly of caffeine molecules where one caffeine molecule is within 6.4 Å distance of a neighboring caffeine molecule in the cluster. For different systems, the probability distributions of caffeine clusters of various sizes n, with respect to the caffeine monomer are calculated. Fig. 3-4 (a) and (b) display cluster size distribution with respect to monomer at different temperatures in pure water and salt water system respectively and the same for single temperature is shown in Fig. 3-5 (c) and (d). The formation of higher order caffeine clusters on all systems is quite evident and their probability of formation is the highest at 275 K temperature. The probability of cluster size greater than 10 is negligible, and is therefore, omitted.

Solvent Accessible Surface Area:

The solvent accessible surface area (SASA) denotes the surface area of a solute over which contact between solute and solvent can occur. Therefore, we have calculated SASA by taking the probe radius of 1.4 Å (which corresponds to the typical size of a water molecule) by using Visual Molecular Dynamics (VMD) program [106]. The SASA for different systems have been estimated and these values are summarized in Table 3-2.

Table 3-2. Solvent accessible surface area per caffeine molecule for different systems

System	SASA (Å^2)	System	SASA (Å^2)
S0	264.09	M0	251.15
S1	275.26	M1	260.03
S2	279.63	M2	265.67
S3	290.12	M3	268.71

At a particular temperature, the average value of surface area accessible to solvent decreases in salt solution, when compared to pure water. This gives an evidence of higher tendency of aggregation of caffeine molecules in salt solution. As temperature increases from 275 K to 350 K, the SASA value per caffeine molecule is found to increase from 264.09 to 290.12 in pure water, and from 251.15 to 268.71 in salt water, which shows that there is a decrease in tendency of aggregation on increasing temperature. These findings act as corroborative evidence of what we have seen in the caffeine-caffeine rdf and caffeine cluster structure analysis discussed above.

Preferential Interaction:

From the above discussions, it is quite evident that association propensity of caffeine with the like molecules increases in presence of salt and the increased temperature is reducing the association tendency. In view of these, it is instructive to calculate the preferential interaction parameter, τ, to further evaluate the effect of temperature and salts on interactions between different solution species. Using Kirkwood-Buff theory, which provides a statistical thermodynamic framework for estimating τ, we calculate the preferential interaction parameters of caffeine with like molecules (over water), τ_{cw}^{c}, by using eq 3.

$$\tau_{cw}^{c} = \rho_c(G_{cc} - G_{cw}) \tag{3.2}$$

where c and w represent the solute caffeine and water molecules, respectively. G_{cc} and G_{cw} are the Kirkwood-Buff integrals [97, 107] and they can be calculated from the caffeine-caffeine and caffeine-water distribution functions. ρ_c is the number density of caffeine in a given system [68]. From the above equation (eq. 2) it is clear that the value of τ_{cw}^{c} becomes positive when a caffeine molecule prefers to interact with other caffeine molecules over water. On the other hand, its negative value implies the preferential hydration of caffeine molecules.

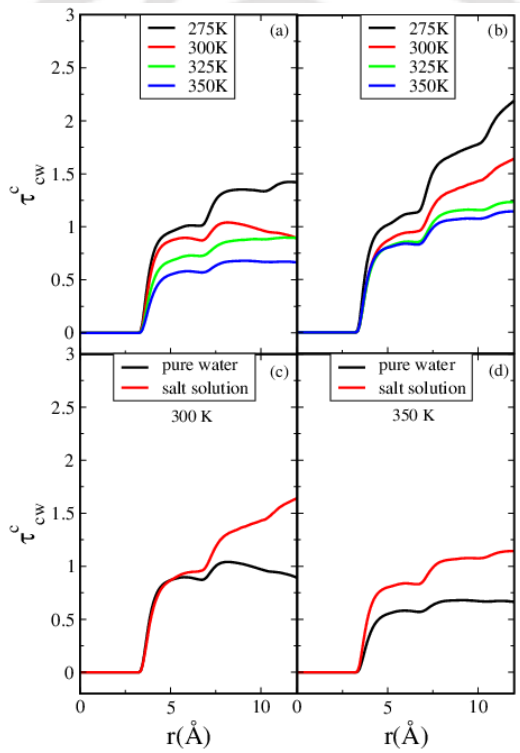

Figure 3-5. *Preferential interaction parameters of caffeine for like molecules over water molecules (τ_{cw}^{c}), in (a) pure water and (b) salt solution. (c) and (d) are at a single temperature.*

Fig. 3-5 (a) and (b) depict how does the value of τ_{cw}^{c} change as function of distance for different temperatures in pure water and salt solution respectively. The comparison of τ_{cw}^{c} values in pure water and salt solution at a particular temperature is shown in Fig. 3-5 (c) and (d). In consistent with previously reported value of τ_{cw}^{c} for caffeine-water binary system [33], we also find that the value of interaction parameter is positive for all systems studied here. Moreover, this finding suggests a greater preference of caffeine to the like molecules

in salt solution suggesting salting-out behavior. Further, by comparing the interaction parameter values at different temperatures, we observe that the value of τ_{cw}^{c} becomes less positive as temperature increases for pure water systems as well for the salt solutions.

Thermodynamics of self-association:

To characterize the thermodynamics of hydrophobic interaction of caffeine molecules, from our temperature-dependent simulations, it will be useful to study the enthalpy-entropy contribution to the free energy of caffeine association. In order to do that, we have first calculated the potentials of mean forces (PMFs), W(r), as a function of caffeine-caffeine center of mass distance r by using equation 3.

$$W(r) = -k_B T ln g_{cc}(r) \tag{3.3}$$

where, k_B and T correspond to the Boltzmann constant and temperature respectively and $g_{cc}(r)$ is the distribution function involving center of mass of caffeine. Then, the entropy is calculated from the PMFs of three temperatures by using the finite difference temperature derivative [108-112].

$$-\Delta S(r) = 1/2[\frac{\delta W(r, T+\delta T)}{\delta T} - \frac{\delta W(r, T-\delta T)}{\delta T}] \tag{3.4}$$

In the above equation (eq. 4) the value of δT is 25 K. From the above value of $\Delta S(r)$ the corresponding enthalpy contribution ($\Delta H(r)$) can be calculated by

$$\Delta H(r) = W(r) + T\Delta S(r) \tag{3.5}$$

Fig. 3-6 (a) and (b) show the entropic (-TΔS(r)) and enthalpic (ΔH) contributions to the PMF at 300 K and 325 K for pure water, and the same for salt solution is shown in Fig. 3-6 (c) and (d). From this figure we make the following observations. (i) There are two distinct minima in each of the PMF plots. The contact minimum (CM) at a distance of 3.7 Å is significantly deeper than the solvent separated minimum (SSM) which appears at 7.2 Å. (ii) The stabilizing effects of entropic and enthalpic contributions to the PMF act in opposite direction to each other, and the relative proportion of the two contribution depends on the caffeine-caffeine distances. (iii) The free energy of association shows a weak temperature dependence in comparison to the temperature dependence of its enthalpic and entropic components.

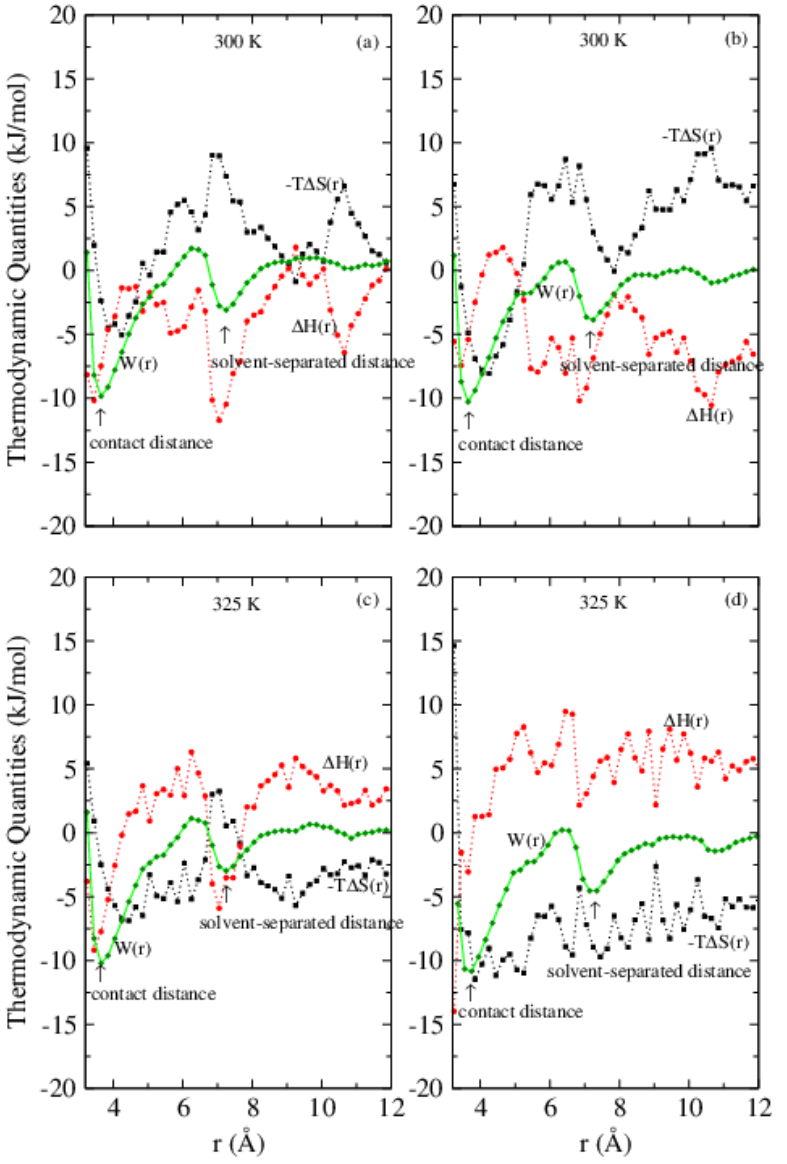

Figure 3-6. *Entropy and enthalpy contribution to caffeine-caffeine PMF, (a) and (c) for pure water; and (b) and (d) for salt solution (basic caffeine model [53]).*

(iv) For pure water, the CM and SSM are stabilized mainly by enthalpy, with a minor contribution of positive entropy, (v) For pure water system, at 325 K, the stabilizing effect of enthalpy contribution at CM is less, when compared to that of 300 K. (vi) The presence of salt in water leads to decrease in enthalpic contribution, though at 300 K, both CM and SSM are still highly stabilized by favorable enthalpy. In presence of salt, the entropic contribution at CM increases slightly when compared to pure water. (vi) Importantly, at 325 K temperature, the presence of salt makes the association phenomenon of caffeine molecules primarily entropy driven.

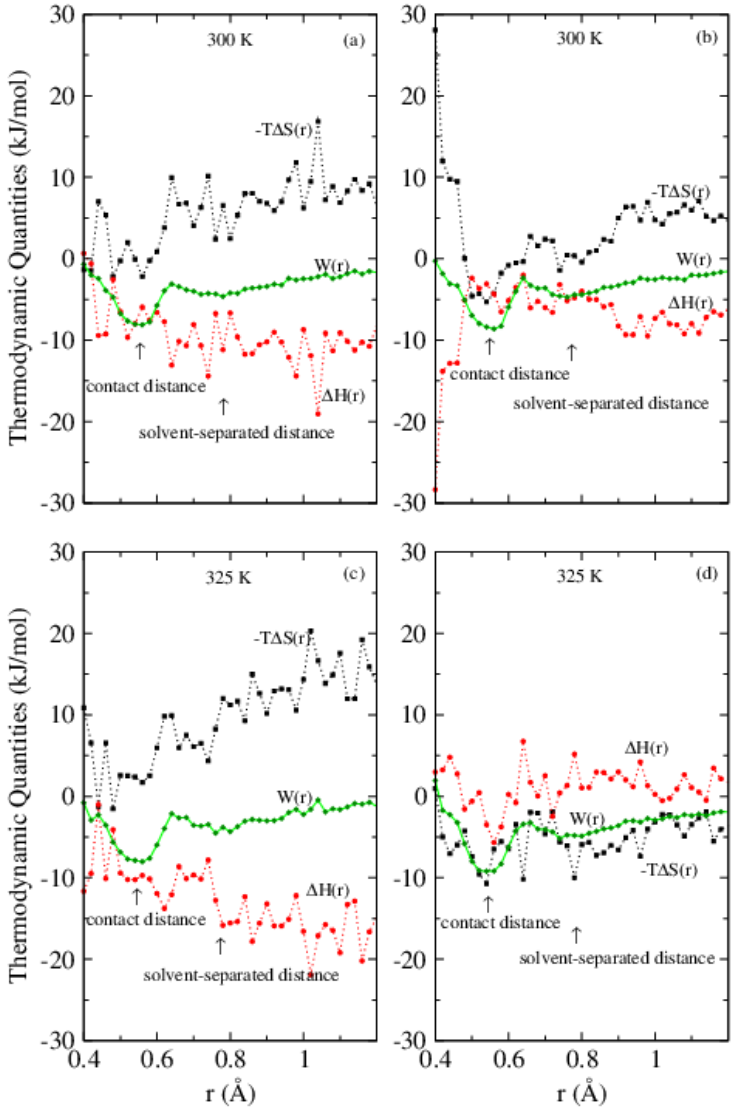

Figure 3-7. *Entropy and enthalpy contribution to caffeine-caffeine PMF, (a) and (c) for pure water; and (b) and (d) for salt solution. A combination of Weerasinghe model of caffeine [33] and Smith model of NaCl [103] are used.*

The entropic and enthalpic contributions to PMFs for the systems containing Weerasinghe model [33] of caffeine molecules (simulated in GROMACS software) as well as for systems containing Smith model of $NaCl$ are displayed in Fig. 3-7. From these figures we have observed stabilization of CM upon salt addition. A closer look in to these figures reveal that in pure water system at 325 K temperature, the caffeine-caffeine aggregation is purely enthalpically driven for Weerasinghe caffeine model whereas the entropic contribution being unfavorable. On the other hand, for the major caffeine model used in this study both enthalpy and entropy contribute to caffeine association and the contribution of the

former is higher than the latter. Moreover, as observed for caffeine molecules used in this study, the decomposition of caffeine-caffeine PMF for these systems into enthalpic and entropic contributions also implies enthalpically driven caffeine self-association in pure water, whereas, at 325 K in salt solution, self-association of caffeine is mostly entropy driven.

The temperature dependence of free energy at 300 K and 325 K shows very similar plots, but the enthalpic and entropic contribution to it are not similar by any means for any systems. Therefore, we will now try to propose an explanation for enthalpy-entropy compensation to get a complete picture of thermodynamics on the association of caffeine molecules. It is now well accepted that for small purely hydrophobic molecule such as methane, its surrounding water structure and hydrogen bonding between water molecules are not much affected. But solute-water attractive interaction plays an important role in wetting/dewetting behaviors of large solutes like caffeine. Together with its bigger size, it can even form H-bonds with solvent water molecules. Therefore, the presence of caffeine molecules in water affects the hydrogen-bonding network of latter. The hydrophobic-driven association process of caffeine will depend on the strength of solute-solvent attraction, which may vary temperature changes and due to the presence of salt NaCl. In the next subsections, we, therefore, will try to understand the hydration of caffeine in water and salt solution and change in water structure due to change in temperature and the presence of salt.

Hydration of Caffeine:

The estimation of number of water molecules in the first solvation shell of solute by using eq. 1 provides information about the hydration pattern of caffeine. This in turn gives, albeit indirectly, the self association of caffeine molecules. Therefore, in this section we discuss the effect of temperature change on the association propensity of caffeine molecules both in presence and in absence of salt. We probe the solvation of caffeine molecules by means of site-site pair correlation functions involving different atomic sites of caffeine and oxygen of water. Due to presence of both hydrophilic and hydrophobic groups in caffeine molecule, it is important to understand the effect of temperature and salt on hydration of these atomic sites which reveals better understanding of caffeine hydration. From the site-site distribution functions (not shown) we have calculated the number of first shell water molecules around the hydrophilic (i.e., O11, O13, N9, and H8) as well as hydrophobic (i.e., C10, C12 and C14) atomic sites of caffeine using equation (eq. 1). Table

3-3 shows the number of water molecules in the first solvation shell of different atomic sites of a caffeine molecule. In the parentheses of the same table we also include the total number of first solvation shell water molecules when a single caffeine is immersed in similar aqueous environments (obtained from a separate set of simulations containing only one solute caffeine molecule). As is evident from these values that the association of caffeine molecules causes a loss in the water molecules from its hydration shell.

Table 3-3. The number of water molecules in the first hydration shell of different atomic sites of caffeine

Temp. (K)	Systems	O11	O13	N9	H8	C10	C12	C14	$Total_{CN}$
275	S0	2.00	1.90	1.27	2.16	14.97	13.84	14.87	51.01 (54.54)
	M0	1.99	1.89	1.26	2.12	14.38	13.39	14.41	49.44 (53.90)
300	S1	1.99	1.88	1.27	2.13	15.25	14.35	15.09	51.96 (53.89)
	M1	1.95	1.85	1.26	2.09	14.55	13.66	14.63	49.99 (53.30)
325	S2	1.99	1.81	1.22	2.06	15.43	14.59	15.31	52.41 (53.43)
	M2	1.90	1.79	1.19	2.02	14.84	13.94	14.68	50.36 (52.75)
350	S3	1.91	1.80	1.19	2.03	15.58	14.76	15.53	52.80 (52.92)
	M3	1.88	1.75	1.15	1.94	15.11	14.02	14.72	50.57 (52.25)

$Total_{CN}$ represents the total number of first shell water molecules around the hydrophobic and hydrophilic atomic sites of caffeine.

Considering the effect of salt at a given temperature first, we observe that the addition of salt causes an exclusion of water molecules from the caffeine sites and this is true for all temperatures considered in this study. Again, the total coordination number is found to be the lowest for system S0 when there is no salt (and system M0 for salt solution). This implies that the association of caffeine molecules is the highest at 275 K, and the association propensity of caffeine decreases with increasing temperature. In regard to the effect of temperature on hydration of atomic sites, one interesting point to be noted is that the effect of temperature does not follow any particular trend for hydrophilic and hydrophobic sites. A closer look into the first coordination number values of different sites reveals that as temperature increases, the interaction of water molecules with hydrogen bonding sites of caffeine viz. O11, O13, N9, and H8 decreases slightly. This suggests exclusion of some water molecules due to breaking of caffeine-water hydrogen bonds at higher temperature. On the other hand, the hydrophobic methyl groups tend to be more

hydrated at higher temperature. This shows that there is a constant competition between hydrophobic self-association and hydrophilic hydration of caffeine, and temperature plays a very crucial role in it. Comparing the total coordination values (CN_{total}) for salt solutions and the systems without salt, we notice that, as temperature is increased the difference between them increases. For example, the difference in the CN_{total} values for systems S0 and M0 is 1.57 and the same for systems S3 and M3 is 2.23. This shows the effect of salt on hydrophobic association is more pronounced as temperature increases.

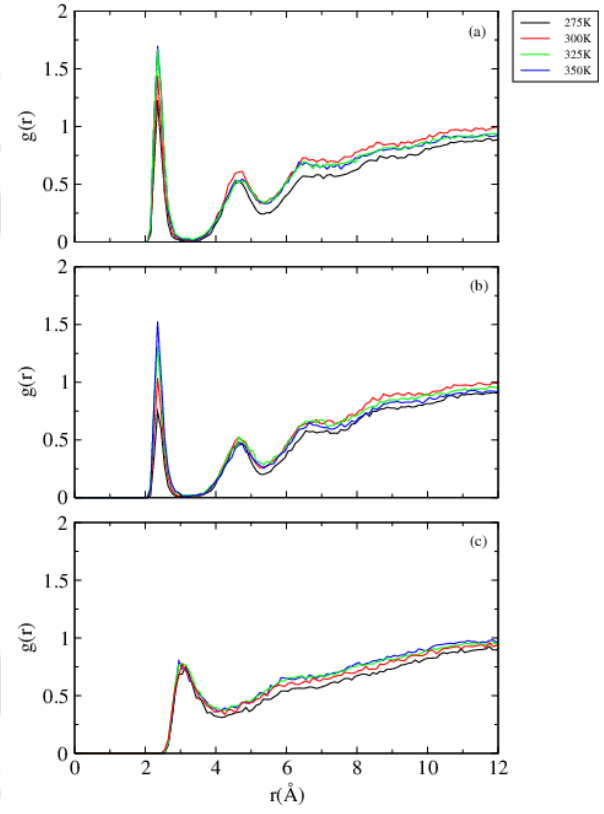

Figure 3-8. *Site-site radial distribution functions involving: (a) Na^+ -O13, (b) Na^+ -O11, and (c) Cl^- -H8. Black, red, green and blue colors are for systems M0, M1, M2 and M3 respectively.*

In our previous work [53], we have reported that $Na^+$and Cl^- ions exhibit an appreciable amount of affinity for caffeine molecule. Therefore, to investigate the effect of temperature on interaction of caffeine molecules with ions in salt solutions, we have shown the rdfs between Na^+ ions around two electronegative carbonyl oxygens O13 (Fig. 3-8 (a)) and O11 (Fig. 3-8 (b)) and Cl^- ions around more electropositive hydrogen H8 of caffeine molecule (Fig. 3-8 (c)). The affinity of Na^+ ions for caffeine increases with temperature as is evident from the formation of stronger first peak in the rdf at higher temperature.

Further, as can be seen from the pair correlation function involving Cl^- ion and H8 of caffeine that the effect of temperature change is not very pronounced. These changes in the rdfs are further confirmed by the spatial distribution plots (with an isovalue of 1.4) of Na^+ and Cl^- ions around these atomic sites of caffeine (see Fig. 3-9).

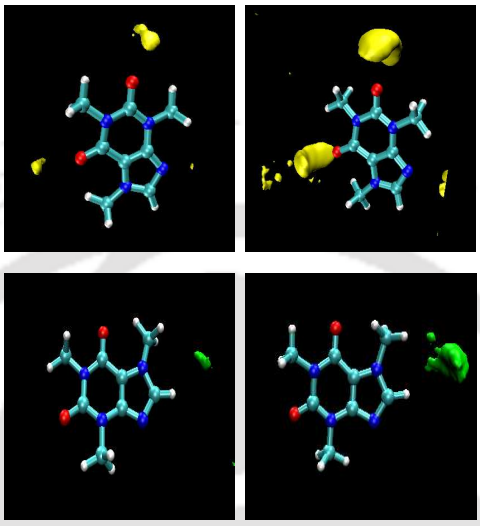

Figure 3-9. *Spatial distribution plot of ions around caffeine, with an isovalue of 1.4 for systems M0 (left) and M3 (right). Top: Na^+ ions around caffeine, bottom: Cl^- ions around caffeine.*

Water Structure

Because of the formation of extensive water-water hydrogen bonds, water molecules are known to be a network forming liquid. The addition of a solute, as large as caffeine, in water causes breaking of water hydrogen bonding network. In this section we discuss the effect of NaCl salt and caffeine on the local structure of water and how the water structure is perturbed as temperature increases. The calculation of water oxygen-water oxygen distribution function is an effective way to examine water structure and the same for different systems is shown in Fig. 3-10 (a) and (b). The appearance of first and second peak (at 2.75 Å and 4.5 Å respectively) in the rdf implies the presence of hydrogen bonded first neighbor and the tetrahedrally located second neighbor. The locations of these peaks in this distribution function are in accordance with those already reported in the literature [113-115]. Considering the effect of increased temperature on water-water interaction in both pure water and salt solution systems, we observe: (a) drop in first peak height, (b) a shallower first minimum and (c) an outward shift of the position of first minimum. Here, we

note that these observations are in consistent with that of already reported elsewhere [116] and suggest the breaking of water structure as temperature increases. The first peak of g(r) in pure water are slightly sharper than those in salt water, but the changes in the first minimum and the second peak are easy to notice. It has been reported that, for salting-out salts like NaCl, the ion-water interaction is stronger than the water-water interaction [117]. The ion-water pair correlation functions are presented in Fig. 3-10 (c) and (d).

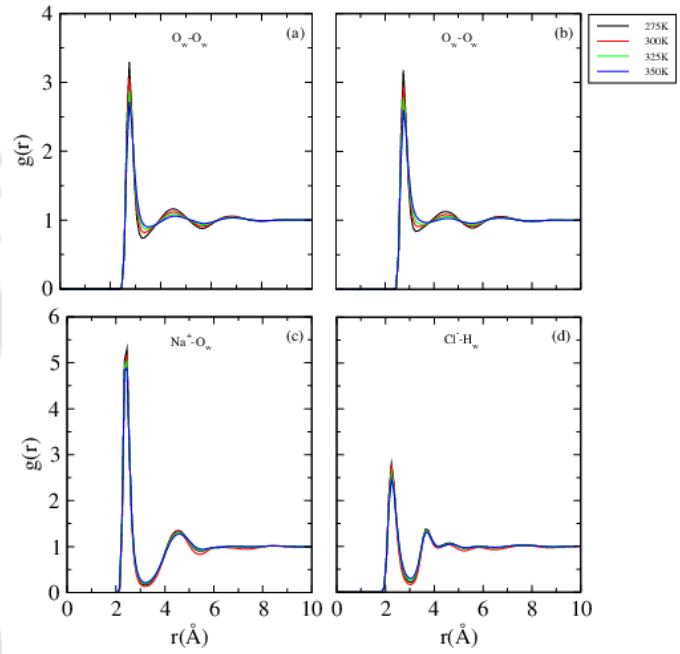

Figure 3-10. *(a) and (b) represent site-site radial distribution functions involving with water oxygen where (a) is for pure water and (b) is for salt solution. (c) and (d) represent pair correlation functions involving sodium ion-water oxygen and chloride ion-water oxygen respectively in salt solution.*

It can be clearly seen that the peak height of Na^+-O_w is much higher than the peak height of water-water rdf. Furthermore, the peak heights of ion-water rdf decreases with increasing temperature indicating increased thermal disorder at higher temperature.

Hydrogen Bond Properties

Water-water and solute-water hydrogen bonding influences many important characteristics of a solvent. As already mentioned, in aqueous solution, caffeine molecules can form hydrogen bonds with water with its three hydrogen bonding sites, and these are two carbonyl oxygen O11 and O13 and ring nitrogen atom N9 [35]. All these atoms act as hydrogen

bond acceptors for caffeine-water hydrogen bonds. We have carried out an analysis of the average number of hydrogen bonds formed between water and these three hydrogen bond acceptor sites of caffeine (in terms of per caffeine). In the same table we also include the average number of water-water hydrogen bonds per water molecule. The results are presented in Table 3-4.

Table 3-4. The number of water-water (per water) and water-caffeine (per caffeine) hydrogen bonds in different systems

System	HB_{w-w}	HB_{O11-w}	HB_{O13-w}	HB_{N9-w}
S0	3.42	1.51	1.52	0.95
S1	3.33	1.50	1.52	0.94
S2	3.23	1.48	1.48	0.93
S3	3.14	1.43	1.46	0.87
M0	3.28	1.50	1.48	0.90
M1	3.15	1.44	1.44	0.89
M2	3.07	1.43	1.41	0.87
M3	2.98	1.39	1.38	0.84

w represents water and O11, O13, and N9 correspond to the different atomic sites of caffeine. The estimated standard errors for all data are less than 0.002.

Following earlier works [118-120], in this study we have used geometric criteria for calculating caffeine-water and water-water hydrogen bonds. According to this hydrogen bonding definition, two molecules are considered to be hydrogen bonded if the distance between donor (D) and acceptor (A) is less than or equal to 3.4 Å and simultaneously the angle of H-D-A is less than 45^o. As expected, the number of water-water hydrogen bonds per water molecule is lower in salt solution compared to that of pure water systems. Again, with increasing temperature, the number of hydrogen bonds per water molecule is decreased from 3.42 to 3.14 in pure water; and 3.28 to 2.98 in salt water. These is due to breaking of water structure at higher temperature. The average number of caffeine-water hydrogen bonds is found to decrease in presence of salt at a particular temperature. This can be attributed to the interaction of ions with caffeine carbonyl atoms (O11, O13), and also due to higher tendency of aggregation of caffeine molecules in presence of salt. As temperature increases, there is a decrease in the number of hydrogen bonds per caffeine

molecules, between water and hydrophilic sites of caffeine due to thermal disorder of water molecules, which is in consistent with the our analysis of caffeine hydration at different hydrophilic atomic sites.

■ Discussions

Our results accounts for the thermodynamics of self-association process of caffeine molecules and demonstrate the determinant role of caffeine-water, caffeine-salt interactions as well as change in water structure due to presence of salt in water.

The free energy of association shows a weak temperature dependent, but contact well in PMF becomes deeper in presence of salt. As already discussed, water density around caffeine is not isotropic. The presence of hydrophilic proton acceptor groups makes caffeine molecule partially soluble in water. But, unlike small solutes, due to its large size and the presence of extended flat hydrophobic surface, a caffeine molecule cannot be accommodated inside the cavity of hydrogen-bonded network of liquid water. As a result, this leads to breaking of hydrogen bonds of some of the water molecules around its surface. The favorable enthalpy and entropy driven association of caffeine molecules at 300 K therefore results from the release of water molecules from caffeine surface to the bulk water. The release of highly ordered water molecules around caffeine contributes to entropy, whereas the liberation of water molecules from the hydrophobic faces leads to regain of lost water-water hydrogen bonds, contributing to enthalpy. In this regard, we further note that, some experimental studies have reported that the association of caffeine molecules in water at room temperature is enthalpic driven [90, 67, 121, 122]. Standard enthalpy for dimerization reaction of aqueous caffeine at 303.15 K and 0.35 MPa pressure is reported to be -14.72 kJ/mol [67] and our calculated enthalpy of caffeine association at 300 K and 1 atm pressure is -7.74 kJ/mol. With increasing caffeine-caffeine separation the enthalpic contribution becomes less favorable, until, at solvent separated distance (7.2 Å) which is highly stabilized by enthalpy, entropic contribution being unfavorable. The rdf plot of water around the center of mass of caffeine (not shown) shows that though water molecules are mostly excluded from the vicinity of caffeine molecules, a stable second peak is formed between 6.3 Å and 7.3 Å . It is also reported earlier that water molecules form a highly structured layer between two solutes at an inter-solute distance of around 7.0 Å and remains so down to around an intersolute distance of 6.0 Å [123]. Therefore, below the solvent separated distance, due to expulsion of water from the intersolute region to the bulk, this highly structured water

layer is released, and the favorable energy arising from water-caffeine interaction is lost, resulting in sharp increase in enthalpy, though it is still favorable (negative).

At 325 K for pure water, we notice that as inter solute distance increases, initially, the CM is stabilized by both enthalpy and a small favorable entropic contribution, but the entropic contribution is slightly less favorable as compared to that at 300 K, which is further compensated by decrease in enthalpy. The enhancement in enthalpic contribution at higher temperature correlates with experimental observations [67]. The hydration of caffeine molecule in water shows that though there is an opposite trend for hydration of hydrophilic and hydrophobic groups of caffeine molecules, overall as temperature increases, caffeine molecules becomes more hydrated (See Table 3-3, and the discussions above). Therefore, aggregation of caffeine at high temperature releases more water molecules, which regain their lost hydrogen bonds at bulk, contributing to more favorable enthalpy. Again, the water oxygen-oxygen rdf plot suggests breaking of water structure as temperature increases (Fig. 3-10). This leads to an increase in entropy at 325 K. Therefore, the change in entropy due to liberation of water molecules from caffeine surface is not much pronounced compared to that at 300 K. The SSM is still stabilized by negative enthalpy due to the formation of highly structured water layer at solvent separated distance. But, the enthalpic contribution is less at higher temperature, due to higher thermal disorder at 325 K, which results in decrease in the favorable energy arising from caffeine-water interaction at solvent separated distance.

The presence of salt in caffeine solution affects the association thermodynamics of caffeine molecules. The addition of NaCl salt significantly stabilizes the contact configuration, as indicated by the decreasing in free energy value establishing the salting out effect of NaCl salt. Here we can note that, the salt-induced strengthening of hydrophobic interactions for small solutes, like methane, are reported to be enthalpic in origin; whereas salting out effect for large length scale hydrophobic moiety is entropic in nature [124, 125]. The origin of these different thermodynamic characteristics is proposed by different mechanism of salting out for small and large scale length molecules. In a simulation study, Mancera [124] explained that the addition of salt results in loss of water-water hydrogen bonds thereby decreasing the enthalpy of the system. On the other hand, for large solutes, Zangi et al [125] reported that in presence of NaCl the salting out effect is entropic. They explained that due to the high charge density of Na^+ and Cl^- ions, there is a greater tendency of water molecules to cluster around these ions forming hydration complexes. As a result, the less polar hydrophobic molecules are pushed away from water. This decreases the available surface area

of solute molecules accessible to water, and thus the salting out effect is described to be dominantly entropic in origin. Therefore, the thermodynamic as well as structural aspects of hydrophobic interaction is highly sensitive to the length scale of the particles, especially in the transition region from small to nanoscale. Though caffeine molecule is smaller than 1 ns scale, from our study and other different experimental studies [67] we have noticed the crossover behavior of thermodynamics of solute association in water. This crossover behavior may also affect the salting out mechanism of caffeine association in salt solution. Unfortunately, we have no experimental data available for association thermodynamics of caffeine molecules in salt solution. However, our study reveals the transition between enthalpic and entropic association, and it seems that both mechanism are on interplay depending upon temperature. At 300 K, though the CM is still stabilized by favorable enthalpy, its contribution is much less compared to pure water, which is compensated by more favorable entropy, arises due to expulsion of water molecules upon aggregation. Again, it has been found that though Na^+ ions are mostly excluded from the caffeine surface, the hydrophilic sites of caffeine show some affinity towards Na^+ ions, and it is more pronounced at higher temperature (see Fig. 3-8). The release of ions from caffeine surface due to aggregation at 325 K temperature further contributes to ion-water clustering, resulting in entropy dominated contact pair formation of caffeine, the contribution of enthalpy becomes small. Due to strong ion-water interaction, the attractive water-water interaction at solvent separated distance decreases in salt solution, contributing less enthalpy (when compared to pure water system) to the free energy at 300 K. On the other hand, the combining effect of ion-water clustering and higher interaction of salt ions with caffeine at 325 K, the favorable energy of water layer at solvent separated distance is totally entropy driven, enthalpic contribution being unfavorable. Our theoretical prediction on self-association thermodynamics of caffeine are further supported by similar trends of enthalpic and entropic to PMF in pure water and salt solution with different caffeine and salt models.

■ SUMMARY AND CONCLUSIONS

In this chapter, we have investigated the effect temperature on the interactions of caffeine molecule with itself and with the solvent molecules in pure water and salt solutions. We have considered caffeine-caffeine center of mass radial distribution function and cluster structure analyses to understand the association propensity of caffeine. Our results show that the overall tendency for aggregation is higher in salt solution than in pure water. As temperature increases, probability of formation of higher order clusters decreases. Spatial distribution plot shows vertical stacking arrangement of caffeine molecules, which gives a trend of decreasing caffeine aggregation at higher temperature. Addition of salt enhances the probability of caffeine distribution around itself. To get a clear picture on thermodynamics of association, we have calculated PMF as a function of caffeine-caffeine distance, and then calculated enthalpic and entropic contribution to PMF for both the two force field model of caffeine, which shows qualitatively similar thermodynamic trends. Interestingly, we have observed that for pure water both enthalpy and entropy changes are favorable for caffeine aggregation, whereas, salt-induced strengthening of caffeine-caffeine interactions at 325 K temperature is found to be mostly entropic in nature. Water molecules form strong hydration complex with ions due to the high charge density, which leads to exclusion of water molecules from caffeine surface, leading to entropy driven aggregation. Salt ions, in particular Na^+ ions, interact more with hydrophilic sites of caffeine at higher temperature, and aggregation of caffeine liberates these ions to the bulk, which adds to the entropy driven association of caffeine. In this regard, it should be noted that though caffeine molecule is smaller than the required 1 nm length as predicted by Chandler [74] for crossover from entropic to enthalpic dependence of aggregation of nonpolar solutes, our analyses point out the transition of thermodynamic behavior of caffeine association to shorter length-scale. The robustness of results is further confirmed by estimating enthalpy-entropy contribution to caffeine-caffeine PMF using a different caffeine (and $NaCl$) model having different force field parameters for different atomic sites. Since size of caffeine molecule falls in between small and large solutes, the thermodynamic property of association is highly sensitive to change in environment. The change in association tendency of caffeine molecules is also reflected in the hydration pattern of caffeine, and we have found excellent correlation between thermodynamics of association and hydration of caffeine molecules. We have observed that the highest exclusion of water molecules from caffeine surface occurs at 275 K in salt water. It is important to note that the hydration pattern of hydrophobic and hydrophilic sites

of caffeine does not follow similar trend and the hydration number analyses reveal that hydrophobic sites tend to be more hydrated as temperature increases, whereas hydrophilic sites show more exclusion of water.

Therefore, in this chapter we have discussed in brief the thermodynamics of self-aggregation of caffeine molecules. The 'hydrophobic effect' is recognized as the major driving force for intermolecular protein-protein interaction, which ultimately leads to amyloid fibril formation. Therefore, in **Chapter 4** we will explore the effect of presence of caffeine on the hydrophobic self-assembly formation.

Chapter 4

Inhibiting Action of Caffeine Association on the Aggregation of di-t-butyl-methane (DTBM)

"Organic molecules can aggregate to form particles in aqueous buffers, and these aggregates can sequester and thereby inhibit protein targets. Aggregation-based inhibition is baffling from a chemical perspective, but viewed biophysically such behavior is expected."

– B. K. Shoichet *Drug Discov. Today* **11**, 607 (2006)

Overview:

Hydrophobic effect is one of the major driving forces in biomolecular interactions. Biological molecules such as proteins and nucleic acids contain numerous hydrophobic components, and their interactions plays a critical role in protein folding-unfolding and protein aggregation. In our study, we have carried out molecular dynamics simulation of aggregation of a model hydrophobic molecule di-t-butyl-methane (DTBM) in a regime of caffeine : DTBM stoichiometric ratio to understand the effect of caffeine on hydrophobic aggregation, and also the mechanism and mode of caffeine action. From the calculations of site-site radial distribution functions followed by coordination number analyses and spatial distribution plots we have observed disruption of hydrophobic moieties of DTBM aggregates in 10 : 1 or more stoichiometric ratio of caffeine : DTBM systems. Calculations of binding affinities, preferential interaction parameters, and effect of caffeine cluster's size on aggregation show that though DTBM affinity with itself is more compared to caffeine, with increasing caffeine number this affinity decreases. On the other hand, in presence of higher number of caffeine in the system, caffeine clusters form a hydrophobic environment in which a DTBM molecule is encapsulated. The presence of a significant number of water molecules in this confinement also ensures the hydration of DTBM. Moreover, these caffeine clusters also act as a barrier and physically block the DTBM molecules to interact with the like molecules leading to disruption of DTBM aggregates in caffeine solution.

■ INTRODUCTION

The tendency for nonpolar molecules to aggregate in solution is often referred to as the 'hydrophobic effect'. The hydrophobic effect is one of the most significant forces in biological systems and is centrally important to biomolecular recognition. Despite extensive research devoted to the hydrophobic aggregation, its molecular mechanisms remain controversial. Hydrophobic hydration and hydrophobic interaction are two subdivision to describe hydrophobic effect. These inter-related phenomena are believed to determine, to a considerable extent, the conformation of macromolecule in aqueous solutions, the aggregation of amphiphiles, enzyme-substrate binding, and the formation of micelles and bilayer membranes. However, aggregation of unfolded proteins, which occurs mainly through the exposed hydrophobic surfaces of protein is also thought to be associated with several disease processes [1-5, 126]. Since biological molecules such as proteins and nucleic acids contain numerous hydrophobic components, the exact nature of these interactions plays a critical role in protein folding-unfolding and protein aggregation.

Therefore, an extensive study of hydrophobic aggregation is important to get a clear understanding of how such aggregation can be inhibited. In this context, molecular dynamics (MD) simulations may become an important computational tool for understanding an accurate account of the physical basis of the inhibition of hydrophobic aggregation of biological macromolecules. Also due to complexity in structure and size in big biomolecules, it is useful to use a small hydrophobic molecule to carry out an atomic and molecular level description of hydrophobic effect. Several studies have shown that a variety of small organic molecules have the potential to inhibit hydrophobic aggregation in biomolecules [14-24]. The inhibition effect of small molecule inhibitors on biomolecular aggregation are sensitive to the stoichiometric ratio of inhibitor and biomolecules [127, 128]. Among small organic molecules, caffeine molecule is particularly of importance for using as a drug for several factors. 1)Caffeine (also known as 1,3,7-trimethylxanthane, (see Fig. 1) (a)) is an inherently safe, inexpensive, readily available chemical stimulant, and probably the world's most widely used psychoactive substance [28, 29]. 2)Due to the amphiphilic nature of caffeine, it passes through all biological membrane and is absorbed into the blood stream after being ingested and easily crosses the blood-brain barrier. 3)Recently different studies on caffeine molecules have shown its ability to prevent aggregation of amyloidogenic protein in human and non-human species [23-26, 129].

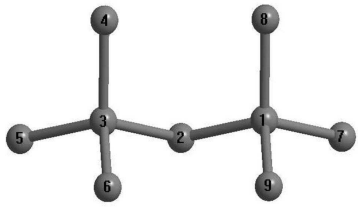

Figure 4-1. *The structure and atomic numbering of di-t-butyl-methane in ball-stick model. Hydrogen atoms are left off for better visual clarity.*

However, the mechanism and mode of inhibition action of caffeine is unclear and till date no attempt has been made to explore the molecular level understanding of the inhibition of hydrophobic aggregation. Therefore, for our study, we have explored the inhibition of self-aggregation of a hydrophobic model probe di-t-butyl-methane (DTBM, Fig. 4-1) by caffeine in water. DTBM molecule is already used as a model hydrophobic solute for atomic level exploration in MD simulation study [130]. From earlier studies it is observed that because of the presence of hydrophobic surface in caffeine molecule, it self-aggregates in water above its solubility limit (0.1M). Caffeine molecule can form complex with different biomolecules, DNA, and drug molecules with $\pi - \pi$ type of stacking interaction [51, 52]. However, in our study, we have considered the hydrophobic DTBM molecule without any aromatic part in it. This rules out any stacking type of interaction between DTBM and caffeine, which allows us to check the mechanism of inhibitory action of caffeine, if any, on purely hydrophobic effect. Clearly, understanding how a small organic molecule like caffeine might play a role on hydrophobic aggregation of model DTBM molecules, will definitely shed some light on the role of caffeine in destabilizing other hydrophobic assemblies. Therefore, in the present work, we have employed classical molecular dynamics (MD) simulation as a tool to understand the effect of different stoichiometric ratio of caffeine on self-association behavior of DTBM molecules in water.

Our goals for this study are:

(i) To investigate the aggregation of DTBM in aqueous solution and in caffeine solution with different caffeine : DTBM stoichiometric ratio. (ii) To explore the self-association of caffeine and size and arrangements of caffeine aggregates; (iii) To understand the underlying mechanism, if any, of inhibition of DTBM aggregation by caffeine.

The organization of the rest of the chapter is as follows. We first present the

models and details of simulations. Results are discussed thereafter, and the last section includes concluding remarks with a brief summary.

■ MODELS AND SIMULATION METHOD

To study the effect of caffeine on the self-aggregation of hydrophobic solute di-t-butyl methane (DTBM) classical molecular dynamics (MD) simulations were performed in pure water as well as in presence of caffeine in water. OPLS/AA force field parameters were employed to characterize the DTBM molecules [131]. The caffeine was modeled using AMBER generated all atom force field as used in previous studies [53, 54]. For water SPC/E model was employed [132].

Table 4-1. Overview of Simulations[a]

System	N_{caff}	N_{DTBM}	N_{wat}	caffeine : DTBM	C_{caff}(M)	box length (Å)	ρ (g cm^{-3})
S0	0	10	4200	-	0	50.52	0.99
S1	15	10	4200	3 : 2	0.19	50.91	1.01
S2	50	10	15000	5 : 1	0.17	76.87	1.00
S3	80	10	25000	8 : 1	0.17	91.89	1.00
S4	100	10	25000	10 : 1	0.20	92.27	1.00
S5	150	10	40000	15 : 1	0.21	106.33	1.01
S6	100	10	25000	10 : 1	0.20	92.24	1.00

N_{caff}, N_{DTBM}, and N_{wat} refer to the number of caffeine, the number of DTBM, and the number of water respectively. C_{caff} and ρ represent the caffeine concentration and the density of the system respectively.

To prepare the initial configurations of all the systems packmol program was used [86]. Here we note that the inhibition effect of small molecule inhibitors on aggregation are sensitive to the stoichiometric ratio of inhibitor and biomolecules [127, 128]. Therefore, to understand the effect of caffeine on DTBM aggregation on molecular basis, we have prepared systems with a regime of caffeine : DTBM stoichiometric ratio. In the initial structure, we have randomly placed 10 DTBM molecules in a cubic box and immersed in water. Considering the same initial separation of DTBM molecules we then added varied number of caffeine molecules to prepare systems with different caffeine : DTBM stoichiometric ratio. In order to understand the effect of caffeine on DTBM aggregation in more detail, we have considered one more simulation where caffeine molecules are added to a equilibrated DTBM-water system with DTBM clusters already formed. It has been ob-

served that different small molecule inhibitors inhibit biomolecular aggregation by forming chemical aggregates with like molecules [133, 134]. Here it is worth mentioning that a varied concentration range of caffeine are generally used in different experimental and theoretical studies [39, 78, 90, 135, 136]. In this study, we have kept the concentration of caffeine just above the solubility limit (0.1 M) to allow the formation of self-aggregated caffeine clusters. This is in line with the our previous studies as well as studies carried out by other researchers in which the caffeine concentrations were kept slightly above its solubility limit in water solvent[53, 54, 68]. An overview of different systems used in this study are presented in Table 4-1.

All MD simulations were performed using the AMBER 12 package [61] in isothermal isobaric (NPT) ensemble at 300 K temperature and 1 atm pressure using a time step of 2 fs. For all the systems, the initial configurations were energy minimized for 5000 steps, with first 2500 steps in steepest descent method followed by the identical number of steps in conjugate gradient method. The systems were then heated slowly from 0 to 300 K over 180 ps in canonical ensemble (NVT). Temperature of each of the systems was controlled by the application of Langevin dynamics method with a collision frequency of 1 ps^{-1}. Then each of the systems was equilibrated for 5 ns followed by 95 ns production runs in an isothermal-isobaric ensemble (NPT). The physical pressure was maintained by employing Berendsen barostat with a pressure relaxation time of 2 ps [87]. For calculating short-ranged nonbonding interactions a cutoff radius of 10 Å was used. For the treatment of long-range electrostatic interactions particle mesh Ewald method was used. For all the systems, the edge effects were removed by considering periodic boundary conditions in all three directions. Bonds involving hydrogens were constrained by the use of SHAKE algorithm [137].

Here we note that the findings of our previous comparative study of different force field parameters of caffeine (in SPC/E water) [54] reveal that in aqueous solution the caffeine model used in this study and the one developed by Weerasinghe and co-workers [33] behave in similar fashion in spite of the fact that our caffeine model showed slightly more self-aggregation tendency. Furthermore, the results of a systematic comparative study of different solute force field parameters (AMBER99, GROMOS 53A6 and OPLS-AA) in combination with five different water models (SPC, SPC/E, TIP3P, TIP4P and TIP4P-Ew) demonstrated that the performance of SPC/E water model is the best with all the three force fields of the solute [138].

■ RESULTS AND DISCUSSION

Hydrophobic aggregation of DTBM and the effect of caffeine on it:

In order to understand the aggregation propensity of DTBM molecules in water and in caffeine solutions we have calculated the number of free monomer DTBM molecules, if any, in all systems and the same is shown in Fig. 4-2 (a) as a function of simulation time (ns).

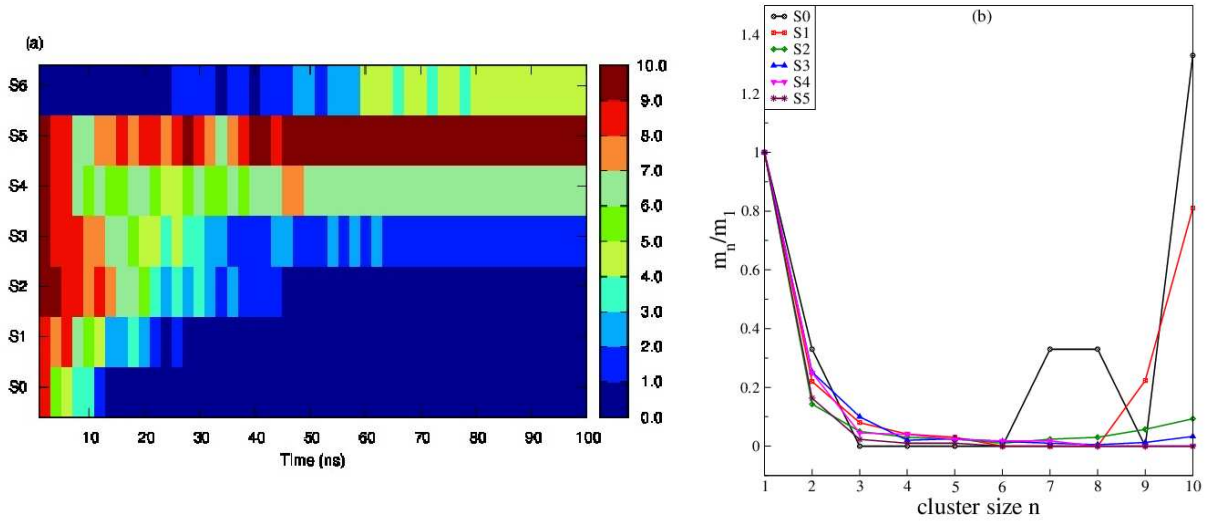

Figure 4-2. *(a) Monomer count of DTBM as a function of simulation time. (b) the probability distribution of clusters of different sizes (m_n) with respect monomer (m_1).*

For system S0 in pure water, there is a sharp drop in monomer count within 10 ns, depicting a strong self-association of DTBM molecules. As a result of this all the DTBM molecules are clustering together in order to reduce the surface contact with water molecules. On addition of 15 caffeine molecules in the system, there is only a slight change in the monomer count. As caffeine number increases, we see a time lag in DTBM cluster formation. In system S5, all the DTBM molecules prefer to be in monomeric form most of the time, showing inhibition of DTBM aggregation by caffeine. In Fig. 4-2 (b) we have shown the probability distribution of different size of DTBM clusters (m_n) with respect to monomer (m_1). For this, we have considered clusters of size two when center of mass of one DTBM molecule is within 7.2 Å of another like molecule. Similarly, a DTBM trimer is formed if a third DTBM molecule is present within 7.2 Å of any of the dimer forming DTBM molecules etc. This cut off distance is obtained from the position of the first minima in DTBM-DTBM rdf (Fig. 4-3 (a)). Monomers are considered as those DTBM molecules

which are not within the cut off distance of any other DTBM molecules. We observe that for system S0, the probability of cluster size 10 is even higher than that of monomer indicating a highly aggregating behavior of DTBM molecules. In presence of caffeine, the number of higher order DTBM clusters decreases, and with increasing caffeine number the probability of finding clusters with respect to monomer tends to zero.

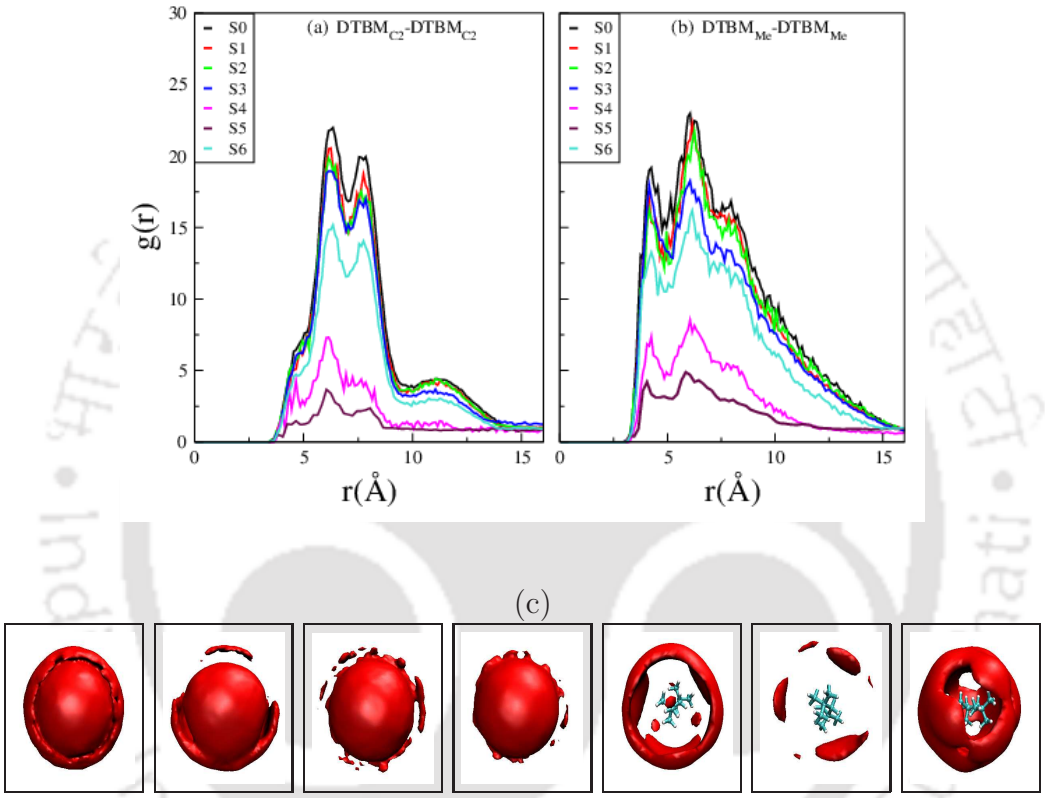

Figure 4-3. *(a,b) Radial distribution functions of DTBM around DTBM involving the central carbon atom (C2), and involving methyl groups of DTBM in different systems, and (c) spatial distribution plots for DTBM around DTBM, with an isovalue of 1.2. Left to right: Systems S0 to S6.*

In order to gain insight into the intermolecular interaction between DTBM molecules we have calculated radial distribution functions (rdf) involving the central carbon atom of DTBM molecule (C2-C2) for all systems, and these are shown in Fig. 4-3 (a). We observe that with increasing caffeine number in the system, the peak height initially decreases slightly for systems S0-S3. However, in system S4 a sharp depletion in the peak height is observed, which continues to decrease even further for system S5. We also present the rdfs involving methyl groups of DTBM in Fig. 4-3 (b). The contact peak, which appears at 4.15 Å, shows a sharp drop in its height for systems S4 and S5. The spatial density plot of DTBM

around DTBM with an isovalue of 1.2 clearly shows the change in the aggregation pattern of DTBM with increasing caffeine number (see Fig. 4-3 (c)). Sdf plot shows negligible density of DTBM around DTBM for system S5, which indicates that almost all the DTBM molecules are separated from each other and there is the least probability of finding DTBM molecule near another like molecule. Furthermore, we have done a quantitative estimation of number of DTBM molecules that are present in the first solvation shell of central atom and methyl carbon of DTBM (and the possible effect of presence of caffeine molecules on to it) from the respective pair correlation functions by the equation: [139]

$$n_{\alpha\beta} = 4\pi\rho_{\beta}\int_{0}^{r_c} r^2 g_{\alpha\beta}(r)dr \tag{4.1}$$

where $n_{\alpha\beta}$ refers to the number of atoms of atom type β surrounding atom type α. r_c and ρ_{β} are the distance of the first minimum in the pair-correlation function, $g_{\alpha\beta}(r)$, and number density of β in the system respectively. It is observed that for DTBM-DTBM interaction, coordination number does not change much up to system S3, however, for S4 and S5 there is a drastic drop in its value (see Table 4-2).

Table 4-2. Number of first shell coordination number of DTBM and water around selected atomic sites of DTBM molecule.

system	$D_{C2} - D_{C2}$	$D_{C4} - D_{C4}$	$D_{C2} - wat$	$D_{C1} - wat$	$D_{C4} - wat$
S0	1.78 (± 0.02)	0.59 (± 0.01)	27.17 (± 0.05)	13.87 (± 0.02)	4.07 (± 0.01)
S1	1.76(± 0.01)	0.56 (± 0.01)	22.44 (± 0.02)	12.52 (± 0.03)	3.78 (± 0.01)
S2	1.33 (± 0.03)	0.45 (± 0.02)	25.80 (± 0.02)	13.91 (± 0.02)	4.01 (± 0.01)
S3	1.01 (± 0.02)	0.36 (± 0.02)	28.89 (± 0.03)	14.08 (± 0.04)	4.09 (± 0.02)
S4	0.34 (± 0.03)	0.08 (± 0.01)	32.34 (± 0.02)	16.93 (± 0.02)	5.23 (± 0.01)
S5	0.16 (± 0.02)	0.03 (± 0.02)	33.61 (± 0.03)	17.40 (± 0.02)	5.33 (± 0.02)

It is a well accepted fact that in aqueous solution the self-aggregation propensity of a non-polar solute molecule is closely related to its hydration pattern. The hydration and concept of dewetting of solute is length-scale dependant When hydrophobic solute molecules are present in water, the solute interact with the surrounding water, and depending on the interaction, the solute self-aggregate in aqueous solution [54, 140-143]. Thus, in order to obtain the molecular details of DTBM hydration, it is important to consider various structural properties which provide the information about it. This instructs us to compute selected site-site rdfs between DTBM (C2, C1 and C4 atoms) and water (oxygen atom) and these are shown in Fig. 4-4 (a,b,c).

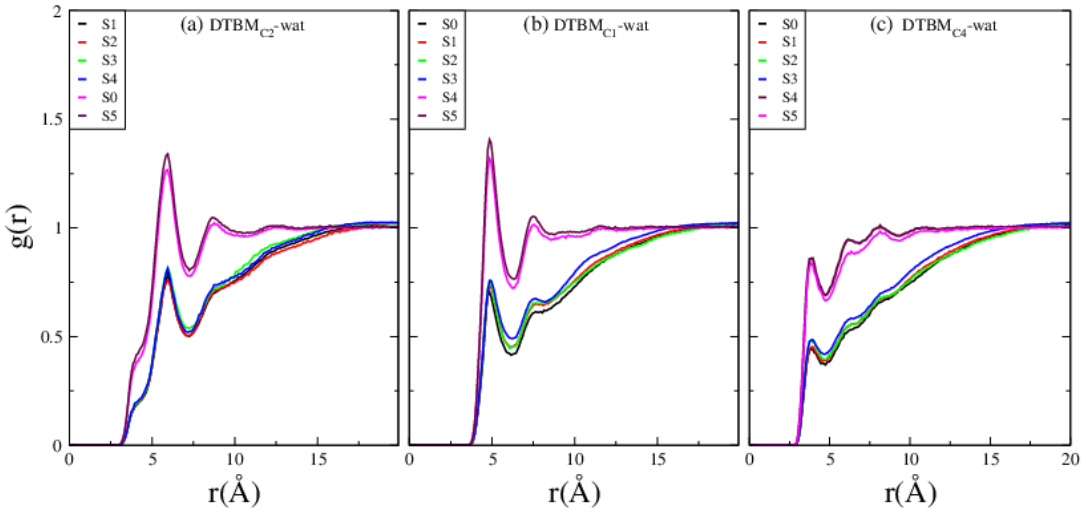

Figure 4-4. *Radial distribution functions involving water and selected atomic sites of DTBM. (a) water around central (C2) atom, (b) water around C1 atom, and (c) water around C4 atom of DTBM for different systems.*

Considering the hydration of DTBM in pure water first, we find that, the height of the first peak is below the bulk density for all these selected atomic sites of DTBM. This indicates the exclusion of water from DTBM surface due to hydrophobic aggregation of DTBM molecules. On addition of caffeine for system S0-S3, the first peak height in DTBM$_{C2}$-water, DTBM$_{C1}$-water and DTBM$_{C4}$-water rdfs remains almost unaffected. This correlates with the fact that there is no apparent enhancement of hydrophobic aggregation of DTBM in these system (see Table 4-2). The hydration tendency of hydrophobic DTBM molecule increases abruptly for systems S4 and S5 due to disruption of DTBM aggregates, and we observe a sharp increase in the peak height of this distribution function. The first peak height of DTBM$_{C2}$-water and DTBM$_{C1}$-water is above the bulk in these two systems suggesting extensive hydration of DTBM in presence of higher caffeine : DTBM stoichiometric ratio in the system. Concentrating on DTBM-water coordination numbers (see Table 4-2), we find that there is only a slight increase in the number of first solvation shell water molecules up to system S3. But for the systems S4 and S5, a sharp increase in its value is observed. This finding is in agreement with the DTBM-water rdfs discussed below.

These findings motivate us to calculate the average solvent accessible surface area (SASA) of DTBM. SASA provides information about the surface area of a solute over which the contact between solute and solvent can occur. In Table 4-3 we have tabulated

the SASA values for different systems.

Table 4-3. Solvent accessible surface area (SASA) per DTBM for different systems.

System	SASA (Å^2)
S0	179.31 (± 2.42)
S1	175.99 (± 3.01)
S2	181.23 (± 2.30)
S3	185.61 (± 2.50)
S4	276.15 (± 2.60)
S5	298.36 (± 3.01)

In accordance with the hydration number analysis discussed above (also see Table 4-2), SASA values also give an evidence of a much higher hydration of DTBM for systems S4 and S5. Focusing on the hydration of methyl group of DTBM (i.e., C4 atom), we find that though the trend of hydration is similar to that of other atomic sites of DTBM, the peak height of DTBM$_{C4}$-water distribution function is always below bulk density even for system S5. In this regard we note that the first peak in this rdf appears at about 3.6 Å with first minimum at 5 Å and a solvent separated minima at 7.3 Å which is in consistent with the hydration of methane in water reported elsewhere [144]. Nevertheless, the first peak height of this rdf gives us an indication that DTBM molecules may prefer to be associated with itself and caffeine molecules through its methyl groups. This fact further implies that these methyl groups of DTBM prefer caffeine over water in its solvation shell even after disruption of DTBM aggregates.

From all the above observations the inhibitory effect of caffeine on hydrophobic aggregation of DTBM molecules is quite evident. But, the underlying mechanism by which caffeine prevents the self-aggregation of DTBM is unclear. Thus, in the following sections we try to define a mechanism by which the aggregation of hydrophobic solutes DTBM is inhibited in presence of higher caffeine : DTBM stoichiometric ratio in the system.

Self-association of caffeine:

It has been found in the literature that the ability of self-assembly is a general property of small organic molecule inhibitors [133, 134, 145]. In view of this we have also analyzed the self-association of caffeine in different systems. Different experimental studies, like, vapor pressure osmometry, sedimentation equilibria, NMR, and other spectroscopic methods [55, 56, 146] have demonstrated that caffeine molecules self-associate in aqueous solution by forming 'vertical-stacking' of clusters. The probability distribution of preferred

'vertical-stacking' is also observed in some theoretical studies [77]. In order to examine the orientational preference of aromatic plane of a caffeine molecule with that of another caffeine molecule, we define the inter-plane angle as the angle between the vectors normal to the respective planes. In Fig. 4-5 we have shown the normalized probability distribution of cosine P(cos(θ)) of inter-plane orientational angles made by the plane normal vectors of two caffeine molecules. The cosine of angle θ close to 1 and -1 corresponds to parallel and anti-parallel orientations, and cos(θ) close to 0 corresponds to perpendicular orientation of aromatic plane of caffeine molecules. We have observed that the preferred arrangement of two caffeine plane are parallel (and anti-parallel), which depicts aromatic stacking of caffeine one above another in parallel arrangement. Similar distribution probabilities of different orientation is also observed for the positively charged guanidium ions in water [147].

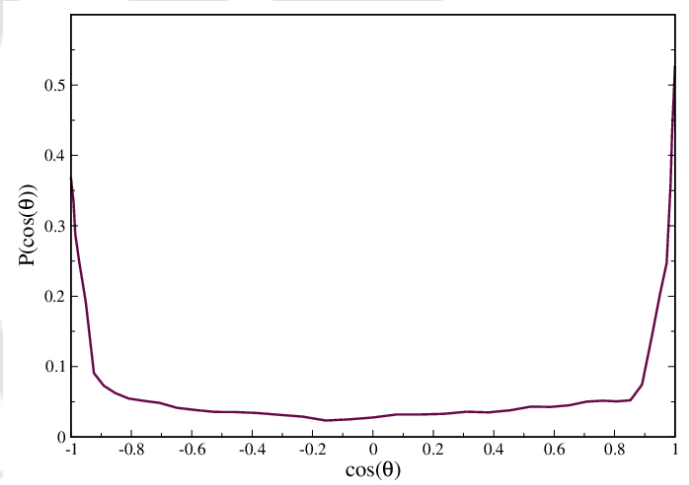

Figure 4-5. *Orientational preference of aromatic plane between two caffeine molecules.*

In order to examine the self-association of caffeine molecules in different solutions considered in this study, we have shown the rdf of center of mass of caffeine around caffeine and are shown in Fig. 4-6 (a). The self-association tendency of caffeine increases only slightly from system S1 to S5 as the concentration of caffeine doesn't change much in the systems. The rdfs of water around caffeine also depicts the same behavior (see Fig. 4-6 (b)) . This indicates that it is not the aggregation propensity of caffeine, however the cluster size and number of aggregates which effects the DTBM aggregation. In order to make a quantitative estimation of self-association of caffeine molecules, we have performed the cluster structure analyses of caffeine and examine the probability distribution of caffeine

clusters of different sizes (m_n) with respect to monomer (m_1). This is shown in Fig. 4-6 (c). Following earlier studies, to estimate the cluster size, we have considered clusters as an assembly of stacked caffeine molecules, with neighboring caffeine molecules within 6.4 Å of each caffeine molecules [53, 54].

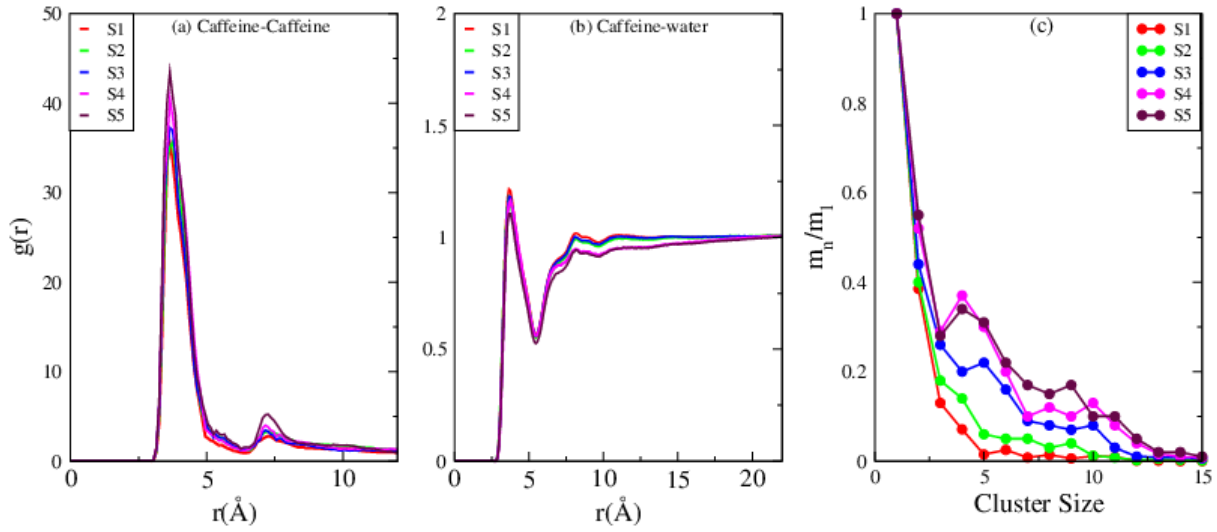

Figure 4-6. *Radial distribution functions involving (a) center of mass of caffeine around caffeine, (b) water around caffeine, and (c) probability distribution of caffeine clusters of different sizes (m_n) with respect to caffeine monomer (m_1).*

From Fig. 4-2 (a) we can see that association tendency of DTBM remains constant after 60 ns. Therefore, we have considered the first 60 ns for caffeine cluster structure analyses to interpret the effect of caffeine clusters on DTBM association. It is observed that although the concentration of caffeine is above the solubility limit, all caffeine molecules does not cluster together to form a single assembly. It has been observed in our analyses that the probability of formation of cluster size greater than 15 is negligible, and therefore those are not shown in the figure. It can further be seen that the probability of formation of caffeine clusters of size 3 to 10 increases from system S0 to S5.

Mechanism of inhibition of hydrophobic aggregation of DTBM by caffeine aggregates:

Now the key question is how these higher numbers of medium order caffeine aggregates inhibits the hydrophobic association of DTBM molecules. From the above analyses of hy-

dration of DTBM molecules, it is clear that in caffeine solutions with higher stoichiometric ratio of caffeine, the hydration of DTBM increases extensively compared to pure water. This relatively higher hydration of DTBM in caffeine solution (despite its water-insolubility) is only possible if 1) The self-association of caffeine provides a hydrophobic environment for DTBM molecule (within the confinement of caffeine aggregates), and/or 2) if there is a strong interaction of DTBM and caffeine, due to which DTBM molecules prefers to bind with caffeine, leading to disruption of DTBM aggregates. In this regard it should also be kept in mind that several factors could results in time-dependent inhibition by aggregates, such as, cluster size of caffeine aggregates, arrangement of caffeine in aggregates, role of interaction of caffeine aggregates with DTBM, number of caffeine, and number of DTBM. As the inhibiting action of organic aggregates is extremely sensitive to the stoichiometric ratio of both of inhibitors and hydrophobic biomolecules [127, 148], therefore, in this study we have kept the number of DTBM molecules fixed in all systems, which helps us to better understand the role of caffeine aggregates solely on hydrophobic association of DTBM.

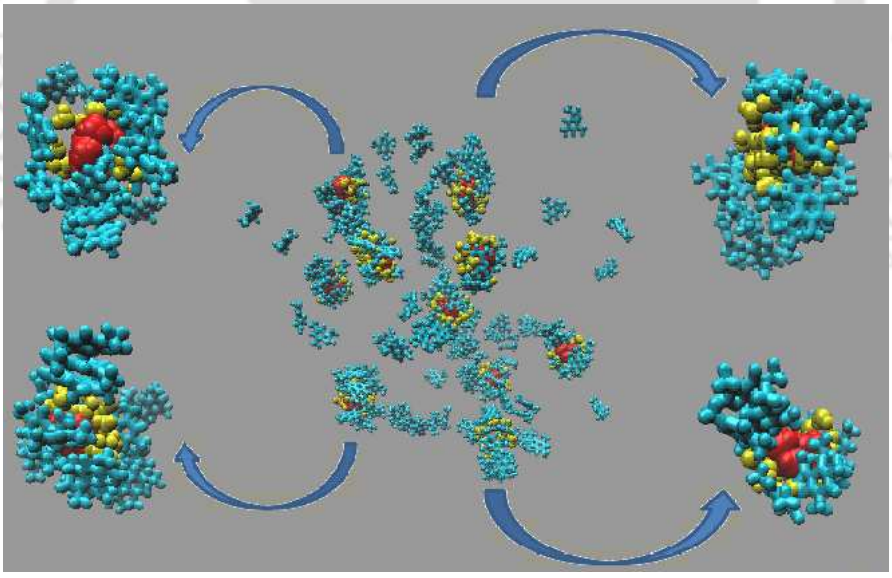

Figure 4-7. *Snapshot of water around DTBM inside the confinement of caffeine for system S5 at 100 ns. Red, cyan and yellow colors are for DTBM, caffeine and water inside the confinement respectively.*

As the hydration of DTBM increases with increasing caffeine ratio, it can be assumed that the only probable location of hydrophobic DTBM molecules is some hydrophobic pocket made by caffeine in aqueous solution of caffeine. The water molecules bound to caffeine aggregates and inside the confinement of caffeine aggregates might interact with

DTBM surface leading to hydration of DTBM. In this regard we have shown the snapshots of systems S5 at 100 ns, which shows clearly how DTBM molecules are encapsulated within caffeine clusters and interaction of water with DTBM within the confinement (see Fig. 4-7).

Here it is to be noted that a single snapshot does not provide the complete picture of a given system, which, in fact, is very dynamical in nature. Therefore, to gain more insights into the interaction of caffeine and DTBM, we have calculated rdf involving center of mass of caffeine and DTBM central atom (C2) and are shown in Fig. 4-8 (a).

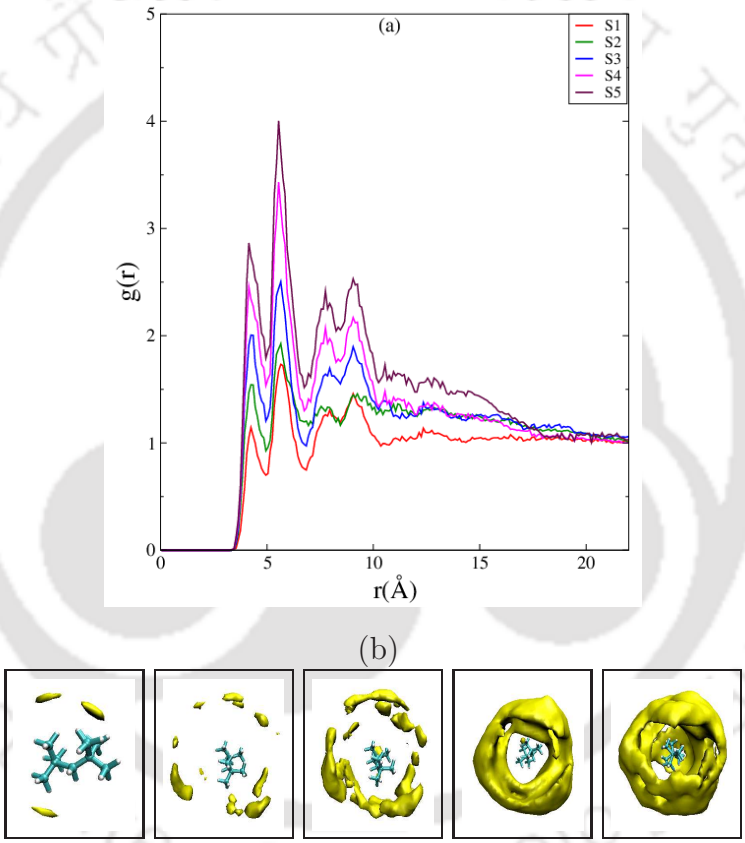

Figure 4-8. *(a) Radial distribution functions involving caffeine around DTBM for different systems, (b) spatial distribution plots for caffeine around DTBM, with an isovalue of 1.2. Left to right: Systems S1 to S5.*

We observe that although the caffeine concentration in all the systems are similar, the peak height of DTBM-caffeine rdf increases with increasing caffeine number in the system. To understand the localized caffeine-DTBM interaction pattern for the whole trajectory, we have shown the sdf plot of caffeine around DTBM with an isovalue of 1.2 for all the systems (see Fig. 4-8 (b)). The spatial density of caffeine around DTBM is

circular, and it increases with increasing caffeine number in the system. This suggests the encapsulation of DTBM molecules by caffeine, which results in inhibition of DTBM self-aggregation. For the encapsulation and physically blocking the DTBM molecules to interact with each other to form aggregates, there should be enough number of medium-sized caffeine clusters, which form a tight confinement around DTBM molecules. Therefore, an increase in caffeine stoichiometric ratio leads to better inhibition by caffeine. Here it is worth to mention that the confinement created by the medium-sized caffeine cluster is not void of any water molecules. Indeed, the average number of water molecules around DTBM inside the confinement of caffeine aggregates is found to be 16.76 for system S5.

In order to understand the binding affinities of DTBM molecules with caffeine and water, we have calculated binding free energies from potentials of mean force (PMF). PMF can be obtained from the corresponding rdf, g(r), using the relation:

$$W(r) = -k_B T ln g(r) \tag{4.2}$$

where k_B is the Boltzmann constant, T is the temperature. The binding free energy [149] of solute-solute and solute-solvent can be calculated from the volume integral of the PMF as

$$E_b = -k_B T ln[4\pi/V \int_0^{r_c} exp(-W(r)/k_B T) r^2 dr] \tag{4.3}$$

where

$$V = 4\pi r_c^3/3 \tag{4.4}$$

is the volume occupied by the associated pair of interacting molecules. A negative value of E_b shows attractive affinity and the larger the value of E_b (absolute value), the higher is the affinity of binding. In Table 4-4 we have shown the binding affinities of DTBM with DTBM, caffeine and water.

Table 4-4. Binding energy (in kcal/mole) of DTBM with itself, Caffeine and Water

Systems	DTBM-DTBM	DTBM-Caff	DTBM-water
S0	-6.68 (± 0.02)		-5.59 (± 0.01)
S1	-6.69 (± 0.02)	-5.75 (± 0.01)	-5.61 (± 0.02)
S2	-6.65 (± 0.01)	-5.88 (± 0.01)	-5.65 (± 0.03)
S3	-6.60 (± 0.02)	-6.09 (± 0.02)	-5.67 (± 0.02)
S4	-6.30 (± 0.03)	-6.29 (± 0.02)	-5.86 (± 0.02)
S5	-6.12 (± 0.02)	-6.47 (± 0.01)	-5.98 (± 0.01)

The binding affinity values of DTBM with different solution species give explanation of our observation of aggregation propensity of DTBM in different caffeine solution. It can be seen that binding free energy of DTBM with itself is the highest, and with water it is the lowest. DTBM-DTBM binding free energy is the highest for S0 and lowest for S5, whereas, DTBM-caffeine binding free energy increases with increasing caffeine number in the system.

On molecular level, the effect of caffeine on DTBM aggregation can be characterized in terms of preferential molecular interaction between DTBM-caffeine and DTBM-water interaction relative to DTBM-DTBM interaction [150]. The distribution functions are directly related to the cosolvent preferential interaction parameter through Kirkwood-Buff integrals [94-98], which provide a statistical thermodynamic framework for evaluating the preferential interaction parameter, τ_{cw}^{d}, for a solute (d, for DTBM), in the solvent mixture of water (w, for water) and a cosolute (c, for caffeine) via-

$$\tau_{cw}^{d} = \rho_c(G_{dc} - G_{dw}) \tag{4.5}$$

where, ρ_c is the number density of the cosolvent (caffeine) and G_{dc} and G_{dw} are Kirkwood-Buff G factors.

Preferential interaction parameter of DTBM with itself over water τ_{dw}^{d} can be calculated by the following expression:

$$\tau_{dw}^{d} = \rho_d(G_{dd} - G_{dw}) \tag{4.6}$$

We have also evaluated the preferential interaction parameter of DTBM with itself over caffeine τ_{dc}^{d} by the expression:

$$\tau_{dc}^{d} = \rho_d(G_{dd} - G_{dc}) \tag{4.7}$$

where ρ_d is the number density of DTBM in a given system. G_{dc}, G_{dw}, and G_{dd} are the Kirkwood-Buff integrals [107, **?**] and they can be evaluated from the DTBM-caffeine, DTBM-water and DTBM-DTBM distribution functions respectively.

For a grand canonical ensemble, G_{ij} is defined as

$$G_{ij} = 4\pi \int_0^\infty [g_{ij}(r) - 1] r^2 dr \tag{4.8}$$

For a closed system, the above equation can be written as

$$G_{ij} \approx 4\pi \int_0^R [g_{ij}(r) - 1] r^2 dr \tag{4.9}$$

where R is the distance where the integral approaches zero.

Preferential interaction parameters for DTBM at different stoichiometric ratio of caffeine are shown in Fig. 4-9.

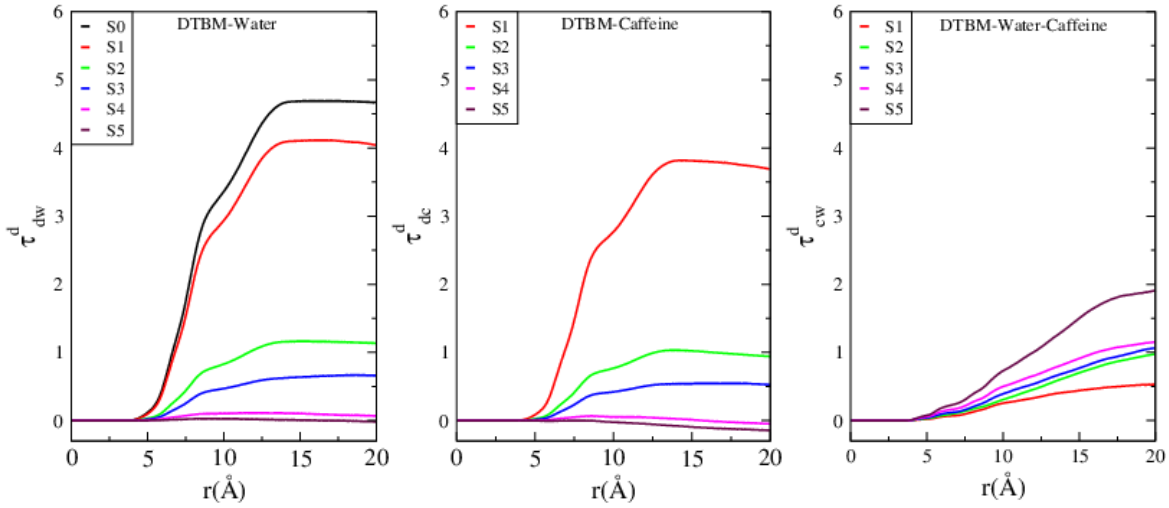

Figure 4-9. *Preferential interaction parameters of DTBM for like molecules, caffeine and water in different systems.*

From the figure we can see that for system S0 to S3 $\tau^d_{dw} > 0$, and $\tau^d_{dc} > 0$ indicating the preferential accumulation of DTBM around itself relative to water and caffeine. However, as caffeine number increases, τ^d_{dw} and τ^d_{dc} decreases, and for system S4 and S5, τ^d_{dc} is negative implying a relatively more preference for caffeine over itself of DTBM molecules in higher stoichiometric ratio of caffeine solutions. Now it seems that there is a constant competition between DTBM hydration and DTBM caffeine interaction as caffeine number increases in the solution. Preferential interaction parameters calculated for DTBM with caffeine over water, τ^d_{cw}, show positive values, indicating more preference towards caffeine over water by DTBM molecule. τ^d_{cw} increases with increasing caffeine number from system S1 to S5 indicating increasing DTBM-caffeine interaction with increasing caffeine number in the system. Given the above observations that there is a sharp drop in τ^d_{dw} and τ^d_{dc} values from S1 to S5 is possible only when DTBM molecule is confined within the caffeine clusters.

Therefore, all the above analyses clearly illustrates the physical blocking of DTBM molecules by caffeine aggregates. Thus, the higher propensity of DTBM-caffeine and

DTBM-water interactions at higher caffeine : DTBM stoichiometric ratio as well as the entrapment of DTBM molecule in caffeine clusters are the reason for the dissolution of DTBM aggregates.

Effect of caffeine on previously aggregated DTBM systems:

It can be assumed from the above analyses that caffeine aggregates, once formed, can physically blocks the DTBM molecules, thereby preventing them to form hydrophobic aggregates. To further characterize whether caffeine clusters can sequester DTBM molecules from aggregates and break the already formed DTBM clusters, we have considered an equilibrated DTBM-water system where DTBM clusters are already formed, and then we added 100 caffeine molecules to it (system S6).

In Fig. 4-2 (a), we have shown the monomer count of DTBM as a function of simulation time (ns). Although the DTBM clusters are already aggregated in the initial structure, we observed the presence of monomers as time progresses. The rdfs involving DTBM-DTBM central carbon and methyl-methyl of DTBM in Fig. 4-3 (a and b) show a decrease in peak height compared to system S0, where all DTBM molecules are aggregated. This change in peak heights depicts the role of caffeine clusters in prohibiting hydrophobic aggregation of DTBM. However, the peak heights of system S6 are higher compared to S4, although the systems have same stoichiometric ratio of caffeine and DTBM. Further, for system S6, the sdf plot of DTBM around DTBM (see Fig. 4-3 (c)) reveals that a complete disruption of already aggregated DTBM molecules is not achieved when caffeine molecules with the same stoichiometric ratio (of that of system S4) are added in DTBM-water binary mixture. Since the stoichiometric ratios of caffeine to DTBM are the same for systems S4 and S6, we have, further, computed potential of mean forces (PMFs) of DTBM association for these two systems. It is found that for system S6 the PMF of DTBM association is -6.71 kJ/mol with a standard error (calculated using block averaging method) of $\pm$ 0.77 and the same for system S4 it is -3.16 kJ/mol with a standard error of $\pm$ 0.60. Here it is worth mentioning that even though our simulations are quite lengthy (100 ns), the difference between the PMF values of DTBM association for systems S4 and S6 might be an outcome of shortage of simulation time for the latter system. Therefore, although caffeine molecules fail to disaggregate already associated DTBM molecules completely, the time dependence of breaking the DTBM aggregates validate our proposed mechanism of inhibition of hydrophobic self-association of DTBM by caffeine aggregates.

■ SUMMARY AND CONCLUSIONS

In this work, we have carried out molecular dynamics simulations of 10 hydrophobic model DTBM molecules in pure water and in a regime of caffeine : DTBM stoichiometric ratio. In order to monitor the effects of caffeine on DTBM aggregation, we have calculated radial distribution functions between the central carbons of DTBM, and between methyl group carbons. We have also analyzed coordination number at first minima in rdf and spatial distribution plot to check the overall interaction of DTBM-DTBM, DTBM-caffeine and DTBM-water in caffeine solution. Our results show that the tendency of DTBM aggregation is only slightly affected at lower stoichiometric ratio of caffeine. Hydration of DTBM is unaffected initially with increasing caffeine number, but as the caffeine : DTBM stoichiometric ratio increases to 10 : 1 or more, the hydration of DTBM increases. The sharp increase in DTBM hydration despite the fact that it is highly hydrophobic in nature shows the disaggregation of DTBM. The preferential interaction of DTBM with caffeine over water is positive for all system, suggesting the more preference of DTBM molecules for caffeine over water. Cluster structure analyses, sdf plots of caffeine around DTBM and snapshots of the trajectory reveals that caffeine aggregates form a hydrophobic environment around a DTBM molecule, and DTBM interacts with water within the confinement of caffeine aggregates. DTBM-DTBM binding free energy is found to be more favorable than DTBM-caffeine for all systems, but it becomes more unfavorable with increasing caffeine number, whereas, DTBM-caffeine binding free energy becomes more favorable. To further verify our observation, we have considered one more system where DTBM molecules are already aggregated and formed cluster, and caffeine molecules are added later to check the sequestering ability of DTBM by caffeine molecules. We have observed the breaking of DTBM cluster in presence of caffeine in the system. These findings ultimately lead us to propose that, at high caffeine : DTBM stoichiometric ratio, due to increase in DTBM-caffeine interaction and presence of higher numbers of caffeine clusters, DTBM molecules are encapsulated within a number of different caffeine clusters. These caffeine clusters form a hydrophobic environment for DTBM in which the presence of considerable amount water molecules also ensures the hydration of DTBM . Moreover, these caffeine clusters then also physically block the other DTBM molecules to interact with the encapsulated DTBM molecule, leading to disruption of DTBM clusters in concentrated caffeine solutions.

As the hydrophobic interaction is a substantial factor to the self-aggregation of proteins,

the atomic level description of disruption of protein aggregates with caffeine may be revealed using molecular simulation study, and work along this direction is already underway.

भारतीय प्रौद्योगिकी संस्थान गुवाहाटी
Indian Institute of Technology Guwahati

Chapter 5

The Role Caffeine as an Inhibitor in Aggregation of Amyloid Forming Peptides

"Protein aggregation is arguably the most common and troubling manifestation of protein instability, encountered in almost all stages of protein drug development. Protein aggregation, along with other physical and/or chemical instabilities of proteins, remains to be one of the major road barriers hindering rapid commercialization of potential protein drug candidates."

– W. Wang *Int J Pharm.* **289**, 1 (2005)

Overview:

In **Chapter 4**, we have observed the inhibiting effect of caffeine on hydrophobic aggregation of purely hydrophobic model DTBM molecules. These results further led us to study the effect of caffeine directly on protein aggregation, which is more complex compared to the purely hydrophobic association. From the results of several studies it is believed that caffeine can prevent the development of Alzheimer's disease. However, the molecular mechanism of the therapeutic potential of caffeine is largely unknown. In this chapter, we have investigated the effect of caffeine on the aggregation of amyloid-β derived switch-peptide with varied stoichiometric ratio of caffeine to peptide. Our molecular dynamics study of peptides in pure water show the formation of β-sheet conformation, which is prevented to a large extent in presence of 10:1 or more caffeine to peptide ratio. We have observed that caffeine can inhibit the formation of β-sheet by interacting with the peptide aromatic moiety. A detailed molecular dynamics analyses on inhibition of peptide aggregation by caffeine further revealed that caffeine molecules form hydrogen bonds with peptide thereby weakening the interstrand hydrogen bonds between peptides. Again, the self-aggregated caffeine clusters form a hydrophobic environment around hydrophobic residues of peptides, and physically blocks them to interact with each other.

■ INTRODUCTION

Physicochemical properties such as conformational constrains, hydrophobicity, net charge and aromatic stacking interactions of aromatic residues play a key role in aggregation of otherwise normally soluble proteins into insoluble amyloid aggregates. Different experimental studies revealed that a notable frequent occurrence of aromatic residues in different amyloid-related peptides raises the possibility of amyloid formation process. Amyloid fibril formation is basically a process of intermolecular recognition. π-stacking interaction can provide specific directionality and orientation by specific pattern of stacking leading to ordered amyloid structure. The immediate previous chapter of this thesis dealt with inhibition action of caffeine on aggregation of purely hydrophobic DTBM molecules. Although the hydrophobic effect is one of the major factors stabilizing the tertiary structures of proteins, however, hydrogen bonding and electrostatic interactions also play crucial roles in protein aggregation. Therefore, in this chapter, we study the inhibiting effect of caffeine on amyloid aggregation with more realistic 18-residue amyloid-β derived switch-peptide. Aggregation of Amyloid peptides (Aβ) plays a central role in the pathogenesis of Alzheimer's disease, the devastating neurodegenerative disease. Since, the Aβ peptide exhibits a high propensity for spontaneous aggregation, the initial stages of oligomer formation are difficult to characterize. Mutter's group have introduced conformational switch-peptides by incorporation of an intramolecular O to an N-acyl migration-based molecular switch that allows the controlled initiation of a folding process even in highly amyloidogenic polypeptides [151]. Therefore, to understand the effect of caffeine on amyloid aggregation and mechanism and mode of caffeine action we have used a switch peptide (SwP) which contains two Phe rings in its side chain [152]. The amino acid sequence of the SwP is as follows:

AcSLSLHQKLVFFSEDVSLGNH$_2$ (S$_{on}$ or Switch-on state)

AcSLSLHQKLVFF(H$^+$)SEDVSLGNH$_2$ (S$_{off}$ or Switch-off state)

In SwP the hydrophobic core of Aβ, which comprises of residues 14-24 (HQKLVFFSEDV), is flanked by two (Leu-Ser)$_n$ oligomers.

In recent study of the investigation of early stages of aggregation of Aβ-derived switch-peptides, it has been revealed that aromatic stacking of phenylalanine (Phe) residues occur prior to aggregate formation, which ultimately leads to the formation of amyloid fibril [152]. This hypothesis (regarding the key role of π-stacking interaction) postulates that drugs that can block π-stacking interaction may inhibit the amyloid formation. Different

theoretical and experimental studies showed that caffeine molecules form complex with different biomolecules, DNA, and drug molecules with π-stacking interaction [51, 52]. Caffeine molecule also self-aggregates in aqueous solution and the aromatic ring of its play a central role to form high-order caffeine clusters [53-56]. Therefore, caffeine molecule seems to be a potential candidate as an inhibitor of amyloid, and can act as a potent drug controlling amyloid disease. Thus, in this work, we attempt to explore the effect of caffeine on protein aggregation and to understand the underlying mechanism of caffeine action.

The organization of the rest of the chapter is as follows. We first present the models and details of simulations. Results are discussed thereafter, and the last section includes concluding remarks with a brief summary.

■ MODELS AND SIMULATION METHOD

The caffeine solute was modeled by using AMBER generated all atom force field as described in **Chapter 2** [53]. For the SwP (S_{on} or Switch-on state) the ff99SB force field parameters were used [153], and the popular extended simple point-charge (SPC/E) model was employed for water molecules [132].

The initial configurations of the systems were prepared with packmol program [86]. At first, five fully stretched SwP were randomly placed and immersed in a cubic box of water with sufficient separation between them. Here we note that the inhibition action of the inhibitor on peptide is found to be extremely sensitive to the stoichiometric ratio of peptide and inhibitor as pointed out by several studies [148, 127]. Increasing the protein concentration dramatically diminishes the potency of different small molecule inhibitors. On the other hand, increasing the inhibitor concentration by similar amount would return efficacy. Therefore, the effects of inhibition of such small molecules on protein aggregation are regarded as a stoichiometric mechanism, with stoichiometries like thousands of inhibitor molecules to one protein [127, 128]. From the studies of different small molecule inhibitors it is revealed that inhibitors inhibit amyloid formation by forming chemical aggregates with the like molecules [133, 134, 145]. In our previous studies we have observed that caffeine molecules self-aggregate above its solubility limit of 0.1 M [53]. Therefore, in this study we kept the concentrations of caffeine for all systems slightly above its solubility limit. To the initial structures of five SwP in water we varied the number of caffeine molecules, and an overview of different systems considered in this study is presented in Table 5-1.

Table 5-1. Overview of Simulations[a]

System	N_{caff}	N_{SwP}	N_{wat}	C_{caff}(M)	caffeine : SwP	box length(Å)	ρ (g cm^{-3})
S0	0	5	4200	0	—	50.52	0.98
S1	15	5	4200	0.19	3:1	50.91	0.99
S2	50	5	15000	0.17	10:1	77.46	1.00
S3	80	5	25000	0.17	16:1	92.22	0.99
S4	100	5	25000	0.20	20:1	92.61	0.99

N_{caff}, N_{SwP}, and N_{wat} represent the number of caffeine, the number of SwP and the number of water molecules respectively. C_{caff} and ρ refer to the caffeine concentration and the density of the system respectively.

The MD simulations were conducted using AMBER 12 package [61] in isothermal isobaric (NPT) ensemble. All simulations were subjected to energy minimization for 5000 steps, with first 2500 steps in steepest descent method followed by the equal number of steps in conjugate gradient method. The systems were then heated gradually by increasing the temperature from 0 to 300 K over 180 ps in a canonical ensemble (NVT). Langevin dynamics method was used to maintain the desired temperature [154]. All the simulations were then equilibrated for 5 ns in an isothermal-isobaric ensemble (NPT) at 1 atm pressure, which were again followed by 95 ns production run in NPT ensemble. Berendsen's barostat [87] with a pressure coupling constant of 2 ps was used to maintain the physical pressure. The short-ranged van der Waals (VDW) interactions were calculated using the switching function, with a cutoff radius of 10 Å . The long-ranged electrostatic interactions were calculated using the particle mesh Ewald method [155]. Bonds involving hydrogens were constrained by use of SHAKE algorithm [137].

■ RESULTS AND DISCUSSION

Self-aggregation of Switch-peptide in pure water and different caffeine solution:

Different proteins have been reported to form amyloid fibrils. A combination of different steps ultimately leads to the formation of the fibrils. In the initial stage, protein monomers self-assemble and oligomers are formed. These oligomers later finally evolve into mature amyloid fibrils by β-sheet formation. Due to the long chain length of the SwP with 18 amino acids present, and as we have started with placing them randomly in the simulation box without any constrains, the formation of the ordered β-sheet structure is least expected in MD simulations. However, we observe the formation of anti-parallel β-sheets in the final state of the oligomer formation of peptides for system S0 (see Fig. 5-1). This indicates the highly amyloidogenic nature of SwP in pure water.

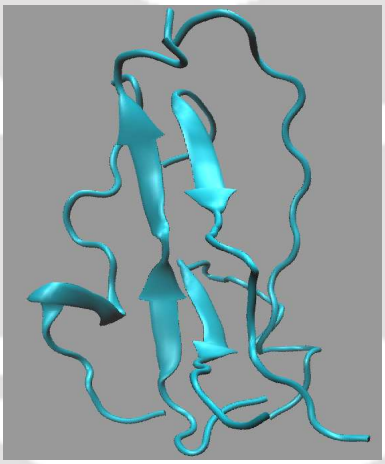

Figure 5-1. *Snap-shot of peptide SwP aggregation in system S0 at the final state.*

To probe the time evolution of peptide aggregation, we have shown the distribution of cluster sizes of peptide with simulation time for all systems (see Fig. 5-2). The two peptides are considered to form clusters when residues of one peptide are within 7 Å of residues of another peptide. We observe that in pure water system all the five peptide aggregate and form stable clusters of size 5 after 30 ns simulation run. In presence of caffeine in system S1, we still observe cluster formation and breaking all throughout the simulation. However, with increasing caffeine number in the system, the aggregate formation tendency of caffeine decreases, and in system S3 and S4, peptide exists as monomers at 100 ns.

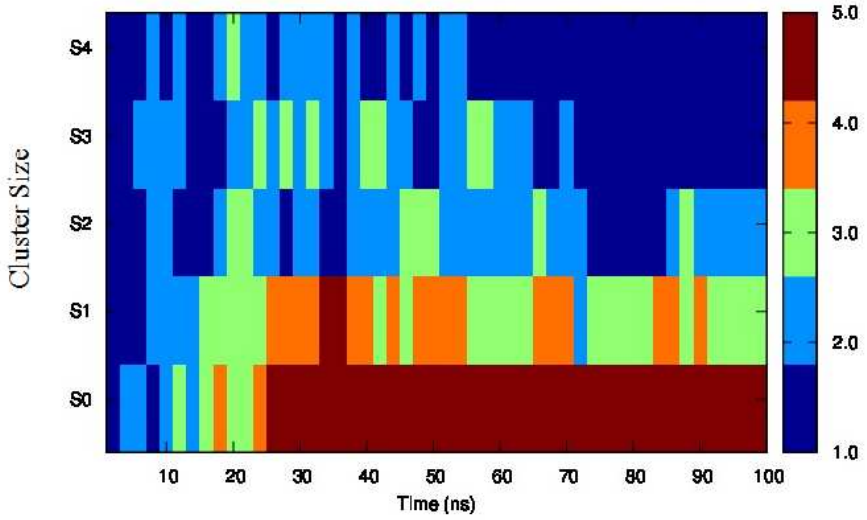

Figure 5-2. *Time evolution of peptide aggregation, shown as the distribution of clusters of different sizes of peptide with simulation time for all systems.*

To probe the initial stages of SwP aggregation, we have shown the snap-shots of all the systems at a fixed time interval (see Fig. 5-3). The hypothesis of aromatic stacking of Phe residues of SwP prior to aggregate formation is well established in our previous study [152]. In system S0, we also notice aromatic interactions between the Phe residues of the peptides, which ultimately leads to aggregation. This observation is in accordance with our earlier study [152]. However, in system S1, the interactions between the Phe residues are hindered to some extent, although peptide molecules aggregate towards the end of simulation. On increasing caffeine : peptide ratio to 10:1 in system S2, we observe a further restriction in the interaction between Phe residues as is observed in the aggregation tendency of the peptides. However, some intermolecular peptide-peptide interactions still persist through other side-chain hydrophobic residues (discussed below). In system S3, all the Phe residues are well separated from each other even up to 100 ns and self-association is restricted. A further increase in caffeine number prevents the peptide aggregation from the very early stage of simulation. Therefore, we observe that in 20:1 stoichiometric ratio of caffeine, the self-association tendency of SwP decreases significantly.

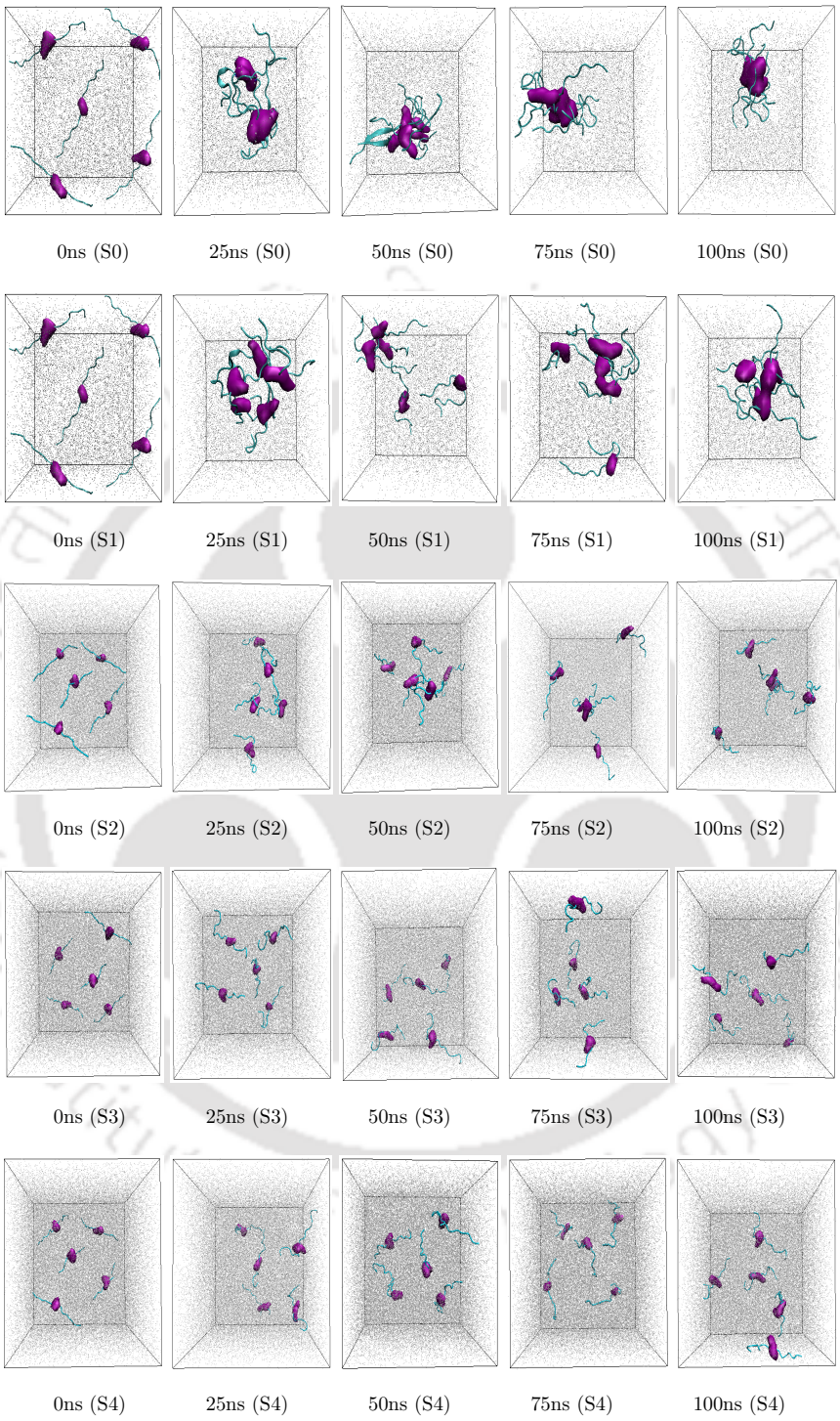

Figure 5-3. *Snapshots of SwP association in all the systems at different time intervals. The contour density of Phe residue is shown in purple color and grey color represents water molecules. Caffeine molecules are left-off to enhance the visual clarity.*

In order to characterize the effect of caffeine on Phe-Phe interaction, we have calculated the radial distribution functions (rdfs) between the intermolecular Phe residues of SwP for all the systems and they are shown in Fig. 5-4 (a). For system S0, the first peak appears at 5 Å along with a well developed second peak at 10.5 Å. With increasing caffeine number in the system, the peak height decreases drastically, and the peak positions shift to higher distances. This implies that the separation between the Phe residues increases, suggesting the blocking of aromatic Phe-Phe interaction in presence of caffeine.

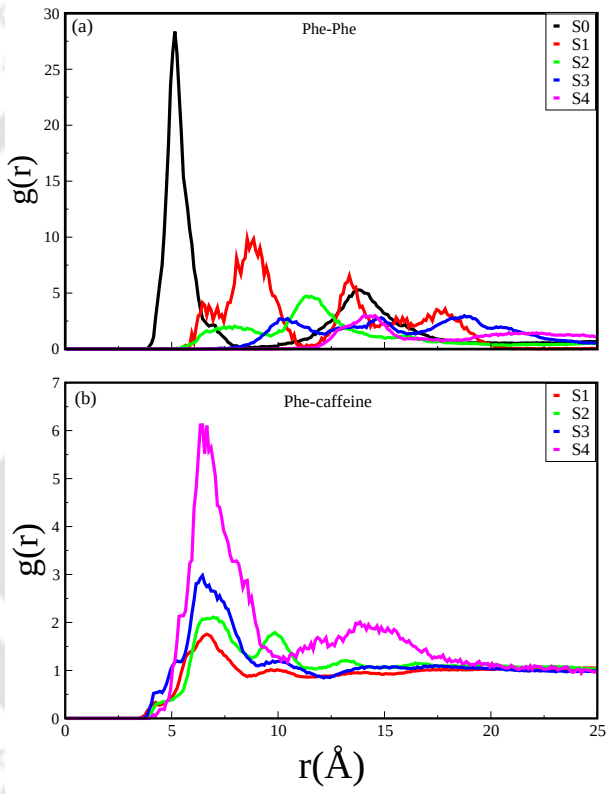

Figure 5-4. *Radial distribution functions of (a) Phe around Phe, and (b) caffeine around Phe for different systems.*

To analyze the conformational changes of the peptides in pure water and in different caffeine solutions, we have shown the dynamics of secondary structure of peptide and these are shown in Fig. 5-5 (a-e).

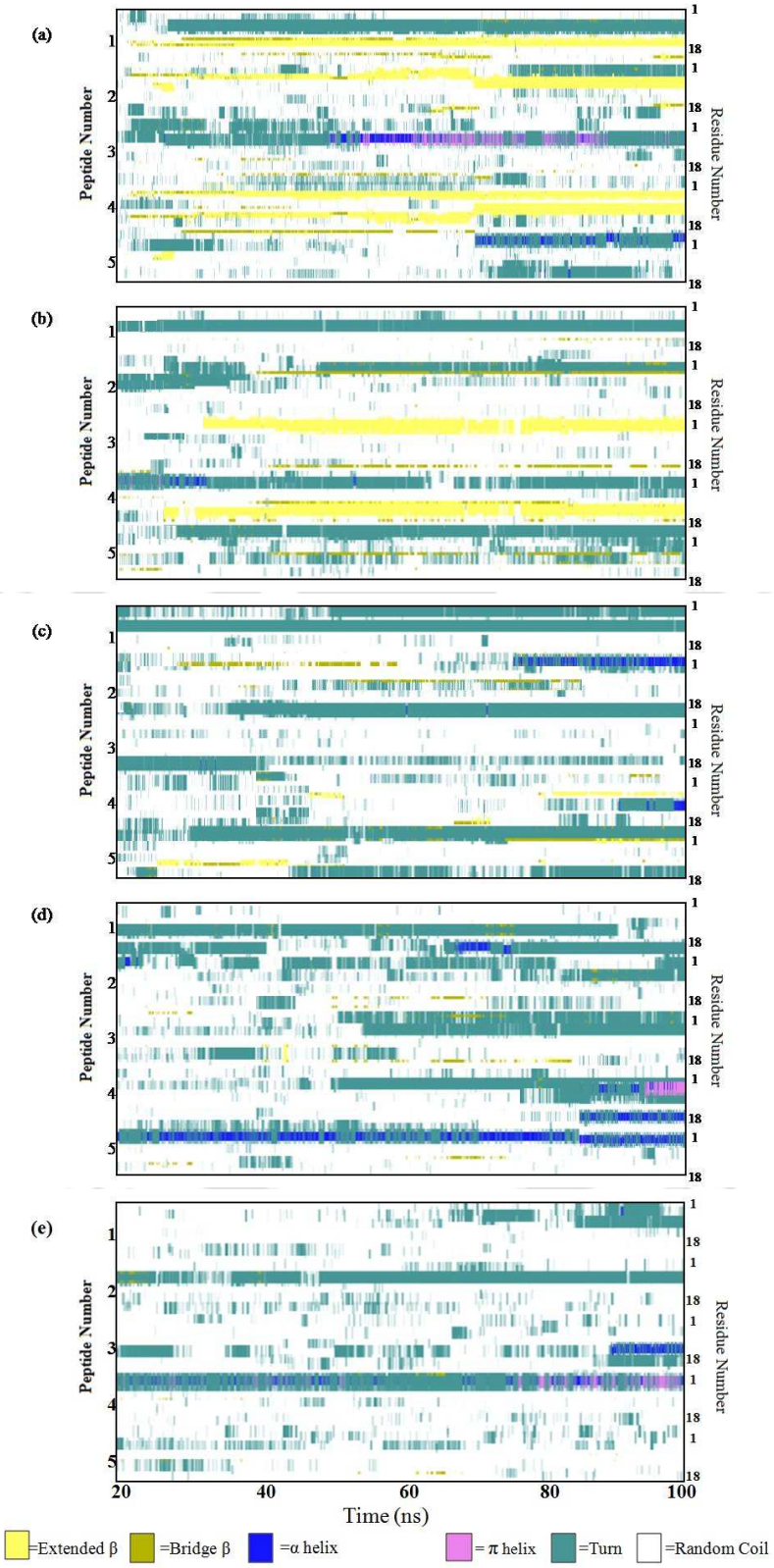

Figure 5-5. *Secondary structure analyses. (a) system S0, (b) system S1, (c) system S2, (d) system S3, and (e) system S4.*

For system S0, we observe the formation of highly ordered β-sheet conformation (yellow color) from the very early stage of the simulation, which remains intact up to 100 ns. The percentage of β-sheet structure slightly decreases in presence of caffeine in system S1, but the system still contains high amount of β-sheets. With further increase in caffeine ratio in the system in S3 and S4, the β-sheet formation is negligible. This indicates that 3:1 stoichiometric ratio of caffeine with peptide is not sufficient to prevent β-sheet formation, however, higher stoichiometric ratio of caffeine and SwP can definitely prevent ordered β-sheet formation as well as the aggregation of SwP.

The residue-residue contact maps of peptides for each pair of residues at the final step of simulation are shown in Fig. 5-6 (a-e). The highest inter-peptide contact is observed for system S0. With increasing caffeine number, the pairwise inter-peptide residue-residue contact decreases, and in system S4, the inter-peptide contact is negligible.

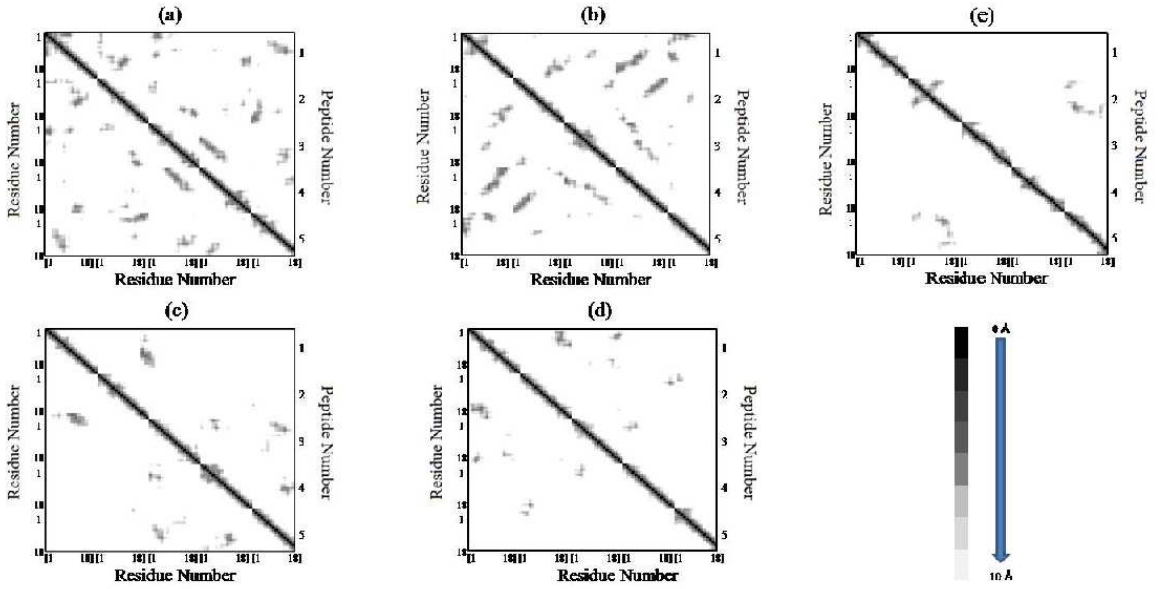

Figure 5-6. *Residue-residue contact maps of peptides. The graph square is colored black at 0.0 Å distance. It is linear gray between distance 0.0 and 10.0 Å and white when it is greater than 10.0 Å . (a) system S0, (b) system S1, (c) system S2, (d) system S3, and (e) system S4.*

To examine the energetic aspects of peptide association and the effect of caffeine on to it, we have decomposed the total interpeptide and peptide-caffeine interactions in to van der Waals (vdw) and electrostatic components, and these are presented in Table 5-2. It is apparent that the inter-peptide vdw interaction energy of system S0 is favorable (more negative) in absence of caffeine. With increasing caffeine number, this vdw energy

increases (less negative), which indicates less favorable interaction between the peptides. In contrast, the average intermolecular electrostatic energy does not change much in all the systems. Furthermore, with increasing caffeine : peptide stoichiometric ratio, both vdw and electrostatic components of caffeine-peptide interaction energy become more and more favorable.

Table 5-2. van der Waals and electrostatic interaction energy (in Kcal/mol) of SwP with itself and with caffeine

Systems	$VDW_{SwP-SwP}$	$Electrostatic_{SwP-SwP}$	$VDW_{SwP-caff}$	$Electrostatic_{SwP-caff}$
S0	-158.48	-2101.26	——	——
S1	-119.22	-2098.58	-96.31	-44.26
S2	-74.76	-2003.43	-228.36	-121.44
S3	-58.56	-1988.35	-299.31	-171.23
S4	-41.95	-1986.44	-323.12	-190.14

Previous studies of the self-association of proteins have already reported that the inter-protein hydrogen bonding interactions contribute significantly to the formation and stabilization of β-rich protein structures [156-159]. Therefore, to further characterize the protein-protein interaction, we have estimated the average number of intermolecular peptide-peptide H-bonds for all the systems (see Table 5-3). A hydrogen bond is assigned if the distance between the donor (D) and acceptor (A) atom is less than 3.5 Å , and simultaneously, a maximum 45^0 angle of H-D-A is considered. The results clearly depict that the average number of intermolecular H-bonds between peptides decreases rapidly with increasing caffeine : peptide ratio.

Table 5-3. Average intermolecular SwP-SwP and SwP-caff hydrogen bonds; and average solvent accessible surface area (SASA) per SwP for different systems

System	$HB_{SwP-SwP}$	$HB_{SwP-caff}$	SASA(Å^2)
S0	22.48	—	1533.48 (± 28.31)
S1	18.57	2.62	1765.59 (± 32.05)
S2	8.77	6.76	2068.52 (± 19.10)
S3	6.02	10.24	2155.03 (± 19.46)
S4	4.21	12.64	2173.81 (± 13.02)

Parentheses show the standard errors of SASA values that are estimated by considering five number of independent blocks of 10 ns each, for last 50 ns.

A comparison of time evolution of inter-peptide hydrogen bond pattern for systems S0 and S4 is shown in Fig. 5-7. We notice a sharp increase in the total number of H-bonds between peptides in system S0 as simulation progresses, whereas the total inter-peptide H-bonds remains almost constant in system S4 over the entire simulation time. This gives a clear picture of the effect of caffeine in solution.

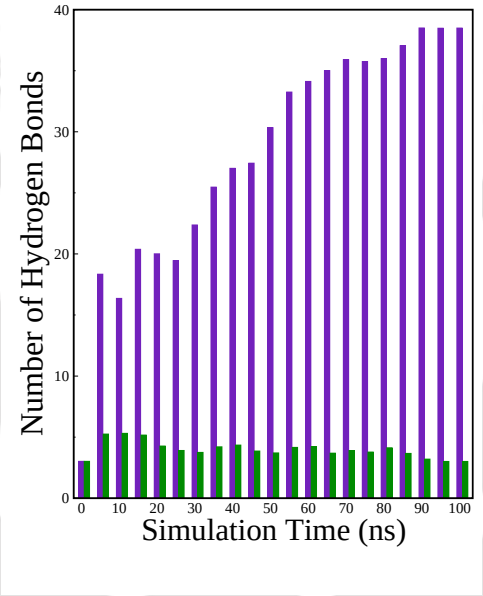

Figure 5-7. *Time evolution of the inter-peptide hydrogen bonds for systems S0 and S4. Indigo is for system S0, and green color indicates system S4.*

Again, to understand the solvation of peptides in different systems, we have calculated the average solvent accessible surface area (SASA) of the peptide in all the systems and they are shown in Table 5-3. We observe a large increase in SASA value for peptides as we move from system S0 to S4, which indicates more surface area of SwP available for solvation.

Interaction between caffeine and Switch-peptide:

The results of our earlier study on amyloid formation of SwP demonstrated that the use of small amyloid β-breaker penta-peptide, which blocks the major recognition region of peptide containing two Phe residues ultimately diminishes the ability to form stable amyloid structures [152]. Here we note that in presence of caffeine, the inter-peptide Phe-Phe interactions are largely affected (see Fig. 5-4 (a) and the discussions above). Caffeine

molecules are known to form complex with different biomolecules, DNA, drugs and other biologically active molecules by forming aromatic π-stacking interaction. Therefore, in order to understand the underlying mechanism by which the caffeine molecules prevent the peptide oligomer formation, it is important to examine the interaction of caffeine with the peptide. In order to understand the interaction of caffeine with aromatic Phe residues of the peptide, we have calculated the rdfs of caffeine around Phe residue of SwP for different systems (see Fig. 5-4 (b)). The first peak height of the rdf appears around 6.5 Å and this peak height increases with increasing the stoichiometric ratio of caffeine : peptide reflecting the enhancement of interaction of caffeine and Phe residues as one moves from system S1 to S4.

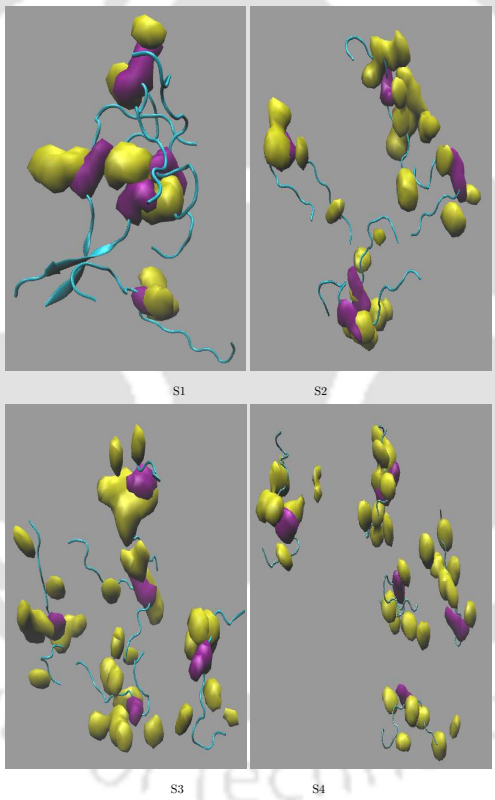

Figure 5-8. *Contour density plot for caffeine yellow around SwP within 7.5 Å of the peptide. From top left to bottom right represent system S1 to S4. Purple color represents the contour density of Phe residues of the peptide*

The contour density plots of caffeine around SwP within 7.5 Å of the peptide (averaged over the last 10 ns of simulation) for different systems show that the caffeine density (yellow) increases as we move from system S1 to S4 (see Fig. 5-8). It is also interesting to note

that although contour density of caffeine is higher around Phe residues, we also observe a non-negligible caffeine density around other residues of the peptides. This indicates that along with the Phe residues, caffeine also interacts with other non-aromatic residues of peptide.

It is worth mentioning here that peptides without any aromatic residues are also reported to form amyloid fibrils, though such structures are formed by larger peptides or over a longer timescale [160]. The presence of aromatic residues significantly accelerates the process of fibrillization. Thus, the blocking of these aromatic groups surely delays the amyloid formation. Therefore, along with the blocking of aromatic residues, it is also important for the inhibitors to possess the capability to block the other H-bonding and hydrophobic sites of the peptide so that the inter-peptide interactions can be prevented significantly.

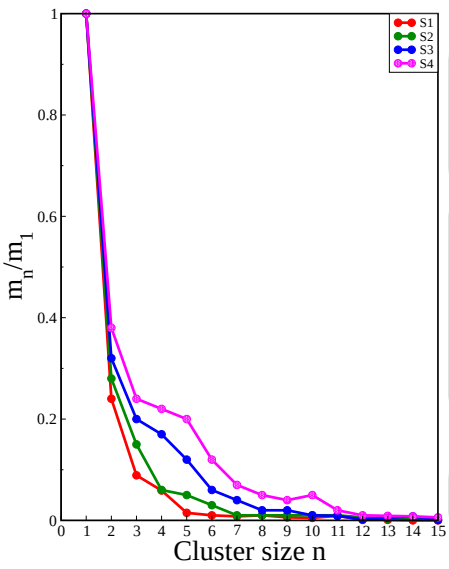

Figure 5-9. *Probability distribution of caffeine clusters of different sizes with respect monomer.*

It has been found in the literature that the ability to form promiscuous aggregates is a general property of many small organic molecule inhibitors [133, 134, 145]. Our earlier studies showed that caffeine molecules self-associate in water and form clusters by vertical stacking of one caffeine above another [53, 54]. The probability distribution of caffeine clusters of different sizes (m_n) with respect to monomer (m_1) is shown in Fig. 5-9. For this we have considered the geometric criterion as adopted in our previous studies [53, 54]. It can be noticed that with increasing caffeine number, the probability of formation of

medium sized clusters of the order of 3 to 10 increases. The probabilities of formation of cluster sizes greater than 15 is negligible, and therefore they are omitted.

In Fig. 5-10 we have shown the snapshots of the last step of simulation of all systems. We observe caffeine clusters around the Phe residues and other hydrophobic residues of the peptide. Here we note that in system S1, although caffeine molecules interact with Phe residues of the peptide, they are not capable of blocking the peptides from interaction with each other fully, leading to the formation of peptide aggregates. When caffeine number increases further, medium sized caffeine clusters are formed in large numbers. These caffeine clusters interact with the Phe residues and other hydrophobic residues and create a hydrophobic environment around them. Due to extensive caffeine-peptide interaction, the aromatic Phe residues and all other hydrophobic residues are blocked to interact with each other. This leads to a significant reduction in the self-assembly formation of the peptides.

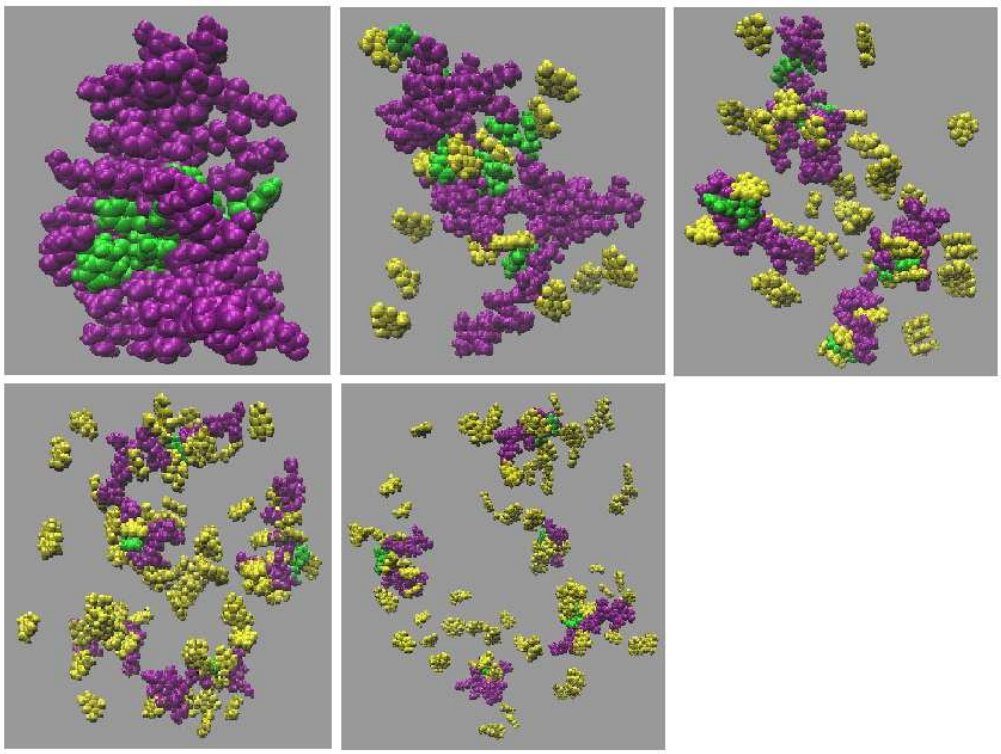

Figure 5-10. *Snapshots of the last step of simulation for different systems. From top left to bottom right represent system S0 to S4. Yellow color represents caffeine molecule, and other colors represent peptide. Phe residues are represented in green color, and other peptides residues are represented in purple color.*

In our earlier studies, we have reported that each caffeine molecule has three hydrogen bonding sites that act as hydrogen acceptors [53, 54]. In order to investigate the formation of

any H-bonds between caffeine and peptides, we have carried out the H-bond analyses. The average number of H-bonds between peptide and caffeine increases with increasing caffeine stoichiometry (see Table 5-3). Therefore, the loss of inter-peptide H-bonds (as discussed above) can be attributed to the fact that caffeine binds to peptide backbone and side-chain residues through its hydrogen acceptors, thereby weakening the backbone-backbone and side-chain H-bonds between peptides. This leads to a decrement in the peptide-peptide hydrogen bonding interaction for the systems with higher number of caffeine molecules.

For a quantitative estimation of number of caffeine in the first solvation shell of the peptide we have calculated the number of caffeine around all the residues from the respective pair correlation functions by using the equation:

$$n_{\alpha\beta} = 4\pi\rho_{\beta}\int_{0}^{r_c} r^2 g_{\alpha\beta}(r)dr \tag{5.1}$$

where $n_{\alpha\beta}$ represents the number of atoms of type β surrounding atom type α in a shell extending from 0 to r_c (the distance of the first minimum in the distribution function, $g_{\alpha\beta}(r)$), and ρ_{β} is the number density of β in the system. The number of first shell caffeine molecules around each of the residues is shown in Fig. 5-11.

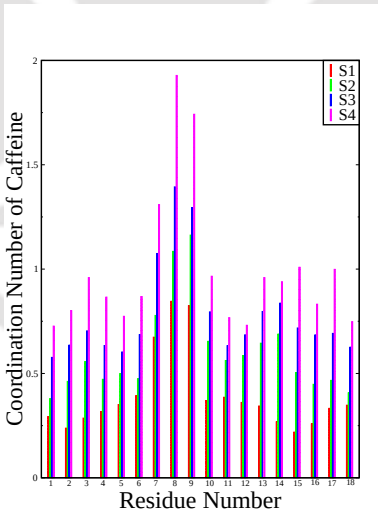

Figure 5-11. *First shell coordination number of caffeine around all the residues of the peptide.*

For system S1, the average number of caffeine molecules in the first coordination shell of each of the residues of the peptide is below one with a maximum coordination number is seen for the two Phe residues (residues 8 and 9). These coordination number values increase for each residue with increasing caffeine stoichiometry, and for system S4 they

reach close to two for the Phe residues. This signifies that there are approximately two caffeine molecules in the immediate vicinity of the Phe residues for system S4. Therefore, from our computational study, we got an insight of the mechanism of inhibiting effect of caffeine on peptide aggregation.

■ SUMMARY AND CONCLUSIONS

In this chapter, we have investigated the effect of caffeine on the aggregation of amyloid-derived switch-peptide with varied stoichiometric ratio of caffeine to peptide by means of a combination of molecular dynamics simulation and experimental analyses. From the secondary structure analyses of peptide, we have observed the formation of highly ordered β-sheet in pure water system. In presence of 3:1 caffeine to peptide ratio, the percentage of β-sheets structure decreases to some extent, although peptides are aggregating heavily. However, in presence of 10:1 ratio and more, the β-sheet formation diminishes. Radial distribution function, residue-residue contact map, interaction energy and solvent accessible surface area calculations have also demonstrated that with 10:1 and more caffeine to peptide ratio, the aggregation tendency of peptide diminishes significantly, and the self-assembly formation is getting ceased. The analysis of interaction of caffeine with switch-peptide showed that caffeine molecules initially interact with the aromatic phenylalanine residues, thereby restricting the Phe-Phe interaction. A detailed analysis of MD simulations further show that caffeine molecules form hydrogen bonds with the peptide molecules and this leads to weakening of the interstrand hydrogen bonds between peptides. On the other hand, caffeine molecules form medium ordered clusters of like molecules of size ranging from 3 to 8 by vertical stacking. These clusters form a hydrophobic environment around the hydrophobic sites of peptides, and physically block them from interacting with each other. All the above results suggested that caffeine has the capacity to inhibit the aggregation of amyloid-forming peptides by reducing hydrophobic interaction between them. The blocking of aromatic Phe residues of the peptides by caffeine clusters through peptide-caffeine π-stacking interaction, and other residues by hydrophobic and hydrogen bonding interaction leads to complete disaggregation of peptide in caffeine solution with 10:1 or higher caffeine to peptide stoichiometric ratio.

Chapter 6

How do the Caffeine Aggregates Inhibit the Fibril Formation of Aβ-Amyloid ?

"The realization of the role of aromatic moieties in fibril formation is currently being used to develop novel inhibitors that can serve as therapeutic agents to treat amyloid-associated disorders."

– E. Gazit *FEBS J.* **272**, 5971 (2005)

Overview:

In order to understand the mechanism of inhibition action of caffeine in more detail, we have considered the seven residue peptide Aβ_{16-22}, which form amyloid fibril in vitro The peptide with sequence KLVFFAE (16-22) is amphiphilic in nature. The LVFF sequence (17-20) in the Aβ_{16-22} peptide is the central hydrophobic core (CHC) in full length Aβ peptide. The N-terminal residue has positively charged lysine and C-terminal has negatively charged glutamic acid. The aromatic residues (FF) in the Aβ_{16-22} peptide play an important role in the molecular recognition and self-assembly process that leads to amyloid fibril formation. Therefore, Aβ_{16-22} is an attractive model system to probe the formation of peptide oligomers for our study. Therefore, in this chapter, we have carried out molecular dynamics simulation of five amyloid forming Aβ_{16-22} peptide in pure water and in a regime of caffeine solutions, with different caffeine : peptide stoichiometric ratios. The secondary structure analyses of peptides in pure water show the formation of β-sheet conformation, whereas on addition of caffeine these ordered conformation become negligible. Radial distribution function, contact map, nonbonding interaction energy, hydrogen bonding, potential of mean force and hydration analyses show less inter-peptide interaction in presence of caffeine, and the effect is more with increasing caffeine ratio. The interaction of aromatic phenylalanine residues of peptide with caffeine restricts the inter-peptide interaction tendency. With increasing caffeine numbers, interaction of caffeine with other hydrophobic residues also increases. Thus, the hydrophobic core recognition motive of amyloid formation of peptide is physically blocked by caffeine, thereby abolishing the self-assembly formation.

■ INTRODUCTION

Alzheimer's disease (AD), the most common form of dementia, that affects more than 44 million people world-wide, is a result of deposition of well-ordered amyloid fibrils in the brain formed due to aggregation of proteins [1-5]. Recent experimental evidences suggested that although the amyloid plaques are one of the hallmarks of the diseases, the neurotoxicity may be caused by oligomers formed in the early stage of fibril formation [48-50]. Thus, drugs that can prevent the formation of early oligomeric intermediates or make them unstable is a major concern in the field of drug discovery against AD. The initial stages of oligomers formation are difficult to characterize in experimental studies, since Aβ peptide is highly amyloidogenic. In this context, we note that computer simulation can provide the information required to capture the early steps of amyloid formation and demonstrate insights of the behavior of the drug that can inhibit Aβ aggregation. In pure aqueous solution, the Aβ monomer exists mainly in random coil conformation, with only a small population of it in local non-random structures. It is suggested that the structural transition from non-aggregated random coil to highly ordered β-sheets conformation followed by fibril formation leads to toxic deposit in plaques. For computational analysis, the aggregation study of full length Aβ_{1-42} is computationally expensive. A number of solid-state NMR studies on fibrils of several short sequences (that are obtained from the full length Aβ fragment) have shown to form amyloid fibril in isolation [160-166]. The seven residue peptide Aβ_{16-22} is one of the shortest length peptide that can form amyloid in vitro [161]. This peptide with sequence KLVFFAE (16-22) is amphiphilic (see Fig. (b)), and found to be critical for fibrillization. The LVFF sequence (17-20) in the Aβ_{16-22} peptide is the central hydrophobic core (CHC) in Aβ peptide. The aromatic residues (FF) in the Aβ_{16-22} peptide play an important role in the molecular recognition and self-assembly process that leads to amyloid fibril formation (due to stacking interaction). Hilbich et al. reported that the substitution of the hydrophobic residues with hydrophilic residues in LVFF hydrophobic core region results a considerable reduction in amyloid fibrillization [167, 168]. Therefore, LVFF region is indeed responsible for β-sheets formation in Aβ peptide. Again, the N-terminal residue of Aβ_{16-22} peptide has positively charged lysine and C-terminal has negatively charged glutamic acid. The electrostatic interaction between peptides due to opposite charges on terminal residues leads to stabilization of antiparallel strands [169]. The Aβ_{16-22} is studied by many different numerical approaches using various force fields

[170-172]. Again, unlike the fibers of larger fragments, the structure of Aβ_{16-22} fibrils may be anticipated to from its sequence alone. Therefore, Aβ_{16-22} is an attractive model system to probe the formation of peptide oligomers. In our previous chapter (**Chapter 5**) we have already observed the inhibiting action of caffeine on aggregation of switch-peptide. In this chapter we have carried out a series of molecular dynamics (MD) simulations to investigate the mechanism of inhibition in more detail. Our goals for this study are:

(i) To examine, in detail, the aggregation of Aβ_{16-22} peptide in pure water, and in caffeine solutions with different caffeine : peptide stoichiometric ratios; (ii) To understand the change in secondary structure of peptide in caffeine solutions; and (iii) To examine the underlying mechanism, of caffeine molecules that act to prevent peptide aggregation.

The organization of the rest of the chapter is as follows. We first present the models and details of simulations. Results are discussed thereafter, and the last section includes concluding remarks with a brief summary.

■ MODELS AND SIMULATION METHOD

The Aβ_{16-22} peptide has been modeled using ff99SB force field [153]. The C-terminals and N-terminals of the Aβ_{16-22} peptides are capped with neutral acetyl and amide groups respectively. To gain the molecular level understanding of the effect of caffeine on aggregation of Aβ_{1-42} peptide, we have performed simulations of five Aβ_{16-22} peptide in aqueous solution with a regime of caffeine : peptide stoichiometric ratios. The initial configurations of the systems were prepared with Packmol program [86]. In the initial structure, the five fully stretched conformation of Aβ_{16-22} peptides were randomly placed in a cubic box with sufficient separation between them and then they are immersed in water. With the same initial configuration of peptide solutions, we then added caffeine molecules in varied numbers to prepare different systems.

In (**chapter 5**) we have already discussed that the inhibition action of inhibitors on protein aggregation is sensitive to the stoichiometric ratio of the peptide and inhibitors. Moreover, for small molecule inhibitors, such stoichiometries range up to thousands of inhibitor molecules to one protein [127, 128]. Therefore, to understand the effect of caffeine on aggregation of Aβ_{16-22} peptide on molecular basis, we have prepared systems with a regime of caffeine : peptide stoichiometric ratio. Since small molecule inhibitors inhibit protein aggregation by forming aggregates with like molecules [133, 134], therefore, we have kept the concentration of caffeine just above the solubility limit (0.1 M), where it can

form self-aggregated caffeine clusters [53, 54]. The number of peptides in all the systems are kept fixed and we varied caffeine : peptide stoichiometric ratios only to better understand the role of caffeine as an inhibitor on peptide aggregation. An overview of different systems used in this study are presented in Table 6-1.

Table 6-1. Overview of Simulations[a]

System	N_{caff}	$N_{peptide}$	N_{wat}	C_{caff}(M)	caffeine : peptide	box length(Å)	ρ (g cm^{-3})
S0	0	5	4200	0	-	50.83	0.96
S1	15	5	4200	0.19	3:1	51.22	0.97
S2	50	5	15000	0.18	10:1	77.40	1.00
S3	80	5	25000	0.17	16:1	91.93	1.00
P0	0	2	3000	0	-	41.80	0.98
P1	8	2	3000	0.18	3:1	42.07	0.99
P2	20	2	6000	0.17	10:1	57.41	1.00
P3	32	2	10000	0.18	16:1	65.93	1.00

N_{caff}, $N_{peptide}$ and N_{wat} represent the number of caffeine, the number of Aβ_{16-22} peptide and the number of water molecules respectively. C_{caff} and ρ refer to the caffeine concentration and the density respectively.

The caffeine solute was modeled using AMBER generated all atom force field as described in (**chapter 2**) [53], and popular extended simple point-charge (SPC/E) model is used for water molecules [132]. Here we like to mention that a comparative study of different force field parameters of caffeine in SPC/E water revealed that the caffeine model used in this study and the one developed by Weerasinghe and co-workers [33] behave in almost similar fashion in qualitative sense, and therefore, it is expected that the change of caffeine force fields should produce the similar qualitative effect of caffeine as an amyloid inhibitor in computational study [54]. The MD simulations were conducted using AMBER 12 package [61] in isothermal-isobaric (NPT) ensemble. The simulation protocols were identical to those described in **Chapter 5**. Simulation runs were subjected to energy minimization for 5000 steps, with first 2500 steps in steepest descent method followed by the same number of steps in conjugate gradient method. The systems were then heated slowly from 0 to 300 K over 180 ps in canonical ensemble (NVT). The temperature was controlled by the application of Langevin dynamics method with a collision frequency of 1 ps^{-1} [154]. All the simulations were then equilibrated for 5 ns followed by 95 ns production runs in NPT ensemble at 1 atm pressure. To analyze our results, we have used PTRAJ module available in AMBER whenever required.

In order to calculate potential of mean force (PMF) between two Phe residues of peptide, we have performed umbrella sampling [173]. For this, we have prepared another four set of systems with two peptides in water and different caffeine solutions maintaining the same stoichiometric ratio of caffeine (system P0 to P3, Table 5-1). Following the same procedure as for our other systems, we then simulate these systems for 75 ns each. The final state of each simulation is then considered as the starting configuration to perform umbrella sampling to calculate PMF.

■ RESULTS AND DISCUSSION

Self-aggregation of Aβ_{16-22} peptide in pure water and in different caffeine solutions:

Previous theoretical studies reported that Aβ_{16-22} monomer predominantly adopts a compact random-coil conformation with only a very small presence of α-helical structure [174, 175]. These random coil monomers when aggregate form highly ordered secondary structure. To probe the formation of oligomers of Aβ_{16-22} in pure water (system S0), we have shown the snapshots of the final state of the peptides at 100 ns in Fig. 6-1 (a-c).

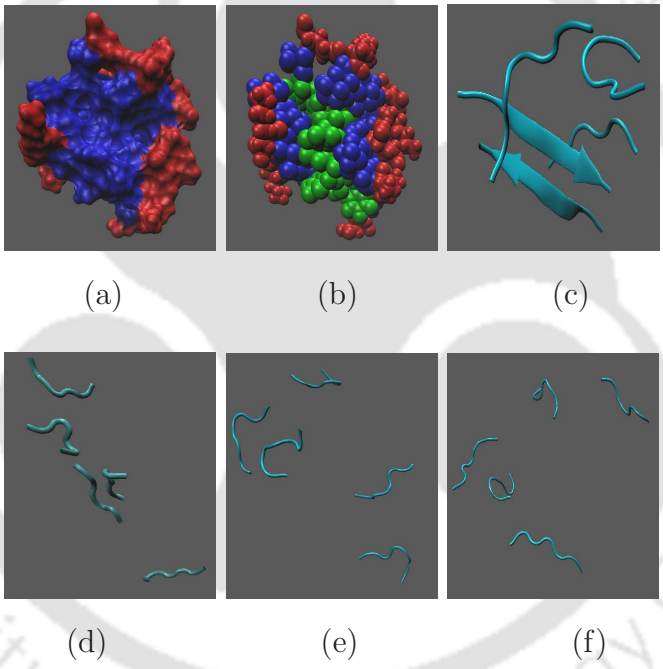

Figure 6-1.*Snapshots of systems S0 at the final state. (a) The arrangement of hydrophobic (blue) and hydrophilic (red) sites in the aggregate, (b) the Phe residues are defined in green) color in the aggregate, and (c) antiparallel β-strand formation by two peptides. d, e, f refer to snapshots of systems S1, S2 and S3 at the final state.*

Fig. 6-1 (a) distinguishes the hydrophobic (blue) and hydrophilic (red) parts of the peptide. We see that all the hydrophobic residues assemble together by inter-peptide hydrophobic interactions to reduce the water contact and form Aβ_{16-22} oligomers with hydrophilic residues pointing outwards. In Fig. 6-1 (b), we have specified the phenylalanine (Phe) residues (green color), which are known to play a key role in fibrillization through

aromatic π-stacking interaction [152]. It can be seen that all the Phe residues are present at the core. Fig. 6-1 (c) shows the formation of anti-parallel β-sheets in the oligomers. The snapshots of the final state of peptides with different caffeine : peptide ratio for systems S1, S2 and S3 are shown in Fig. 6-1 (d-f). We observe that with increasing number of caffeine, the self-aggregation tendency of peptides decreases.

Here, it is to be noted that a single snapshot does not necessarily produce correct picture of a particular simulated system. Thus, we also examined, in detail, the effect of caffeine on the oligomer formation of peptide Aβ_{16-22} (see below).

In order to examine how the conformation of the peptide changes in different caffeine solutions, we have analyzed the changes in the secondary structure of the peptide as time progresses (for last 80 ns) and these are shown in Fig. 6-2 (a-d).

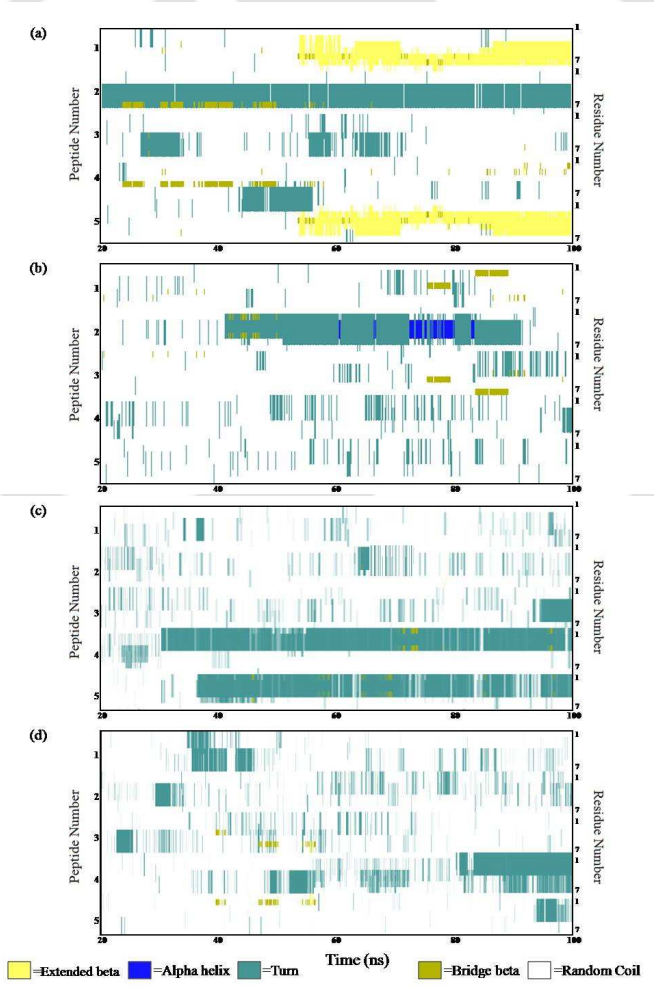

Figure 6-2. *Secondary structure analyses. (a) system S0, (b) system S1, (c) system S2, and (d) system S3.*

Using the definitions of secondary structure conformations (i. e., β-sheet, α-helix, random coil etc.), we noticed that in system S0, the percentage of β-strand of Aβ_{16-22} in the oligomer is 16 %. The two peptides (peptide 1 and 5) show fast conversion into β-strand (yellow color), and remains intact up to 100 ns once formed. The percentage random-coil conformation is found to be 66 % in this system. Though, we started the simulation by placing the peptides randomly in the simulation box with sufficient separation between them, the formation of β-strand structure denotes the high amyloidogenic ability of the peptide in pure water. However, in caffeine solution, we observe a significantly large probability of random coil conformation and with increasing caffeine number in the systems, the probability of finding ordered secondary conformation becomes negligible.

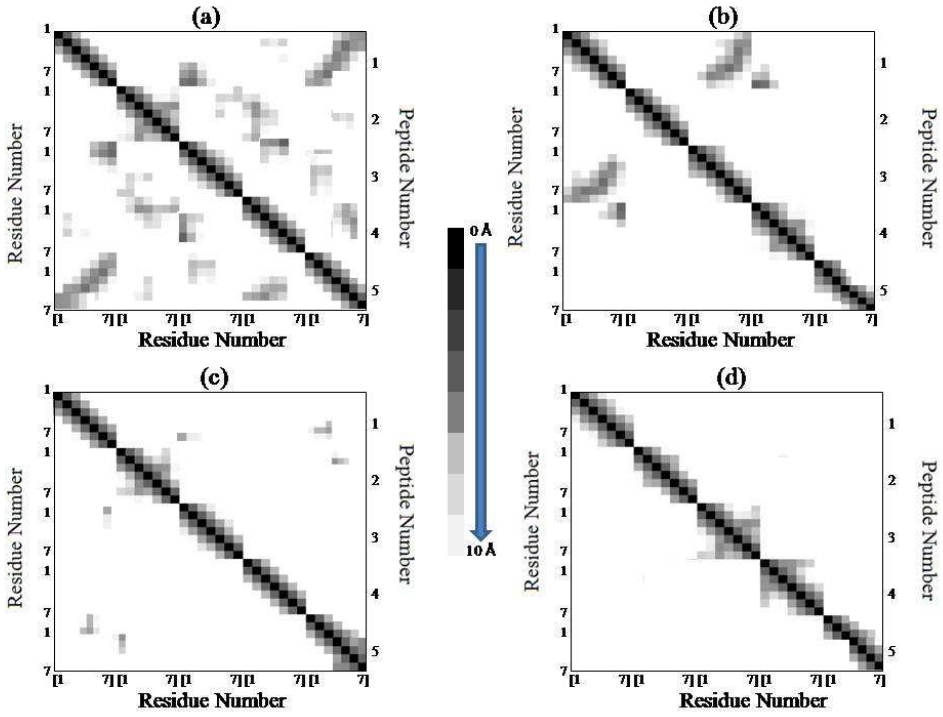

Figure 6-3. *Residue-residue contact maps of peptides. The graph square is colored black at 0.0 Å distance, to a linear gray scale between 0.0 and 10.0 Å and white when it is greater than 10.0 Å . (a) system S0, (b) system S1, (c) system S2, and (d) system S3.*

The residue-residue contact map of each pair of residues for all the peptides, considering the Cα-Cα distances, is shown in Fig. 6-3 (a-d). It is apparent from the figure that in system S0, the residues of one peptide are in contact with the residues of other peptides. For example, all the residues of peptide 1 and the residues of peptide 5 are in contact with

each other. The residues of other peptides are also interacting significantly, as the colored region is very prominent in system S0. However, as the number of caffeine increases, the pairwise residue-residue inter-peptide contact decreases, and in system S3 all the peptides are separated, as there seems to be no inter-peptide residue-residue interaction.

To probe the time evolution of peptide clusters formation and lifetime of clusters, we have shown the distribution of cluster sizes of peptide with simulation time for all systems (see Fig. 6-4). The two peptides are considered to form clusters when residues of one peptide are within 7 Å of residues of another peptide. We observe that in pure water system, cluster formation starts from very early stage of simulation and after 30 ns all five peptides are aggregated. In presence of caffeine in system S1, the cluster size fluctuates between 4 and 3 which ultimately stabilizes at 3 after 70 ns. System S2 shows initial fluctuation in dimer formation. However, after 10 ns, the system remains mostly as a monomer upto 30 ns, then again dimer and trimer starts to form ultimately leading to dimer after 65 ns. It can be seen that the peptides in system S3 prefer to remain in monomeric form for most of the simulation time. Although initially peptides interact to form a dimer, after 50 ns only monomers are observed in the system, without any trace of higher order cluster.

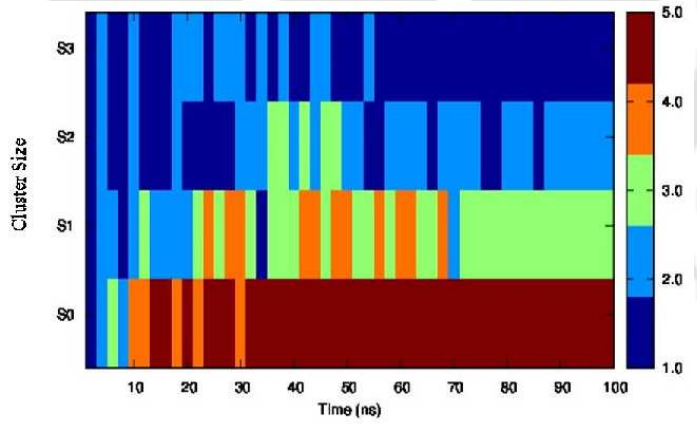

Figure 6-4. *Distribution of $A\beta_{16-22}$ peptide clusters of different sizes as a function of simulation time.*

The two aromatic Phe residues in Aβ peptide are regarded to play a key role in amyloid formation [152]. The aromatic stacking interactions have been suggested to provide an energetic contribution to the self-assembly of ordered amyloid fibrils. Therefore, to investigate the effect of caffeine molecules on the inter-peptide Phe-Phe interaction, we have calculated the radial distribution functions (rdfs) involving inter-peptide Phe-Phe for all systems and

these are shown in Fig. 6-5 (a). The Phe-Phe rdf in system S0 shows appearance of a strong first peak at 5 Å with a well developed second peak at 7.5 Å. The hydrophobic Phe residues of one peptide interact with the Phe residues of other peptides leading to aggregation. Interestingly, the presence of caffeine molecules in system S1 causes a sharp decrease in the peak height of Phe-Phe distribution function. With further increasing the number of caffeine molecules in systems S2 and S3, the peak position also shifts to higher distance, indicating the separation of Phe residues from one another.

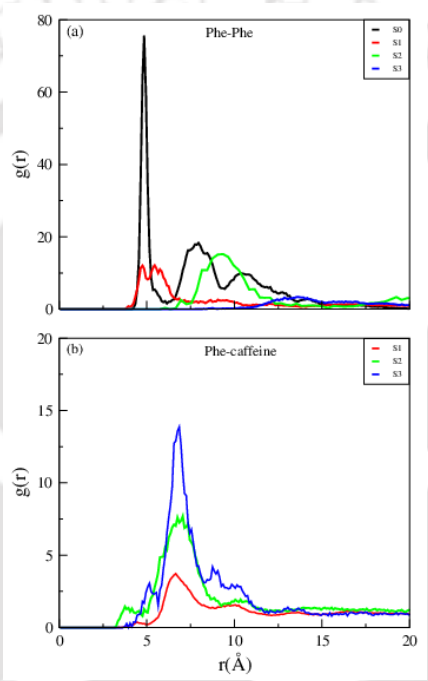

Figure 6-5. *Radial distribution functions of (a) Phe around Phe, and (b) caffeine around Phe in different systems.*

The peptide Aβ_{16-22} is amphiphilic in nature and the hydrophobic core is present in its middle part, whereas the charged terminal residues are present at the terminal positions. The hydrophilic terminal portions interact with water, and the hydrophobic middle portion tends to keep itself away from water. Therefore, to gain insight into the changes in the pattern of hydration of different residues in presence of caffeine, we have estimated the number of first shell water molecules around each residues from the corresponding rdfs by using the equation [53, 54]:

$$n_{\alpha\beta} = 4\pi\rho_{\beta}\int_{0}^{r_c} r^2 g_{\alpha\beta}(r)dr \tag{6.1}$$

where $n_{\alpha\beta}$ represents the number of atoms of type β surrounding atom type α in a

shell extending from 0 to r_c (the distance of the first minimum in the distribution function, $g_{\alpha\beta}(r)$), and ρ_β is the number density of β in the system. Hydration numbers of each of the peptide residues in different systems are shown in Fig. 6-6.

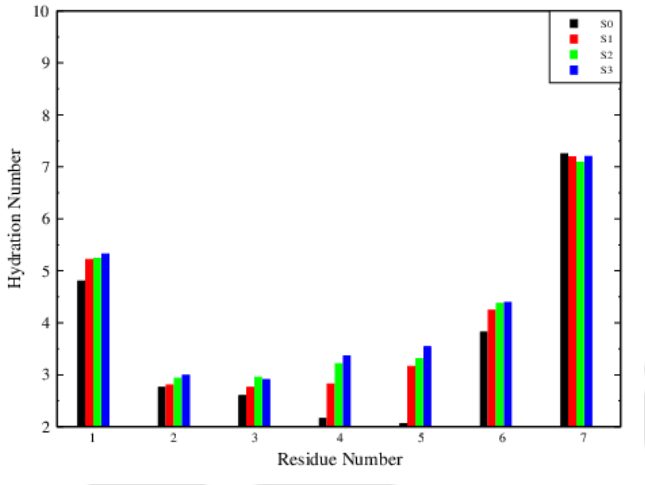

Figure 6-6. *Hydration number (the number of first shell water molecules) around all the residues of peptide.*

We see that glutamic acid (residue 7) has the highest hydration number value which is followed by lysine (residue 1), and these hydration numbers do not change much as caffeine number is increased. Furthermore, a close examination in to these hydration numbers for other peptide residues suggests that the effect of caffeine on these numbers is not very profound except for the Phe-residues (residue 4 and 5) in which a moderate increase in the hydration number value is observed as caffeine is added. Considering the fact that the effective Phe-Phe interaction decreases dramatically as caffeine : peptide stoichiometric ratio is increased (as revealed by Phe-Phe rdf, Fig. 6-5 (a)), this relatively smaller change in the hydration number is not that significant. This gives an indication that caffeine molecules may directly interact with the hydrophobic residues of the peptides, by creating a hydrophobic environment around them. This further implies, albeit indirectly, that the caffeine-peptide interaction may play a significant role and prevents the inter-peptide interaction.

In order to examine the effect of caffeine on peptide-peptide interaction for different systems, we have decomposed peptide-peptide interaction energy in to electrostatic and van der Waals components and these are plotted as a function of simulation time (see Fig. 6-7 (a) and (b)). In the same figure, we also show the average peptide-peptide electrostatic and van der Waals (vdw) energies for different systems (Fig. 6-7 (c)). As can be seen

that, the electrostatic energy component dominates over the van der Waals component in peptide-peptide interactions.

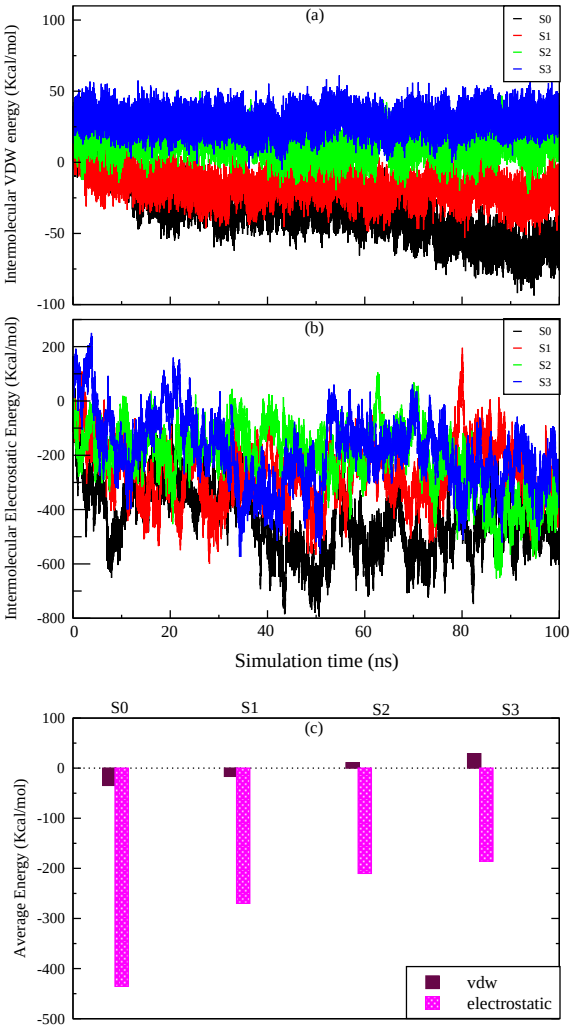

Figure 6-7. *Time evolution and average van der Waals and Electrostatic peptide-peptide interaction energy.*

Here it is worth mentioning that the electrostatic interaction of inter-peptide Lys 16 and Glu 22 is reported to confer stabilization to the anti-parallel β-strand arrangements [176]. In comparison to pure water system, addition of caffeine makes both electrostatic and van der Waals interactions more unfavorable. Here, we would also like to mention that the electrostatic energy component (of peptide-peptide interaction) is not a strong function of caffeine : peptide stoichiometric ratio. Similar observation was also made for myricetin, a

natural polyphenol, as inhibitors of amyloid aggregation of GNNQQNY heptapeptide [177]. Nevertheless, it is interesting to observe that for caffeine solutions with higher number of caffeine molecules, peptide-peptide van der Waals interactions become positive.

Further, the importance of inter-peptide hydrogen bonds is a well known fact in the context of stabilization of peptide oligomers, which ultimately leads to the formation of β-rich protein structures [159]. To probe the role of hydrogen bonds in the oligomers formation of Aβ_{16-22} in different solutions, we have estimated the average inter-peptide hydrogen bonds for all systems and the same are shown in Fig. 6-8. A hydrogen bond is assigned if the distance between donor (D) and acceptor (A) is less than 3.5 Å and simultaneously, and the angle of H-D-A is considered as less than or equal to 45^0. The total inter-peptide hydrogen bonds in S0 is found to be 13. As caffeine number is increased a sharp decrease in this hydrogen bond is observed and for system S3, a complete abolish of the same is found.

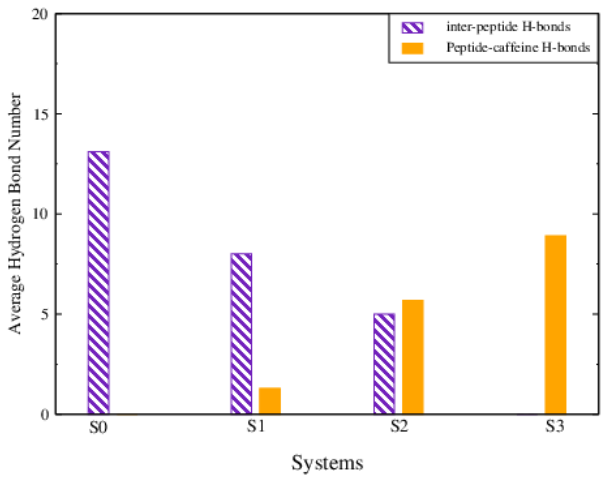

Figure 6-8. *Inter-peptide and peptide-caffeine hydrogen bonds.*

Interaction between caffeine and Aβ_{16-22} peptide:

It is discussed above that increased caffeine : peptide ratio makes peptide-peptide interactions unfavorable (see Fig. 6-7). Moreover, as shown above in Fig. 6-5 (a) that in presence of caffeine molecules, the inter-peptide interactions between the Phe-residues are greatly affected. Thus, it is instructive to estimate peptide-caffeine interaction energies for different systems. The average peptide-caffeine electrostatic and van der Waals interaction

energies for different systems are shown in Table II. We observe that both vdw and electrostatic components are favorable. Unlike peptide-peptide interactions, peptide-caffeine interactions are dominated by van der Waals interactions. The caffeine-peptide interaction energy decreases (more negative) rapidly with increasing number of caffeine molecules, depicting more favorable interaction between them. In the same table we have also shown the solvent accessible surface area (SASA) of peptides. We observe an increase in SASA value with increasing the caffeine : peptide stoichiometric ratio, which depicts that more surface area of peptides are available to solvent, indicating less aggregation propensity of the peptide with increasing the stoichiometric ratio. Different experimental and theoretical studies reported that caffeine molecules form complex with different biomolecules, DNA and aromatic drug molecules by π-stacking interaction [146, 55, 56]. Furthermore, previous studies of amyloid aggregation revealed that the blocking of the two aromatic Phe residues of amyloidogenic peptides diminishes the ability of peptide to form stable amyloid fibrils [152]. The shifting in position of the first peak to large-r value in Phe-Phe rdf indicates that Phe residues are blocked to interact with each other (see Fig. 6-5 (a)). Therefore, in order to understand the interaction of caffeine with Phe residues, we have calculated the rdfs of caffeine around Phe for different systems and these are shown in Fig. 6-5 (b). The first peak of this rdf appears at 6.5 Å and the peak height increases with increasing number of caffeine molecules, implying enhancement in the caffeine-peptide interaction. Furthermore, caffeine molecule is known to possess three hydrogen bonding sites, viz. two carbonyl oxygen and one ring nitrogen [53]. The average number of hydrogen bonds between caffeine and peptide for different systems are shown in Fig. 6-8. It can be seen that total number of caffeine-peptide hydrogen bond increases with increasing number of caffeine molecules. As the number of oligomers is reduced and peptides get separated in presence of caffeine, more hydrogen bonding sites of peptide are available for caffeine to form hydrogen bonds. The calculation of average number of water-peptide (per peptide) and water-caffeine (per caffeine) hydrogen bonds show a slight reduction in their values as caffeine : peptide stoichiometric ratio increases (data not shown). To characterize the interaction of caffeine with peptide in more detail, we have shown how the number of caffeine molecules within 7.5 Å of peptide surface changes as simulation progresses (see Fig. 6-9). We observe that almost 10 caffeine molecules are present near the vicinity of peptide in system S1. With increasing caffeine stoichiometric ratio in the system, the number of caffeine molecules around peptide surface increases, and in system S3 we observe the presence of approximately 30 caffeine molecules within 7.5 Å of peptide.

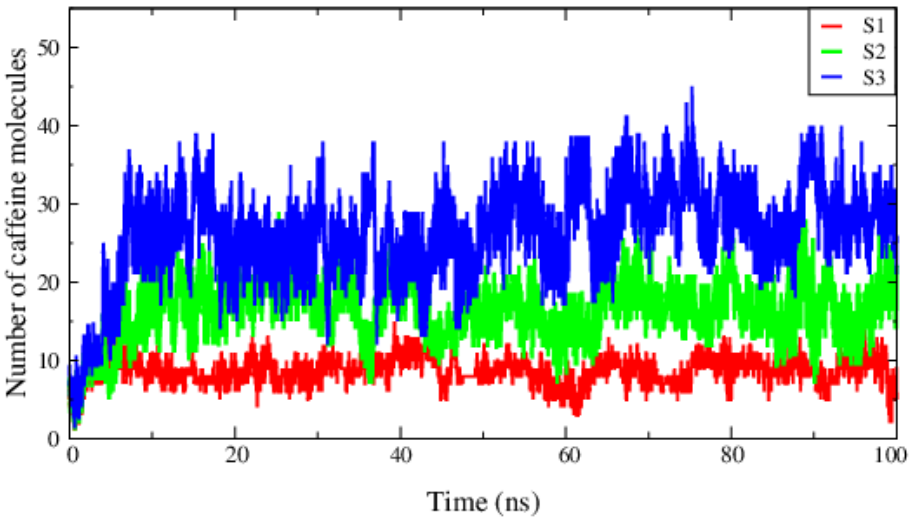

Figure 6-9. *Time evolution of number of caffeine molecules within 7.5 Å of peptide surface.*

To get a pictorial description of contour density of caffeine around Aβ_{16-22} peptide, we have shown the spatial density plot of caffeine molecules that are present within 7.5 Å of peptide, (averaged over the last 10 ns of simulation (see Fig. 6-10).

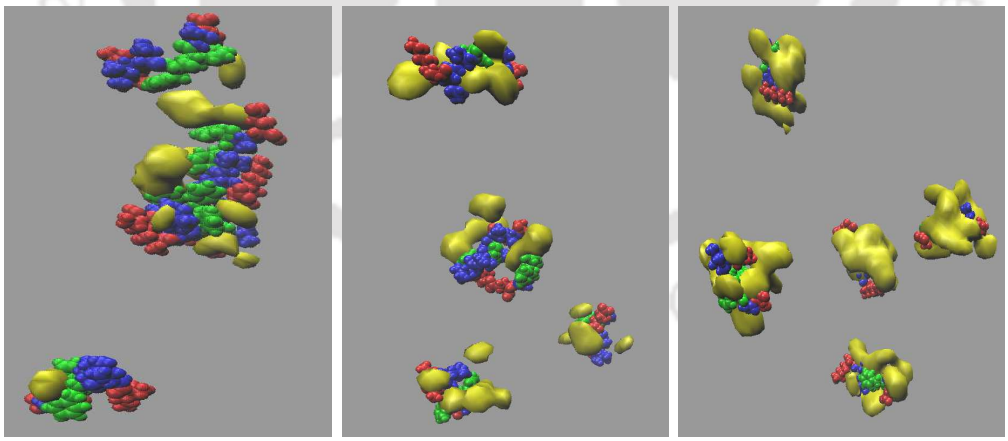

Figure 6-10. *Contour density plots for caffeine around Aβ_{16-22} peptides within 7.5 Å of peptide for the last 10 ns of simulation. Yellow color represents caffeine density, and other colors represent peptide. Hydrophobic parts are represented in blue, hydrophilic parts in red, and Phe residues are represented in green color.*

We find that caffeine density (yellow) within this interaction distance increases with increasing the caffeine number. In system S1, with the presence of 15 caffeine molecules in the system, the caffeine density is mostly populated around the Phe residues (purple) of peptide. However, with increasing caffeine : peptide ratio, caffeine density has also started appearing around other residues of the peptide. These findings suggest that once the Phe residues are blocked, the caffeine molecules interact with other parts of the peptide through hydrophobic and/or hydrogen bonding interaction. A comparison of contour density of Phe residues (around another Phe residues) in system S0 with other systems shows the separation of Phe residues in presence of caffeine. For a quantitative analysis, we have further calculated the first shell coordination number of caffeine around each residues of the peptide from the corresponding rdf using equation 1 and the same is presented in Fig. 6-11.

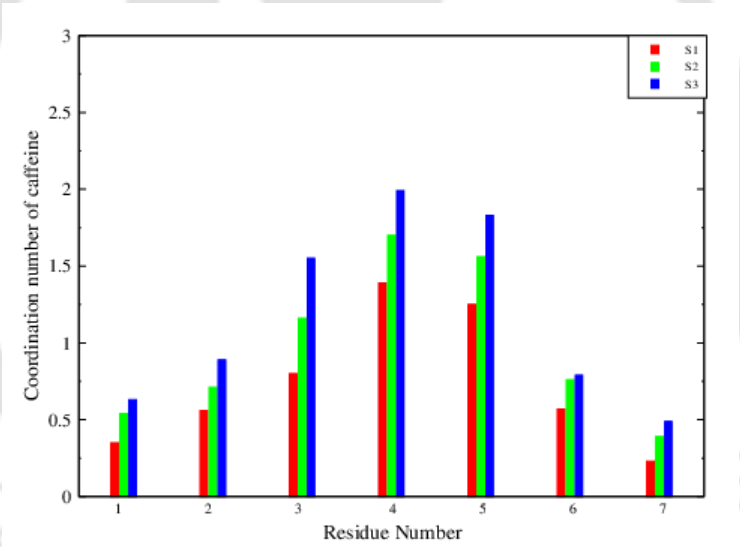

Figure 6-11. *First shell coordination number of caffeine around all the residues.*

The coordination number of caffeine for system S1 is below one for all the residues except Phe residues (residue 4 and 5), where it is above one. This means that on average, at least one caffeine molecule is present around Phe residues. With increasing caffeine number, the caffeine coordination number increases for all residues. The snapshots of caffeine around peptide at the final stage of simulation for different systems are shown in Fig. 6-12. It is found that caffeine molecules (yellow) form clusters around peptide. Here we note that, small organic molecules, which act as inhibitors in amyloid formation, have the general property of forming chemical aggregates with itself. These colloidal aggregates range in

size from 50 nm^3 to over 600 nm^3, and once formed, they physically sequester proteins and inhibit enzymes nonspecifically [133, 134, 145]. Many recent investigations depicted extensive aggregation of the caffeine molecules in aqueous solution above its solubility limit [54, 77, 178]. These studies reveal that caffeine aggregates are formed by planar stacking of the hydrophobic faces one above another [77]. Dipolar interaction between the caffeine molecules is the driving force for caffeine cluster formation [178]. These vertical clusters can be upto the size of 10 in a single cluster [54].

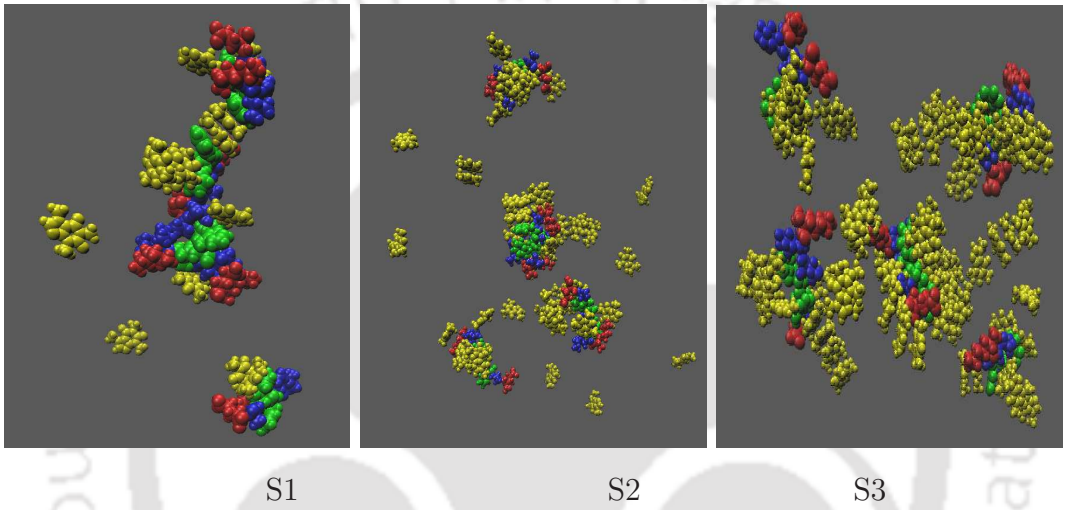

Figure 6-12. *Snapshots of the last state of simulation for different systems. Yellow color represents caffeine molecules, and other colors represent peptide. Hydrophobic parts are represented in blue, hydrophilic parts in red, and Phe residues are represented in green color.*

In this study, we have analyzed the cluster formation of caffeine for all the systems and they are shown in Fig. 6-13. Following our earlier studies, we have estimated the cluster size, by considering clusters as an assembly of stacked caffeine molecules, with neighboring caffeine molecules within 6.4 Å of each caffeine molecule [53, 54]. We observe that with increasing caffeine number, the probability of formation of medium ordered caffeine cluster increases. Therefore, it can be proposed that with enough number of caffeine clusters in the system, caffeine molecules physically sequester the peptides and enclose the peptide hydrophobic sites within the hydrophobic confinement of caffeine clusters, which ultimately prevent the peptides from further inter-peptide interaction. As a result, in systems with higher caffeine : peptide ratio, the oligomer formation tendency of peptides is ceased.

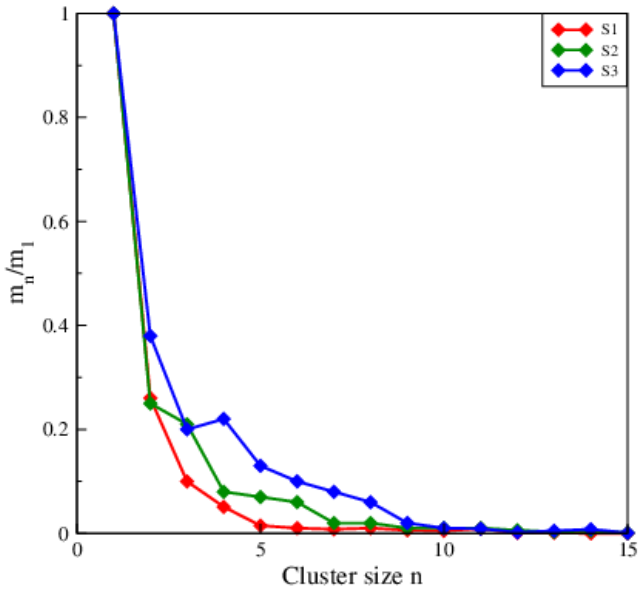

Figure 6-13. *Probability distribution of caffeine clusters of different sizes (m_n) with respect monomer (m_1).*

Potential of mean force calculation:

In order to provide a more comprehensive view on how peptide-peptide interaction is affected in presence of caffeine in the system, we plot the potential of mean force (PMF) between two Phe residues of two different peptides. We have used a spring constant of 1000 kcal/mol to compute the properties of the system at different windows, ranging from 3 Å to 15 Å. Windows are seperated from each other by 0.25 Å. Each window was simulated for 10 ns leading to a total of 460 ns for 46 windows. The PMFs are computed using the Weighted Histogram Analysis Method (WHAM) [179]. Fig. 6-14 shows the PMF at 300 K for the interaction of Phe residues between two peptides as a function of distance. The global minimum in the PMF in pure water system (system P0) is observed at 4.6 Å. In presence of caffeine in the system, the minima shifts to a larger distance, and pmf increases (more positive) with increasing caffeine number in the system. In addition to the global minimum, the PMF of Phe residues in P0 also show a well-defined second minimum at a distance of 9.6 Å.

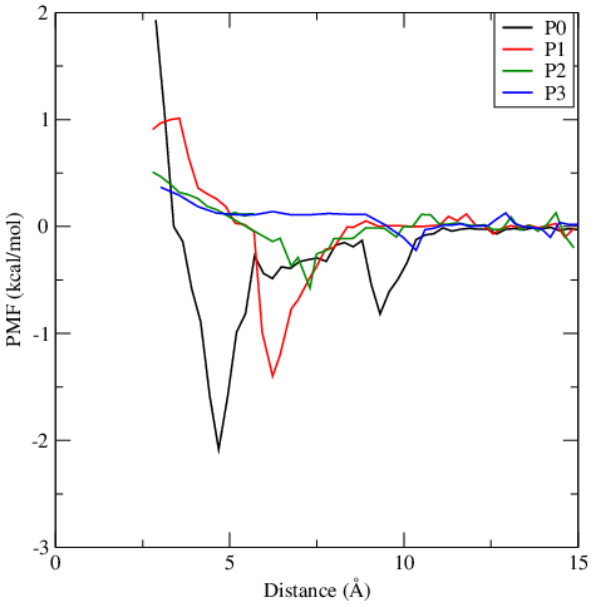

Figure 6-14. *Phe-Phe PMF for different systems.*

To get a more clear picture on the interaction of caffeine with peptide, we have carried out different analyses (such as coordination number, hydrogen bonds, secondary structure) when two peptides are separated 12 Å apart and compared this with the results when peptides are 5 Å apart. Here it is worth mentioning that due to the presence of different populations of peptide clusters in our main system, the information for single peptide will provide important view on affect of caffeine solution on peptide. To probe the solvation of single peptide in water and in different caffeine solutions, we have computed hydration number around different residues of peptide and these and are shown in Fig. 6-15 (a). When peptides are separated (12 Å window), we observe that in pure water the hydration of charged Lys and Glu residues are higher. Presence of caffeine leads to a slight decrease in these values. However, the hydration of hydrophobic residues Leu, Val, and Ala increases in system P1 compared to system P0. On the contrary, hydration of Phe residues decreases in P1. In system P1, the coordination number of caffeine is found to be the highest around Phe residues (4 and 5), and it is very small around other hydrophobic residues (see Fig. 6-15 (b)). Due to less number of caffeine molecules present in this system, the caffeine molecules mostly prefer to interact with Phe residues of the two peptides which results in to lower hydration. On the other hand, the coordination number of caffeine around the hydrophobic sites increases sharply from system P1 to P3 with increasing caffeine number in these system. Therefore, we observe a monotonous decrease in hydration of all residues

compared to pure water system. Therefore, the slight increase in hydration of different residues of peptides in caffeine solution in our main systems (i. e. system S0 to S3) can be attributed to the relative decrease in aggregation tendency of peptides which leads to higher hydration, and not on higher solvation of single peptide in caffeine solution. We observe that when the two peptides are 5 Å apart, the hydration number doesn't follow any definite trend. On the other hand, coordination number of caffeine around peptide residues increases with increasing caffeine number.

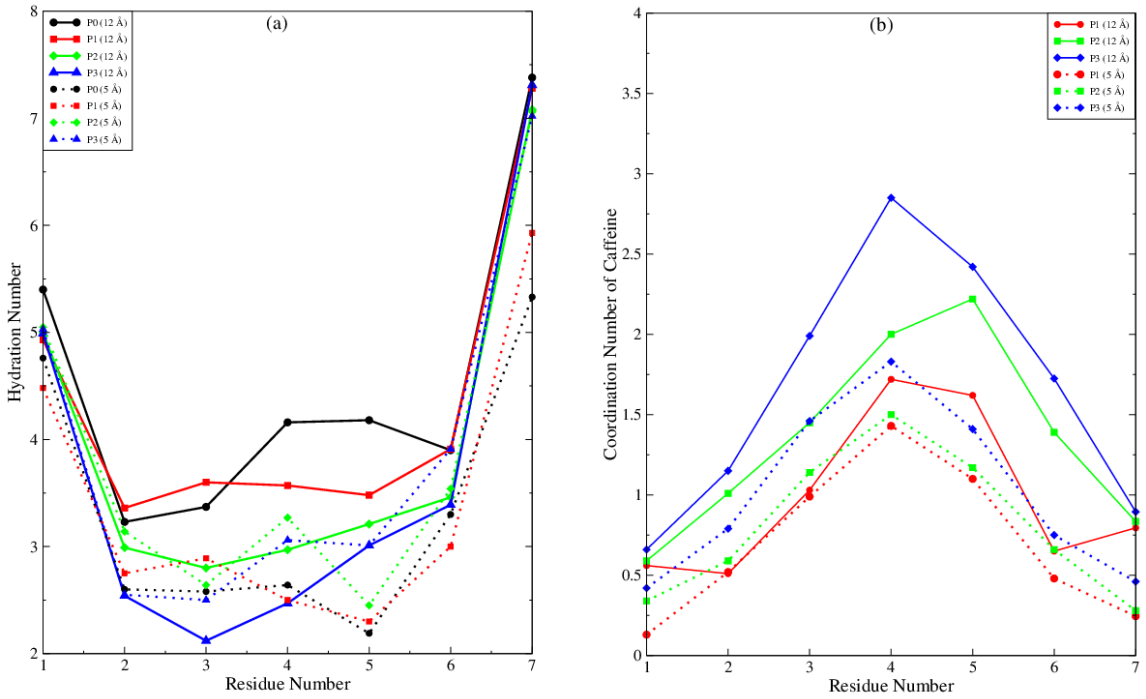

Figure 6-15. *Coordination number of (a) water and (b) caffeine around different residues of the peptide when peptides are 5 Å and 12 Å apart respectively.*

We have also obtained information about the peptide-peptide and peptide-caffeine hydrogen bond formation for two windows, when peptides are away from each other (12 Å) and when peptides are close to each other (5 Å), and the same are shown in Fig. 6-16. When the peptides are far apart (12 Å distance) the average number of inter-peptide hydrogen bonds (see Fig. 6-16 (a)) show a modest change as caffeine number is increased (from 1.5 for system P0 to 0.3 for system P3). But, interestingly, when the two peptides are close to each other (i.e. 5 Å distance) a sharp drop in inter-peptide hydrogen bonds is noticed. For example, the inter-peptide hydrogen bond is reduced from 5 (in system P0) to 1 (in system P3).

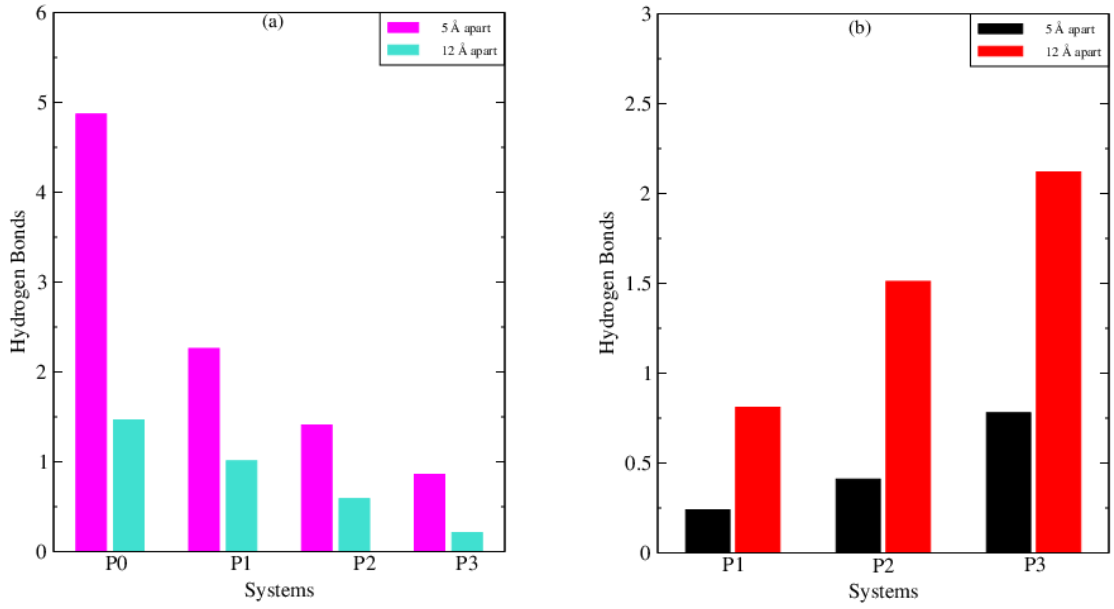

Figure 6-16. *(a) Inter-peptide and (b) peptide-caffeine hydrogen bonds when peptides are 5 Å and 12 Å apart respectively.*

On the other hand, hydrogen bonds between caffeine and peptide (see Fig. 6-16 (b)) increases with increasing caffeine number in the system. When peptides are separated, more peptide-caffeine hydrogen bonds are formed as more hydrogen bonding sites of the peptide residues are available. We have also observed that although all three hydrogen acceptor (two oxygen and ring nitrogen) atoms in caffeine can form hydrogen bonds with hydrogen donor sites of peptide, the two carbonyl oxygen atoms have much higher propensity for hydrogen bond formation (not shown). The residues having more hydrogen bond forming affinity with caffeine are found to be Glu, (followed by) Lys, Ala and Val. However, we observe that Phe residue has a stronger propensity to interact with caffeine among all the residues. Therefore, we may assume that hydrophobic interaction is the main force that drive the peptide-caffeine interaction. However, hydrogen bonding interactions also contribute significantly in caffeine-peptide interaction.

The secondary structure analyses of the two peptides for system P0 and P2 are performed and they are shown in Fig. 6-17 (a-d). In pure water, when the peptides are 5 Å apart, we observe that all the hydrophobic residues of the two peptides are in β-strand conformation, and the terminal residues are in random coil or turn conformation (see Fig. 6-17 (a)).

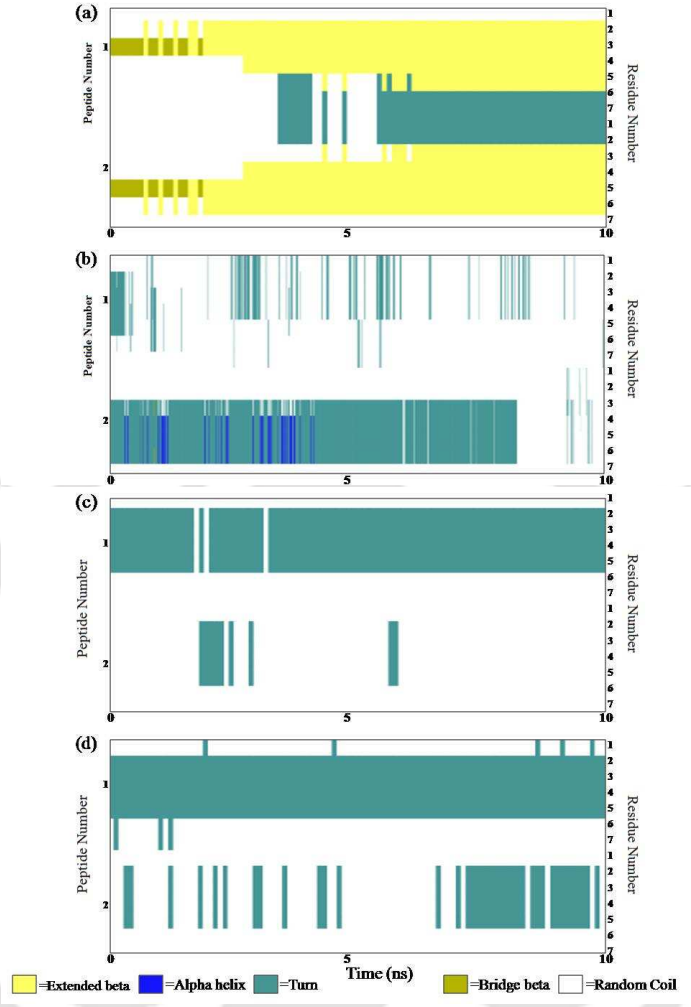

Figure 6-17.*Secondary structure analyses of peptides. (a) system P0, 5 Å apart; (b) system P0, 12 Å apart; (c) system P2, 5 Å apart and (d) system P2, 12 Å apart.*

However, when the peptides are far apart (12 Å), we don't observe any β-strand and the peptide residues are mostly in random coil or in turn conformation. Moreover, during the first 5 ns, we also observe α-helix conformation (see Fig. 6-17 (b)). It is worth mentioning here that in the secondary structure analyses of peptides in system S1 we also observe the formation of small amount of α-helix conformation (see Fig. 6-2 (b)). Due to less number of caffeine molecule present in system S1, caffeine molecules mostly block the Phe residues and thereby preventing the oligomer formation tendency of peptide. Therefore, to avoid water contact, other hydrophobic sites in peptide monomer turn themselves and transform into α-helical structure. With increasing number of caffeine molecules, the formation of ordered β-sheet structure are totally prevented even when peptides are close to each other (see Fig.

6-17 (c)). When peptides are separated the caffeine-peptide interaction increases, and the hydrophobic residues of the peptide are stabilized within the hydrophobic confinement of caffeine clusters. Therefore, residues of both the peptides are mostly in random coil or turn conformation in caffeine solution (Fig. 6-17 (d)).

■ SUMMARY AND CONCLUSIONS

Alzheimer's disease, a common form of dementia, is caused due to aggregation of Aβ peptide and it is characterized by the deposition of aggregated fibrils in the brain. Several clinical and preclinical studies on human and non-human species have shown the disease curing ability of caffeine on Alzheimer's disease. However, the mechanism and mode of action of caffeine is not studied either experimentally or theoretically. Therefore, in this study, we have investigated the aggregation tendency of amyloid forming short peptide Aβ_{16-22} in both pure water as well as in different caffeine solutions. In pure water, the secondary structure analyses of Aβ_{16-22} peptide showed the formation of highly ordered β-sheets structure. All the five peptides present in the system aggregate together to shield the hydrophobic central core from solvent water molecules and the hydrophilic terminal residues are well exposed to water. The non-bonded inter-peptide interaction energy of such oligomer formation is found to be favorable (negative) for different systems. The calculations of potential of mean forces between phenylalanine residues of two peptides show a global minimum at 4.6 Å in pure water, which shifts to a larger distance in presence of higher number of caffeine in the system. In presence of caffeine, the hydrophobic central core of peptides is blocked by the caffeine clusters to interact with other peptides. The interaction between caffeine and the phenylalanine residues of peptide restricts the self-assembly formation of peptide. The secondary structure analyses showed mostly random coil conformation of the peptide in presence of caffeine, which is the predominant conformation of Aβ_{16-22} peptide as a monomer. The formation of small amount of α-helix conformation in system S1 suggests that, as the number of caffeine in this system is small, caffeine molecules mostly interact with phenylalanine residues of the peptide and therefore, other small hydrophobic sites turn themselves around resulting in to α-helical structure. For the full length Aβ peptide, with relatively long stretches of hydrophobic residues, we believe that the possibility of α-helix conformation due to the hydrophobic collapse will be more. Radial distribution function, hydrogen bond analyses, residue-residue contact map calcula-

tion, interaction energy calculation and solvent accessible surface area calculation showed the disaggregation tendency of peptide in presence of caffeine, and with increasing number of caffeine in the system, the self-assembly formation is getting ceased. The contour density analyses of caffeine within 7.5 Å of peptide showed higher caffeine density with increasing caffeine number. We also observed that as the number of caffeine increases, the interaction of caffeine with hydrophobic residues and hydrogen bonding sites of the peptide increases. However, we observed that hydrophobic interaction is the driving force of peptide-caffeine interaction. The cluster structure analyses of caffeine in all systems indicates the formation of higher number of medium ordered caffeine clusters with increasing number of caffeine. These clusters form a hydrophobic environment around the hydrophobic residues of peptide, and physically block them from interaction. Therefore, our simulation study showed that caffeine molecules inhibit the oligomers formation of Aβ_{16-22} peptide, by reducing hydrophobic interaction between peptides. Again, as the self-aggregation tendency of peptide decreases in presence of caffeine, the hydrogen bonding sites of peptide are available to form hydrogen bonds with hydrogen accepting atomic sites of caffeine, which further stabilizes the caffeine-peptide interaction.

भारतीय प्रौद्योगिकी संस्थान गुवाहाटी
Indian Institute of Technology Guwahati

Chapter 7

Summary and Our View on Action of Caffeine as an Inhibitor

"We are at the very beginning of time for the human race. It is not unreasonable that we grapple with problems. But there are tens of thousands of years in the future. Our responsibility is to do what we can, learn what we can, improve the solutions, and pass them on."

– Richard P. Feynman

We have carried out classical MD simulation to explore the underlying mechanism of effect of caffeine on aggregation of protein. We systematically investigated the self-association property of caffeine molecules first and then the changes in protein aggregation tenancy in presence of caffeine aggregates. We started our investigation to explore the self-association of caffeine molecules in presence of NaCl salt, as salt ions are an essential component of living systems. We observed that caffeine molecules self-aggregate by forming clusters by intermolecular π-stacking interaction. Addition of NaCl salt causes the exclusion of water molecules from caffeine hydrophobic surface. To investigate the solvation of caffeine more closely we have calculated preferential interaction parameters. We have found that with increasing salt concentrations, a caffeine molecule prefers to interact with another caffeine over water molecules. Cluster structure analyses and SASA calculations have revealed higher association of caffeine molecules at high NaCl concentration. We have also observed a slight decrease in the caffeine-water average number of hydrogen bonds on addition of salt. An investigation of the effect of temperature on self-association of caffeine molecules in pure water and salt solutions showed that as temperature increases, the probability of formation of higher order clusters decreases. Spatial distribution plot shows vertical stacking arrangement of caffeine molecules, which shows a trend of decreasing caffeine aggregation at higher temperature. Addition of salt enhances the probability of caffeine distribution around itself. Calculation of potential of mean force and the enthalpic and entropic contribution to it shows that thermodynamics of caffeine association is enthalpy driven in pure water. However, presence of salt leads to entropy driven association specifically at higher temperature. Interestingly, although caffeine molecule is smaller than the required 1 nm length as predicted by Chandler [74] for crossover from entropic to enthalpic dependence of aggregation of nonpolar solutes, our analyses point out the transition of thermodynamic behavior of caffeine association to shorter length-scale as the chemical and physical environments are changed.

To shed lights on the effect of caffeine on hydrophobic aggregation of biomolecules, at first we have examined the self-aggregation of hydrophobic di-t-butyl-methane (DTBM) molecules in a regime of caffeine : DTBM stoichiometric ratios. Calculations of site-site radial distribution functions followed by the coordination number analyses and spatial distribution plots showed the disruption of hydrophobic moieties of DTBM aggregates in 10 : 1 or more stoichiometric ratio of caffeine : DTBM. Cluster structure analyses, spatial distribution function plots of caffeine around DTBM and the snapshots of the trajectory reveal that caffeine aggregates form a hydrophobic environment around a DTBM molecule

in which a DTBM molecule is encapsulated, and DTBM interacts with water within the confinement of caffeine aggregates. Moreover, these caffeine clusters also physically block the other DTBM molecules to interact with the encapsulated DTBM molecule, leading to disruption of DTBM clusters in solutions with 10:1 or higher caffeine to DTBM molecules.

Next, we have explored the effect of caffeine on protein aggregation, which is more complex compared to purely hydrophobic associtions. Our studies on effect of caffeine on the aggregation of amyloid-β derived switch-peptide with varied stoichiometric ratios of caffeine to peptide showed that formation of β-sheet conformation is prevented to a large extent in presence of 10:1 or more caffeine to peptide ratio. We have observed that caffeine can inhibit the formation of β-sheet by interacting with the peptide aromatic moiety. In order to understand the mechanism of inhibition action of caffeine in more detail, we have considered the seven residue peptide Aβ_{16-22}, which form amyloid fibril in vitro. In pure water system, the peptides aggregate together to shield the hydrophobic central core from the solvent water molecules and the hydrophilic terminal residues are well exposed to water. However, radial distribution function, hydrogen bond analyses, residue-residue contact map calculation, interaction energy calculation and solvent accessible surface area calculations showed the disaggregation tendency of peptide in presence of caffeine, and with increasing number of caffeine in the system, the self-assembly formation is getting ceased. In presence of caffeine the hydrophobic central core of peptides is blocked by the caffeine clusters to interact with other peptides. The interaction between caffeine and the phenylalanine residues of peptide restricts the self-assembly formation of peptide. We also observed that as the number of caffeine increases, the interaction of caffeine with the hydrophobic residues and hydrogen bonding sites of the peptide increases. For all systems, the cluster structure analyses of caffeine indicate the formation of higher number of medium ordered caffeine clusters with increasing number of caffeine. These clusters form a hydrophobic environment around the hydrophobic sites of peptides, and physically block them from interacting with each other. Again, as the self-aggregation tendency of peptide decreases in presence of caffeine, the hydrogen bonding sites of peptide are available to form hydrogen bonds with hydrogen accepting atomic sites of caffeine, which further stabilizes the caffeine-peptide interaction.

Therefore, we conclude that caffeine has the ability to inhibit amyloid formation of peptide, and the blocking of aromatic Phe residue of the Aβ_{16-22} peptide by caffeine clusters through peptide-caffeine π-stacking interaction, and other residues by hydrophobic and hydrogen bonding interactions lead to complete disaggregation of peptide in caffeine solution

with 10:1 or higher caffeine to peptide stoichiometric ratio.

Bibliography

1. D. J. Selkoe, *Nature* **426**, 900 (2003).
2. C. Soto, *FEBS Lett.* **498**, 204 (2001).
3. C. Soto, *Nat. Rev. Neurosci.* **4**, 49 (2003).
4. C. M. Dobson, *Nature* **418**, 729 (2002).
5. M. S. Forman, J. Q. Trojanowski, V. M. Lee. *Nat. Med.* **10**, 1055 (2004).
6. C. B. Anfinsen, *Science* **181**, 223 (1973).
7. A. Brüning, J. Jückstock, *Cancer Molecular Targets and Therapeutics* **5**, 47 (2015).
8. P. Hammarstrm, R. L. Wiseman, E. T. Powers, J. W. Kelly, *Science* **299**, 713 (2003).
9. I. V. Baskakov, G. Legname, M. A. Baldwin, S. B. Prusiner, F. E. Cohen, *J. Biol. Chem.* **277**, 21140 (2002).
10. F. U. Hartl, M. Hayer-Hartl, *Nat. Struct. Mol. Biol.* **16**, 574 (2009).
11. H. C. Huang, Z. F. Jiang, *J. Alzheimers Dis.* **16**, 15 (2009).
12. A. Mudher,S. Lovestone, *Trends in Neurosci.* **1**, 22 (2002).
13. D. J. Selkoe, *Nature* **399**, 23 (1999).
14. R. Kayed, E. Head, J. L. Thompson, T. M. Mclntire, S. C. Milton, C. W. Cotman, C. G. Glabel, *Science* **300**, 486 (2003).
15. K. P. Nilsson, *FEBS Lett.* **583**, 2593 (2009).
16. T. L. Kukar, *Nature* **453**, 925 (2008).
17. J. Chen, A. H. Armstrong, A. N. Koehler, M. H. Hecht, *J. Am. Chem. Soc.* **132**, 17015 (2010).
18. Y. Hong, L. Meng, S. Chen, C. W. T. Leung, L.-T. Da, M. Faisal, D.-A. Silva, J. Liu, J. W. Y. Lam, X. Huang, B. Z. Tang, *J. Am. Chem. Soc.* **134**, 1680 (2012).

19. T. Takahashi, H. Mihara, *Acc. Chem. Res.* **41**, 1309 (2008).

20. K. Giger, R. P. Vanam, E. Seyrek, P. L. Dubin, *Biomacromolecules* **9**, 2338 (2008).

21. C. Cabaleiro-Lago, F. Quinlan-Pluck, I. Lynch, K. A. Dawson, S. Linse, *ACS Chem. Neurosci.* **1**, 279 (2010).

22. P. Frid, S. V. Anisimov, N. Popovic, *Brain Research Reviews* **53**, 135 (2007).

23. G. W. Arendash, T. Mori, C. Cao, M. Mamcarz, M. Runfeldt, A. Dickson, K. Rezai-Zadeh, J. Tane, B. A. Citron, X. Lin, V. Echeverria, H. Potter, *J Alzheimers Dis.* **17**, 661 (2009).

24. C. Cao, J. R. Cirrito, X. Lin, L. Wang, D. K. Verges, A. Dickson, M. Mamcarz, C. Zhang, T. Mori, G. W. Arendash, D. M. Holtzman, H. Potter, *J Alzheimers Dis.* **17**, 681 (2009).

25. G. W. Arendash, W. Schleif, K. Rezai-Zadeh, E. K. Jackson, L. C. Zacharia, J. R. Cracchiolo, D. Shippy, J. Tan, *Neuroscience.* **142**, 941 (2006).

26. H. Qosa, A. H. Abuznait, R. A. Hill, A. Kaddoumi, *J Alzheimers Dis.* **31**, 151 (2012).

27. C. Laurent, S. Eddarkaoui, M. Derisbourg, A. Leboucher, D. Demeyer, S. Carrier, M. Schneider, M. Hamdane, C. E. Müller, L. Buée, D. Blum, *Neurobiol. Aging* **35**, 2079 (2014).

28. H. Terada, Y. Sakabe, *J. Chromatogr.* **291**, 453 (1984).

29. T. Kumazawa, H. Seno, X. P. Lee, A. Ishii, K. W. Suzuki, K. Sato, O. Suzuki *Anal. Chim. Acta* **387**, 53 (1999).

30. M. Melnik, *J. Inorg. Nucl. Chem.* **43**, 3035 (1981).

31. S. A. Shaker, Y. Farina, S. Mahmmod, M. Eskender, *J. Basic Appl. Sci.* **3**, 3337 (2009).

32. Y.-S. Kim, H. Sano *Phytochem.* **69**, 882 (2008).

33. R. Sanjeewa, S. Weerasinghe, *J. Mol. Struct. THEOCHEM* **944**, 116 (2010).

34. Y. Cui, *Int. J. Pharm.* **397**, 36 (2010).

35. A. V. Shestopalova, *Biophysics* **51**, 335 (2006).

36. L. Tavagnacco, O. Engström, U. Schnupf, M-L Saboungi, M. E. Himmel, G. Widmalm, A. Cesàro, J. W. Brady, *J. Phys. Chem. B* **116**, 11701 (2012).

37. A. Cesàro, E. Russo, D. Tessarotto, *J. Solution Chem.* **9**, 221 (1980).

38. T. H. Lilley, H. Linsdell, A. Maestre, *J. Chem. Soc. Faraday Trans.* **88**, 2865 (1992).

39. A. Al-Maaieh, D. R. Flanagan, *J. Pharm. Sci.* **91**, 1000 (2002).

40. H. Kimura, T. Aoyama, *J. Pharmacobiodyn* **12**, 589 (1989).

41. R. W. Larsen, R. Jasuja, R. Hetzler, P. T. Muraoka, V. G. Andradaand, D. M. Jameson, *Biophys. J.* **70**, 443 (1996).

42. D. M. Davis, D. A. Veselkov, V. V. Kodintsev, M. P. Evstineev, A. N. Veselkov, *Mol. Phys.* **23**, 1961 (2000).

43. D. B. Davis, D. A. Veselkov, L. N. Dijmant, A. N. Veselkov, *Eur. Biophys. J.* **30**, 354 (2001).

44. M. B. Lyles, I. L.Cameron, *Cell Biol. Int.* **26**, 145 (2002).

45. G. Fisone, A. Borgkvist, A. Usiello, *Cell. Mol. Life. Sci* **61**, 857 (2004).

46. P. Svenningsson, G. G. Nomikos, E. Ongini, B. B. Fredholm *Neuroscience* **79**, 753 (1997).

47. D. Shi, O. Nikodijevic, K. A. Jacobson, J. W. Daly, *Arch Int Pharmacodyn Ther* **328**, 261 (1994).

48. Chiti, F.; Dobson, C. M. *Annu. Rev. Biochem.* **75**, 333 (2006).

49. Ellis, R. J.; Pinheiro, T. J. T. *Nature* **416**, 483 (2002).

50. Lesné, S.; Koh, M. T.; Kotilinek, L.; Kayed, R.; Glabe, C. G.; Yang, A.; Gallagher, M.; Ashe, K. H. *Nature* **440**, 352 (2006).

51. W. Pohle, H. Fritzsche, *Nucleic Acids Res.* **3**, 3331 (1976).

52. S. Banerjee, P. K. Verma, R. K. Mitra, G. Basu, S. K. Pal, *J Fluoresc.* **22**, 753 (2012).

53. B. Sharma, S. Paul, *J. Chem. Phys.* **139**, 194504 (2013).

54. B. Sharma, S. Paul, *J. Phys. Chem. B* **119**, 6421 (2015).

55. H. Fritzsche, H. Lang, H. Sprinz, W. Pohle, *Biophys. Chem.* **11**, 121 (1980).

56. L. S. Kan, P. N. Borer, D. M. Cheng, P. O. Tso, *Biopolymers* **19**, 1641 (1980).

57. H. Fritzsche, H. Lang, H. Sprinz,W. Pohle, *Biophys. Chem.* **11**, 121 (1980).

58. L.-S. Kan, Ph. N. Borer, D. M. Cheng, P. O. P. Ts'o, *Biopolymers* **19**, 1641 (1980).

59. J. W. Ponder and D. A. Case *Adv. Prot. Chem.* **66**, 27 (2003).

60. D. A. Case, T. A. Darden, T. E. Cheatham III, C. L. Simmerling, J. Wang, R. E. Duke, R. Luo, M. Crowley, R. C. Walker, W. Zhang, K. M. Merz, B. Wang, S. Hayik, A. Roitberg, G. Seabra, I. Kolossváry, K. F. Wong, F. Paesani, J. Vanicek, X. Wu, S. R. Brozell, T. Steinbrecher, H. Gohlke, L. Yang, C. Tan, J. Mongan, V. Hornak, G. Cui, D. H. Mathews, M. G. Seetin, C. Sagui, V. Babin, P. A. Kollman, AMBER 10, University of California, San Francisco (2008).

61. D.A. Case, T.A. Darden, T.E. Cheatham, III, C.L. Simmerling, J. Wang, R.E. Duke, R. Luo, R.C. Walker, W. Zhang, K.M. Merz, B. Roberts, S. Hayik, A. Roitberg, G. Seabra, J. Swails, A.W. Gtz, I. Kolossvry, K.F. Wong, F. Paesani, J. Vanicek, R.M. Wolf, J. Liu, X. Wu, S.R. Brozell, T. Steinbrecher, H. Gohlke, Q. Cai, X. Ye, J. Wang, M.-J. Hsieh, G. Cui, D.R. Roe, D.H. Mathews, M.G. Seetin, R. Salomon-Ferrer, C. Sagui, V. Babin, T. Luchko, S. Gusarov, A. Kovalenko, P.A. Kollman, AMBER 12, University of California, San Francisco (2012).

62. J. E. Lennard-Jones *Proc. R. Soc. London, Ser. A* **106**, 463 (1924).

63. J. D. van der Waals *Verhandelingen der Koninklijke Akademie der Wetenschappen* **1**, 1 (1893).

64. C. A. Coulomb, G Villars*Collection de ḿemoires relatifs à la physique* **569**, (1884).

65. L. Verlet *Phys. Rev.* **159**, 98 (1967).

66. R. W. Hockney *Meth. Comp. Phys.* **9**, 136 (1970).

67. M. L. Origlia-Luster, B. A. Pattersn, E. M. Woolley, *J. Chem. Thermodynamics* **34**, 1909 (2002).

68. R. Sanjeewa, S. Weerasinghe, *Comp. Theor. Chem.* **966**, 140 (2011).

69. J. W. Brady, L. Tavagnacco, L Ehrlich, M. Chen, U. Schnupf, M. E. Himmel, M-L Saboungi, A. Cesàro, *Eur Biophys J.* **41**, 369 (2012).

70. A. Geiger, P. Mausbach, J. Schnitker, R. L. Blumberg, H. E. Stanley, *J. de Physique* **45**, 13 (1984).

71. J. N. Israelachvili, H. Wennerström, *Nature* **379**, 219 (1996).

72. F. H. Stillinger, *Science* **209**, 451 (1980).

73. R. Zangi, B. J. Berne, *J. Phys. Chem. B* **112**, 8634 (2008).

74. D. Chandler, *Nature* **437**, 640 (2005).

75. C.-Y. Lee, J. A. McCammon, P. J. Rossky, *J. Chem. Phys.* **80**, 4448 (1984).

76. S. H. Lee, P. J. Rossky, *J. Chem. Phys.* **100**, 3334 (1994).

77. L. Tavagnacco, U. Schnupf, P. E. Mason, M-L Saboungi, A. Cesàro, J. W. Brady, *J. Phys. Chem. B* **115**, 10957 (2011).

78. A. Cesàro, G. Starec, *J. Phys. Chem.* **84**, 1345 (1980).

79. F. Hofmeister, *Arch. Exp. Pathol. Pharmakol.* **24**, 247 (1888).

80. I. Jelesarov, E. Durr, R. M. Thomas, R. Bosshard, *Biochemistry* **37**, 7539 (1998).

81. J. H. Stern, E. Lowe E., *J. Chem. Eng. Data* **23**, 341 (1978).

82. M. J. Frisch, G. W. Trucks, H. B. Schlegel, G. E. Scuseria, M. A. Robb, J. R. Cheeseman, J. A. Montgomery Jr., T. Vreven, K. N. Kudin, J. C. Burant, J. M. Millam, S. S. Iyengar, J. Tomasi, V. Barone, B. Mennucci, M. Cossi, G. Scalmani, N. Rega, G. A. Petersson, H. Nakatsuji, M. Hada, M. Ehara, K. Toyota, R. Fukuda, J. Hasegawa, M. Ishida, T. Nakajima, Y. Honda, O. Kitao, H. Nakai, M. Klene, X. Li, J. E. Knox, H. P. Hratchian, J. B. Cross, V. Bakken, C. Adamo, J. Jaramillo, R. Gomperts, R. E. Stratmann, O. Yazyev O., A. J. Austin, R. Cammi, C. Pomelli, J. W. Ochterski, P. Y. Ayala, K. Morokuma, G. A. Voth, P. Salvador, J. J. Dannenberg, V. G. Zakrzewski, S. Dapprich, A. D. Daniels, M. C. Strain, O. Farkas, D. K. Malick, A. D. Rabuck, K. Raghavachari, J. B. Foresman, J. V. Ortiz, Q. Cui, A. G. Baboul, S.

Clifford, J. Cioslowski, B. B. Stefanov, G. Liu, A. Liashenko, P. Piskorz, I. Komaromi, R. L. Martin, D. J. Fox, T. Keith, M. A. Al-Laham, C. Y. Peng, A. Nanayakkara, M. Challacombe, P. M. W. Gill, B. Johnson, W. Chen, M. W. Wong, C. Gonzalez, J. A. Pople, Gaussian 03, (2003)

83. M. Žółkiewski, *J. Solution Chem.* **16**, 1025 (1987).

84. I. S. Joung, T. E. Cheatham, *J. Phys. Chem. B* **112** 9020 (2008).

85. H. J. C. Berendsen, J. R. Grigera, T. P. Straatsma, *J. Phys. Chem.* **91**, 6269 (1987).

86. L. Martinez, R. Andrade, E.G. Birgin, J. M. Martinez, *J. Comput. Chem.* **30**, 2157 (2009).

87. H. J. C. Berendsen, J. P. M. Postma, W. F. van Gunsteren, A. DiNola J. R. Haak, *J. Phys. Chem.* **81**, 3684 (1984).

88. M. Falk, M. Gil, N. Iza, *Can. J. Chem.* **68**, 1293 (1990).

89. S. Chowdhuri, A. Chandra, *J. Chem. Phys.* **115**, 3732 (2001).

90. A. Cesàro, E. Russo, V. Crescenzi, *J. Phys. Chem. B* **80**, 335 (1976).

91. P. R. Stoesser, S. J. Gill, *J. Phys. Chem. B* **71**, 564 (1976).

92. A. Shrake, J. A. Rupley, *J. Mol Bio* **79**, 351 (1973).

93. J. C. Kirkwood, F. P. Buff, *J. Chem. Phys.* **19**, 774 (1951).

94. E. Matteoli, G. A. Mansoori, *Fluctuation Theory of Mixtures, Taylor and Francis*, New York, (1990).

95. A. Ben-Naim, *Statistical Thermodynamics for Chemists and Biochemists*, Plenum Press, New York, (1992).

96. A. Ben-Naim, *Molecular Theory of Solutions, Oxford University Press*, New York, (2006).

97. P. E. Smith, *J. Phys. Chem. B* **110**, 2862 (2006).

98. P. E. Smith, *Biophys. J.* **91**, 849 (2006).

99. M. Falk, W. Chew, J. A. Walter, W. Kwiatkowski, K. D. Barclay, G. A. Klassen, *Can. J. Chem.* **76**, 48 (1998).

100. T. Ghosh, A. E. Garcia, S. Garde, *J. Chem. Phys.* **116**, 2480 (2002).

101. Y. Zhang, P. S. Cremer, *Curr. Opin. Chem. Boil.* **10**, 658 (2006).

102. H. S. Ashbaugh, M. E. Paulaitis, *J. Am. Chem. Soc.* **123**, 10721 (2001).

103. V. Pierce, M. Kang, M. Aburi, S. Weerasinghe, P. E. Smith, *J. Chem. Theory Comput.* **7**, 1369 (2011).

104. D. van der Spoel, E. Lindahl, B. Hess, G. Groenhof, A. E. Mark, H. J. C. Berendsen, *J. Comp. Chem.* **26**, 1701 (2005).

105. E. Lindahl, B. Hess, D. van der. Spoel, *J. Mol. Mod.* **7**, 306 (2001).

106. W. Humphrey, A. Dalke, K. Schulten, *J. Molec. Graphics.* **14**, 33 (1996).

107. J. C. Kirkwood, F. P. Buff, *J. Chem. Phys.* **19**, 774 (1951).

108. D. E. Smith, A. D. J. Haymet, *J. Chem. Phys.* **98**, 6445 (1993).

109. S. Ludemann, R. Abseher, H. Schreiber, O. Steinhauser, *J. Am. Chem. Soc.* **119**, 4206 (1997).

110. T. Head-Gordon, *J. Am. Chem. Soc.* **117**, 501 (1995).

111. S. Shimizu, H. S. Chan, *J. Am. Chem. Soc.* **123**, 2083 (2001).

112. N. Choudhury, B. M. Pettitt, *J. Phys. Chem. B* **110**, 8459 (2006).

113. R. Sarma, S. Paul, *J. Chem. Phys.* **135**, 174501 (2011).

114. C. Vega, C. McBride, E. Sanz, J. L. F. Abascal, *Phys. Chem. Chem. Phys.* **7**, 1450 (2005).

115. R. Sarma, S. Paul, *J. Chem. Phys.* **136**, 114510 (2012).

116. A. K. Soper, *Chem. Phys.* **258**, 121 (2000).

117. S. Chowdhuri, A. Chandra, *J. Chem. Phys.* **115**, 3732 (2001).

118. A. Luzar, D. Chandler, *Phys. Rev. Lett.* **76**, 928 (1996).

119. A. Chandra, *Phys. Rev. Lett.* **85**, 768 (2000).

120. A. Chandra, *J. Phys. Chem. B* **107**, 3899 (2003).

121. J. H. Stern, J. A. Devore, S. L. Hansen, O. Yavuz, *J. Phys. Chem.* **78**, 1922 (1974).

122. J.-X. Dong, Q. Li, Z.-C. Tan, Z.-H. Zhang, Y. Liu, *J. Chem. Thermodynamics* **39**, 108 (2007).

123. N. Choudhury, B. M. Pettitt, *J. Am. Chem. Soc.* **127**, 3556 (2005).

124. R. L. Mancera, *J. Phys. Chem. B* **103**, 3774 (1999).

125. R. Zangi, M. Hagen, B. J. Berne, *J. Am. Chem. Soc.* **129**, 4678 (2007).

126. O. Keskin, A. Gursoy, B. Ma, R. Nussinov, *Chem. Rev.* **108**, 1225 (2008).

127. S. L. McGovern, B. T. Helfand, B. Y. Feng, B. K. Shoichet, *J. Med. Chem* **46**, 4265 (2003).

128. B. K. Shoichet, *Drug Discovery Today* **11**, 607 (2006).

129. J. R. P. Prasanthi, B. Dasari, G. Marwarha, T. Larson, X. Chen, J. D. Geiger, O. Ghribi, *Free Radic Biol Med.* **49**, 1212 (2010).

130. S. Das, S. Paul, *J. Phys. Chem. B* **120**, 173 (2016).

131. W. L. Jorgensen, D. S. Maxwell, J. Tirado-Rives, *J. Am. Chem. Soc.* **118**, 11225 (1996).

132. H. J. C. Berendsen, J. R. Grigera, T. P. Straatsma, *J. Phys. Chem.* **91**, 6269 (1987).

133. K. E. D. Coan, B. K. Shoichet, *J. Am. Chem. Soc.* **130**, 9606 (2008).

134. B. Y. Feng, B. H. Toyama, H. Wille, D. W. Colby, S. R. Collins, B. C. May, S. B. Prusiner, J. Weissman, B. K. Shoichet, *Nat. Chem. Biol.* **4**, 197 (2008).

135. I. Pavel, A. Szeghalmi, D. Moigno, S. Cîntă, W. Kiefer, *Biopolymers* **72**, 25 (2003).

136. U. Kopcak, R. S. Mohamed, *J Supercrit Fluids* **34**, 209 (2005).

137. J. P. Ryckaert, G. Ciccotti, H. J. C. Berendsen, *J. Comput. Phys.* **23**, 327 (1977).

138. B. Hess, N. F. A. van der Vegt, *J. Phys. Chem. B* **110**, 17616 (2006).

139. S. Paul, G. N. Patey, *J. Phys. Chem. B* **116**, 4991 (2012).

140. X. Huang, C. J. Margulis, B. J. Berne, *Proc. Nat. Acad. Sci. U.S.A.* **100**, 11953 (2003).

141. N. Choudhury, B. M. Pettitt, *J. Am. Chem. Soc.* **127**, 3556 (2005).

142. N. Choudhury, *J. Phys. Chem. B* **112**, 6296 (2008).

143. N. Choudhury, *J. Chem. Phys.* **131**, 014507 (2009).

144. R. Sarma, S. Paul, *Chem. Phys.* **407**, 115 (2012).

145. K. E. D. Coan, D. A. Maltby, A. L. Burlingame, B. K. Shoichet, *J. Med. Chem* **52**, 2067 (2009).

146. D. B. Davied, D. A. Veselkov, L. N. Djimant, A. N. Veselkov, *Eur. Biophys. J.* **30**, 354 (2001).

147. D. Bandyopadhyay, K. Bhanja, S. Mohan, S. K. Ghosh, N. Choudhury, *J. Phys. Chem. B* **119**, 11262 (2015).

148. S. L. McGovern, E. Caselli, N. Grigorieff, B. K. Shoichet, *J. Med. Chem* **45**, 1712 (2002).

149. J. Timko, D. Bucher, S. Kuyucak, *J Chem Phys.* **132**, 114510 (2010).

150. M. Hamsa Priya, H. S. Ashbaugh, M. E. Paulaitis, *J. Phys. Chem. B* **115**, 13633 (2011).

151. M. Mutter, A. Chandravarkar, C. Bovat, J. Lopez, S. D. Santos, B. Mandal, R. Mimna, K. Murat, L. Patiny, L. Saucede, G. Tuchscherer, *Angew Chem. Int. Ed.* **43**, 4172 (2004).

152. A. Paul, B. Sharma, T. Mondal, K. Thalluri, S. Paul, B. Mandal, *Med. Chem. Commun.* **7**, 311 (2016).

153. W. D. Cornell, P. Cieplak, C. I. Bayly, I. R. Gould, K. M. Merz, D. M. Ferguson, D. C. Spellmeyer, T. Fox, J. W. Caldwell, P. A. Kollman, *J. Am. Chem. Soc.* **117**, 5179 (1995).

154. P. H. Hünenberger, *Adv. Polym. Sci.* **173**, 105 (2005).

155. U. Essmann, L. Perera, M. L. Berkowitz, T. Darden, H. Lee, L. G. Pedersen, *J. Chem. Phys.* **103**, 8577 (1995).

156. M.-S. Lin, L.-Y. Chen, H.-T. Tsai, S. S.-S. Wang, Y. Chang, A. Higuchi, W. Y. Chen, *Langmuir* **24**, 5802 (2008).

157. W. B. Stine, K. N. Dahlgren, G. A. Krafft, M. J. LaDu, *J. Biol. Chem.* **278**, 11612 (2003).

158. A. Banerjee, S. K. Maji, M. G. B. Drew, D. Haldar, A. K. Das, A. Banerjee, *Tetrahedron* **60**, 5935 (2004).

159. S. Trobro, J. Åqvist, *Biochemistry* **45**, 7049 (2006).

160. E. Gazit, *FEBS J.* **272**, 5971 (2005).

161. J. J. Balbach, Y. Ishii, O. N. Antzutkin, R. D. Leapman, N. W. Rizzo, F. Dyda, J. Reed, R. Tycko, *Biochemistry* **39**, 13748 (2000).

162. D. A. Kirschner, H. Inouye, L. K. Duffy, A. Sinclair, M. Lind, D. J. Selkoe, *Proc. Natl. Acad. Sci.* **84**, 6953 (1987).

163. T. H. J. Huang, P. E. Fraser, A. Chakrabartty, *J. Mol. Biol.* **269**, 214 (1997).

164. T. S. Burkoth, T. L. S. Benzinger, V. Urban, D. M. Morgan, D. M. Gregory, P. Thiyagarajan, R. E. Botto, S. C. Meredith, D. G. Lynn, *J. Am. Chem. Soc.* **122**, 7883 (2000).

165. T. L. S. Benzinger, D. M. Gregory, T. S. Burkoth, H. Miller-Auer, D. G. Lynn, R. E.Botto, S. C. Meredith, *Biochemistry* **39**, 3491 (2000).

166. T. L. S. Benzinger, D. M. Gregory, T. S. Burkoth, H. Miller-Auer, D. G. Lynn, R. E.Botto, S. C. Meredith, *Proc. Natl. Acad. Sci.* **95**, 13407 (1998).

167. C. Hilbich, B. Kisters-Woike, J. Reed, C. L. Masters, K. Beyreuther, *J. Mol. Biol.* **218**, 149 (1991).

168. C. Hilbich, B. Kisters-Woike, J. Reed, C. L. Masters, K. Beyreuther, *J Mol Biol.* **228**, 460 (1992).

169. D. K. Klimov, D. Thirumalai, *Structure* **11**, 295 (2003).

170. W. Hwang, S. Zhang, R. D. Kamm, M. Karplus, *Proc. Natl. Acad. Sci.* **101**, 12916 (2004).

171. G. Favrin, A. Irbäck, S. Mohanty, *Biophys. J.* **87**, 3657 (2004).

172. U. F. Röhrig, A. Laio, N. Tantalo, M. Parrinello, R. Petronzio, *Biophys. J.* **91**, 3217 (2006).

173. G. M. Torrie, J. P. Valleau, *J. Comput. Phys.* **23**, 187 (1977).

174. D. K. Klimov, J. E. Straub, D. Thirumalai, *Proc. Natl. Acad. Sci.* **101**, 14760 (2004).

175. P. H. Nguyen, M. S. Li, G. Stock, J. E. Straub, D. Thirumalai, *Proc. Natl. Acad. Sci.* **104**, 111 (2007).

176. D. K. Klimov, D. Thirumalai, *Structure* **11**, 295 (2003).

177. W. M. Berhanu, A. E. Masunov, *Biophys Chem.* **149**, 12 (2010).

178. L. Tavagnacco, S. Di Fonzo, F. D'Amico, C. Masciovecchio, J. W. Bradyc, A. Cesáro, *PCCP* **18**, 13478 (2016).

179. A. Grossfield, http://membrane.urmc.rochester.edu/Software/WHAM/WHAM.html, 2008, April, 14

List of Publications

1. Bhanita Sharma and Sandip Paul, Effects of dilute aqueous NaCl solution on caffeine aggregation. *J. Chem. Phys.* **139**, 194504 (2013).

2. Bhanita Sharma and Sandip Paul, Understanding the Role of Temperature Change and the Presence of NaCl Salts on Caffeine Aggregation in Aqueous Solution: From Structural and Thermodynamics Point of View. *J. Phys. Chem. B*, **119**, 6421 (2015).

3. Ashim Paul, Bhanita Sharma, Tanmay Mondal, Kishore Thalluri, Sandip Paul and Bhubaneswar Mandal, Amyloid β derived switch-peptides as a tool for investigation of early events of aggregation: a combined experimental and theoretical approach. *Med. Chem. Commun.*, **7**, 311 (2016).

4. Bhanita Sharma and Sandip Paul, Action of Caffeine as an Amyloid Inhibitor in the Aggregation of Aβ_{16-22} Peptides. *J. Phys. Chem. B*, **120**, 9019 (2016).

5. Bhanita Sharma, Sourav Kalita, Bhubaneswar Mandal and Sandip Paul, The role of caffeine as an inhibitor in the aggregation of amyloid forming peptides: a unified molecular dynamics simulation and experimental study. *RSC Adv.*, **6**, 78548 (2016).

6. Bhanita Sharma and Sandip Paul, Role of caffeine as an inhibitor in aggregation of hydrophobic molecules: A molecular dynamics simulation study *J. Mol. Liq.* (Just Accepted).

7. Bhanita Sharma and Sandip Paul, Role of caffeine as a tau aggregation inhibitor. (Manuscript under preparation).

Conferences Attended

1. Presented a poster entitled "Self-association of caffeine in Dilute Aqueous NaCl Solution" in the conference "Theoretical Chemistry Symposium (TCS)" held at Department of Chemistry, IIT Guwahati from 19-22 December 2012.

2. Presented a poster entitled "Effects of Dilute Aqueous NaCl Solution on Caffeine Aggregation" in the conference "Current Trends in Theoretical Chemistry (CTTC)" held at BARC, Mumbai from 26-28 September 2013.

3. Presented a poster entitled "Effect of Temperature Change and the Presence of NaCl Salts on Caffeine Aggregation in Aqueous Solution" in the conference "Dynamics of Complex Chemical and Biological Systems (DCCBS)" held at Department of Chemistry, IIT Kanpur in January 2014.

4. Awarded the 'best poster award' for a poster entitled "Understanding the Role of Temperature Change and the Presence of NaCl Salts on Caffeine Aggregation in Aqueous Solution: From Structural and Thermodynamical Point of View" in the conference "Theoretical Chemistry Symposium (TCS)" held at Department of Chemistry, NCL Pune from 21-24 December 2014.

5. Presented a poster entitled "Role of caffeine as an inhibitor in aggregation of hydrophobic molecules: A molecular dynamics simulation study" in the conference "18th CRSI National Symposium in Chemistry" held at Department of Chemistry, Panjab University from 5th-7th February 2016.